MECHANISMS OF PROTEIN MISLOCALIZATION IN NEURODEGENERATIVE DISEASE

APPROVED BY SUPERVISORY COMMITTEE

Philip J Thomas, Ph.D

YuhMin Chook, Ph. D

Ilya Bezprozvanny, Ph. D

Gang Yu, Ph. D

DEDICATION

To my family

ACKNOWLEDGMENTS

First, I would like to thank my mentor, Phil Thomas, for his support, his guidance, and especially for his confidence in my ability to succeed. Also all of the Thomas lab members, for making the Thomas Lab a great place to work, in particular my fellow conspirator I-Hui Wu. I would also like to thank my committee members: Ilya Bezprovanny, Gang Yu, Steve McKnight, and Yuh Min Chook for your support and insight. A special thanks to Yuh Min Chook, her former student Joyce Fung, and her postdoc Tolga Cagatay, who were instrumental in studies of the putative NES in TDP-43. Thanks to Ege Kavalali, and former students Ying Li and Austin Reese for their donations of hippocampal cultures. Thanks to Jerry Shay, his former student Laura Yuan, former post-doc Andrew Ludlow, and postdoc Jen Peters-Hall for their help culturing patient fibroblasts. And thanks to former postdoc in the Thomas Lab, Andrey Karamyshev, for his work on elucidating RAPP, and for performing *in vitro* translation and photocrosslinking experiments.

MECHANISMS OF PROTEIN MISLOCAIZATION IN NEURODEGENERATIVE DISEASE

by

EMIL SEVIM PINARBASI

DISSERTATION

Presented to the Faculty of the Graduate School of Biomedical Sciences

The University of Texas Southwestern Medical Center at Dallas

In Partial Fulfillment of the Requirements

For the Degree of

DOCTOR OF PHILOSOPHY

The University of Texas Southwestern Medical Center at Dallas

Dallas, Texas

May 2019

MECHANISMS OF PROTEIN MISLOCALIZATION IN NEURODEGENERATIVE DISEASE

Publication No. _____

Emile Sevim Pinarbasi, M.D. Ph.D.

The University of Texas Southwestern Medical Center at Dallas, Graduation Year

Supervising Professor: Philip J. Thomas, Ph.D.

Fronto Temporal Lobar Degeneration (FTLD) and Amyotrophic Lateral Sclerosis (ALS) are two fatal and rapidly progressing neurodegenerative diseases. A unifying characteristic of these diseases is the mislocalization of an RNA-binding protein, TDP-43. In unstressed cells, TDP-43 is predominantly nuclear and constantly shuttling to the cytosol; in ALS/FTLD, TDP-43 is aggregated in the cytosol. Two lines of evidence suggest this shift is a cause, rather than an effect, of disease. First, point mutations in the C-terminus of TDP-43, which enhance its aggregation, are a rare cause of familial ALS. Second, animal models which replicate the disease-linked redistribution of TDP-43 in motor neurons demonstrate the progressive muscle weakness and loss of spinal cord mass seen in patients.

However, little is known about the cellular insults that promote TDP-43 mislocalization. My graduate work makes two contributions to this understanding. First, I elucidated a major determinant of normal TDP-43 trafficking. TDP-43 localization is governed by the balance between nuclear import and nuclear export. While a model for TDP-43 nuclear export had been proposed, there was no direct experimental evidence supporting it.

I have shown that the proposed model of TDP-43 nuclear export is incorrect; the putative nuclear export signal (NES) does not mediate nuclear export, and TDP-43 nuclear export is XPO1 independent. Additionally, my data suggest no discrete trafficking signal within TDP-43. Rather, I propose that TDP-43 nuclear export is primarily driven by diffusion through the nuclear pore.

Second, I focused on an upstream event known to affect TDP-43 localization: progranulin secretion. One genetic cause of FTLD is a single loss-of-function mutation in *GRN*, which causes progranulin haploinsufficiency. For reasons that are still unclear, a lifetime of progranulin haploinsufficiency in a patient causes FTLD with TDP-43 mislocalization. I focused on how a subset of *GRN* mutations- the signal sequence mutations- prevent progranulin secretion. I found that the W7R and A9D mutations disrupt co-translational recruitment of the targeting factor SRP (Signal Recognition Particle). This triggers a quality control pathway called RAPP (Regulation of Aberrant Protein Production), which results in degradation of both mutant protein and mutant mRNA. Thus, RAPP mediates progranulin haploinsufficiency in these patients.

TABLE OF CONTENTS

PRIOR PUBLICATIONS

Pinarbasi, E.S, Karamyshev A. K., Hudson, H.H, Thomas, P.J. (2017) Pathogenic signal sequence mutations in progranulin disrupt SRP interactions required for mRNA stability. *Submitted*.

Pinarbasi, E.S. *et al*. Primary determinants of TDP-43 localization are active nuclear import and passive nuclear export. *In preparation*

LIST OF FIGURES

LIST OF TABLES

LIST OF ABBREVIATIONS

3’ UTR - 3’ Untranslated Region

3-AT - 3-amino-1, 2, 4-triazole, a drug which inhibits Histidine biosynthesis

ABC - ATP Binding Cassette

ABCE1 – ATP Binding Cassette sub-family E member 1

Ago2 – Argonaute 2

ALS – Amyotrophic Lateral Sclerosis

Aminoacyl tRNA – Aminoacyl transfer RNA

APP – Amyloid Precursor Protein

ATP – Adenosine Tri Phosphate

C9ORF72 – Chromosome 9 Open Reading Frame 72

cDNA – complementary Deoxyribo Nucleic Acid

CFTR – Cystic Fibrosis transmembrane conductance Regulator

CHMP2B – Charged Multivesicular Body Protein 2B

CLIP-Seq – Cross Linking Immuno Precipitation combined with high-throughput RNA Sequencing

CNS – Central Nervous System

COL5A1 - Collagen, type V, alpha 1

Cre-ER - Cre Estrogen Receptor

CRISPR – Clustered Regularly Interspaced Palindromic Repeats

CRM1 – Chromosomal Region Maintenance 1 (yeast homolog of XPO1)

Cryo EM – Cryogenic Electron Microscopy

CSF – Cerebrospinal Fluid

DNA – Deoxy ribo Nucleic Acid

Dom34 – Duplication of Multilocus region (yeast homolog of Pelota)

DSPP – Dentine Sialo PhosphoProtein

eIF4G – eukaryotic Initiation Factor 4G

EJC - Exon Junction Complex

ER – Endoplasmic Reticulum

eRF1 – eukaryotic Release Factor 1

eRF3 – eukaryotic Release Factor 3

EWSR1 – Ewing's Sarcoma breakpoint Region 1

FTLD – Fronto Temporal Lobar Degeneration

FTLD-Tau – Fronto Temporal Lobar Degeneration, Tau subtype

FTLD-U - Fronto Temporal Lobar Degeneration, Ubiquitinated subtype

FUS – Fused in Sarcoma

G- Protein – Guanine nucleotide binding protein

GDP – Guanosine Di Phosphate

GFP – Green Fluorescent Protein

GRN - Progranulin

GSP1 – Genetic Suppressor of Prp20

GTP – Guanosine Tri Phosphate

Hbs1 – Hsp70 subfamily B Supressor

hnRNP – Heterogenous Ribonuclear Protein particle

hnRNPA1 - Heterogenous Ribonuclear Protein particle A1

hnRNPA2B1 - Heterogenous Ribonuclear Protein particle A 2 B1

hnRNPC - Heterogenous Ribonuclear Protein particle C

Kd – Dissociation constant

kDa – Kilo Dalton

LMB – Leptomycin B, an irreversible XPO1 inhibitor

LOF – Loss of function

mRNA – Messenger RNA

Mtr4 – mRNA transport 4

NCL – Neuronal Ceroid Lipfuscinosis

ND- Neurodegenerative Disease

NES – Nuclear Export Signal

NGD – No-Go Decay

NLS – Nuclear Localization Signal

NMD – Nonsense Mediated Decay

NMR – Nuclear Magnetic Resonance

NSD – Non-Stop Decay

OPTN - Optineurin

P2 – Post-natal day 2

PABP – Poly A Binding Protein

P-body – Processing Body

POMC – Proopiomelanocortin

PPL – Preprolactin

PSEN1 – Presenilin 1

PSEN2 – Presenilin 2

PTC - Premature Termination Codon

PTH – Parathyroid Hormone

qPCR – Semi-quantitative Polymerase Chain Reaction

Ran – Ras-related Nuclear Protein

RAPP – Regulation of Aberrant Protein Production

Ribosome QC – Ribosome Quality Control

RIP-Seq –Immuno precipitation of an RNA-binding protein followed by high-throughput

RNA sequencing

RNA – Ribonucleic Acid

RRM – RNA Recognition Motif

SDS-PAGE – Sodium Dodecyl Sulfate Polyacrylamide Gel Electrophoresis

SI – Shuttling Index (metric of shutting in heterokaryon experiments)

siRNA – silencing RNA

Ski7 – Superkiller 7

SMG1 – Suppressor with Morphogenic effect on Genitalia 1

SMG5 - Suppressor with Morphogenic effect on Genitalia 5

SMG7 - Suppressor with Morphogenic effect on Genitalia 7

SOD1 – Superoxide Dismutase 1

SOX10 – Sex determining Region of Y Box 10

SRP - Signal Recognition Particle

SRP54 - 54 kDa subunit of the Signal Recognition Particle

TAF15 – TATA box binding protein associated factor 15

TDP-43 - Transactive response DNA binding protein 43 kDa

tdTomato – Tandem dimer Tomato

tRNA – transfer Ribo Nucleic Acid

UBQLN2 – Ubiquilin 2

UGT1A1 – UDP glucuronosyltransferase 1 A1

Upf1- Up frame shift helicase 1

Upf2- Up frame shift helicase 2

Upf3 - Up frame shift helicase 3

UTR – Un Translated Region

UV – Ultra Violet

VCP – Valosin Containing Protein

WT – Wild-type

XPO1 – exportin 1

Xrn1 - exoribonuclease 1

CHAPTER ONE

Introduction and Literature Review

Neurodegenerative Disease

Neurodegenerative diseases (ND) are characterized by a progressive loss of neurons which manifests as a gradual decline in nervous system function. NDs represent a huge burden of morbidity and mortality in the developed world. In fact, two of the top fifteen causes of death in the United States in 2014 were neurodegenerative diseases: Alzheimer's, #6, and Parkinson's, #14 [1]. Moreover, as the population ages, the impact of these diseases will only increase; increasing age is the primary risk factor for Parkinson's and Alzheimer's, and is correlated with increasing incidence in other neurodegenerative diseases, such as ALS (Amyotrophic Lateral Sclerosis) [2-4]. However, despite the threat posed by these diseases, we still lack a detailed understanding of the pathological changes which drive them.

Neurodegenerative diseases share several unique features. First, rather than a diffuse effect on the nervous system, most neurodegenerative diseases display a striking specificity for a type of neuron; for example, dopaminergic neurons in the *substantia nigra* are preferentially targeted in Parkinson's disease [5]. Second, brain regions affected by a neurodegenerative disease have characteristic intra or extra cellular protein aggregates: accumulations of misfolded proteins. The makeup of these aggregates is not random; rather, aggregates have a dominant protein that varies by patient, and segregates by disease. A

critical question in the field is the role these aggregates play in disease. Do aggregates cause toxicity in affected neurons, or are they merely a byproduct of disease?

The elaboration of the genetics of neurodegenerative diseases provided strong support for the former. For all described NDs, a subset of cases are familial: directly inherited by a parent. Detailed genetic analyses of these familial cases, as well as sporadic cases, has yielded comprehensive lists of ND-causing mutations. Many of these mutations strongly suggest an aggregate-driven mechanism. For example, the three fully penetrant mutations which cause Alzheimer's disease – in which aggregates are composed of the β-amyloid protein-- are in *APP*, *PSEN1*, and *PSEN2*, all genes involved in amyloid production or processing[6]. However, not all ND-causing mutations have such obvious potential to induce aggregate formation. Moreover, many patients with neurodegenerative diseases do not carry any known disease-causing mutation. This suggests a role for additional environmental factors or genetic modifiers.

In summary, neurodegenerative diseases share two unique features: specificity for a select population of neurons, and characteristic aggregates within affected brain regions. These features are critical for defining and distinguishing between the different neurodegenerative diseases.

FTLD/ALS: Two sides of a spectrum

The neurodegenerative diseases FTLD (FrontoTemporal Lobar Degeneration) and ALS (Amyotrophic Lateral Sclerosis) were originally classified as two distinct entities, due to their differing clinical presentations: patients with ALS present with motor defects, while patients with FTLD present with cognitive deficits [7, 8]. These presenting symptoms stem

directly from the type of neuron preferentially lost in disease; primarily motor neurons in ALS versus cortical neurons in FTLD.

However, several advances have led to the reclassification of FTLD and ALS as two extremes of a clinical spectrum [9]. Neurodegenerative diseases are distinguished from each other by 1) the population of neurons affected 2) the protein component of aggregates and 3) causative mutations, all of which co-segregate. In FTLD/ALS, all of these characteristics present in a spectrum in the patient population.

First, FTLD/ALS patients rarely exhibit pure motor or pure cognitive deficits. Around 50% of patients diagnosed with ALS demonstrate some degree of cognitive impairment; in 15% of patients this impairment was severe enough to meet criteria for FTLD [10]. Furthermore, clinical signs of motor disease are often seen in FTLD patients [9].

Second, the composition of aggregates in FTLD and ALS patients are very similar. Historically, FTLD was divided into two pathological subtypes: FTLD-Tau, in which aggregates are composed of tau, and FTLD-U, in which aggregates were composed of an unknown, ubiquitinated protein [11]. Similarly, while rare ALS patients with SOD1 mutations had SOD1 positive aggregates, the majority of patients had aggregates composed of an unknown ubiquitinated protein[12]. In 2006, an antibody-based screen revealed that both types of aggregates were composed of the RNA-binding protein TDP-43 [13]. Several large-scale follow up studies demonstrated that TDP-43 positive aggregates are found in the majority of ALS and FTLD-U patients [14, 15]. Moreover, a sizeable minority of both FTLD-U and ALS patients with TDP-43 negative aggregates have aggregates composed of

the related RNA-binding protein FUS [16]. However, there are still a small number of patients whose aggregates are an unknown ubiquitinated protein (<1% FTLD patients) [17].

Finally, the genetics of FTLD and ALS are closely intertwined. Many of the mutations which cause familial ALS (representing ~10% of total ALS cases) can also cause FTLD, or a neurodegenerative disease with features of both ALS and FTLD [18]. For example, a hexanucleotide repeat expansion in *C9ORF72* is the most common genetic cause of both ALS and FTLD [19]. Additionally, mutations in proteins involved in the ubiquitin-proteosome pathways, such as *UBQLN2*, *VCP*, and *CHMP2B*, can cause both FTLD and/or ALS [20-23].

There are some notable exceptions: SOD1 mutations are almost exclusively associated with ALS, and Tau mutations are primarily associated with FTLD [12, 24]. However, the similarity of genetics and aggregate composition, and the symptoms of the patient population, support the spectrum model of disease.

Therapeutic strategies for FTLD/ALS

FTLD/ALS is a fatal and rapidly-progressing neurodegenerative disease. Currently, there are few therapies which slow the progression of FTLD/ALS; most existing therapies are aimed at alleviating symptoms. One example of the former is riluzole, which is thought to mitigate glutamate excitotoxicity, a pathological adaptation seen in dying neurons [25, 26]. Unfortunately, this drug only modestly extends life by 2-3 months [25]. To develop more efficacious therapies, we need to target pathological processes which occur earlier in the disease. One such process is the accumulation of protein aggregates.

TDP-43 aggregation is a mechanism of neurotoxicity in FTLD/ALS:

One of the earliest bases for subtyping FTLD and ALS came from the protein component of aggregates. To a large degree, the identity of the ALS/FTLD- causing mutations predicts the makeup of the protein aggregates (Table 1). For example, patients with SOD1 mutations develop SOD1 aggregates, and patients with FUS mutations develop FUS aggregates [27-29]. However, TDP-43 aggregation appears to be a more general pathway.

TDP-43 mutations which increase the protein's propensity to aggregate are a rare cause of familial ALS/FTLD (~0.5% of ALS patients), suggesting TDP-43 aggregation is sufficient to cause neurotoxicity [30, 31]. However, TDP-43 aggregates are not limited to patients with TDP-43 mutations. The majority of ALS/FTLD patients have protein aggregates composed of TDP-43: ~97% of ALS patients, and ~45% of FTLD patients.

These TDP-43 aggregates are seen both in patients with disparate ALS/FTLD causing mutations (see table 1), and in patients with no known genetic cause of ALS/FTLD. The intracellular aggregates and course of disease in these patients are identical, suggesting that TDP-43 aggregation is a root cause of toxicity, and that TDP-43 aggregation can result from many different environmental and/or genetic causes.

Table 1.1: Aggregates in FTLD/ALS

Main component of Aggregates	**Prevalence in ALS**	**Associated mutations in ALS**	**Prevalence in FTLD**	**Associated mutations in FTLD**
TDP-43	97%	Sporadic; C9ORF72 VCP; CHMP2B; TDP-43; ANG; OPTN UBQLN2	45%	C9ORF72; PGRN; VCP; OPTN
FUS	<1%	FUS UBQLN2	9 %	Sporadic [32] FUS
Tau	None observed		45%	MAPT mutations
SOD1	2%	SOD1 mutations	None observed	
Unknown ubiquitinated protein				

Figure 1.1: TDP-43 aggregation in FTLD/ALS

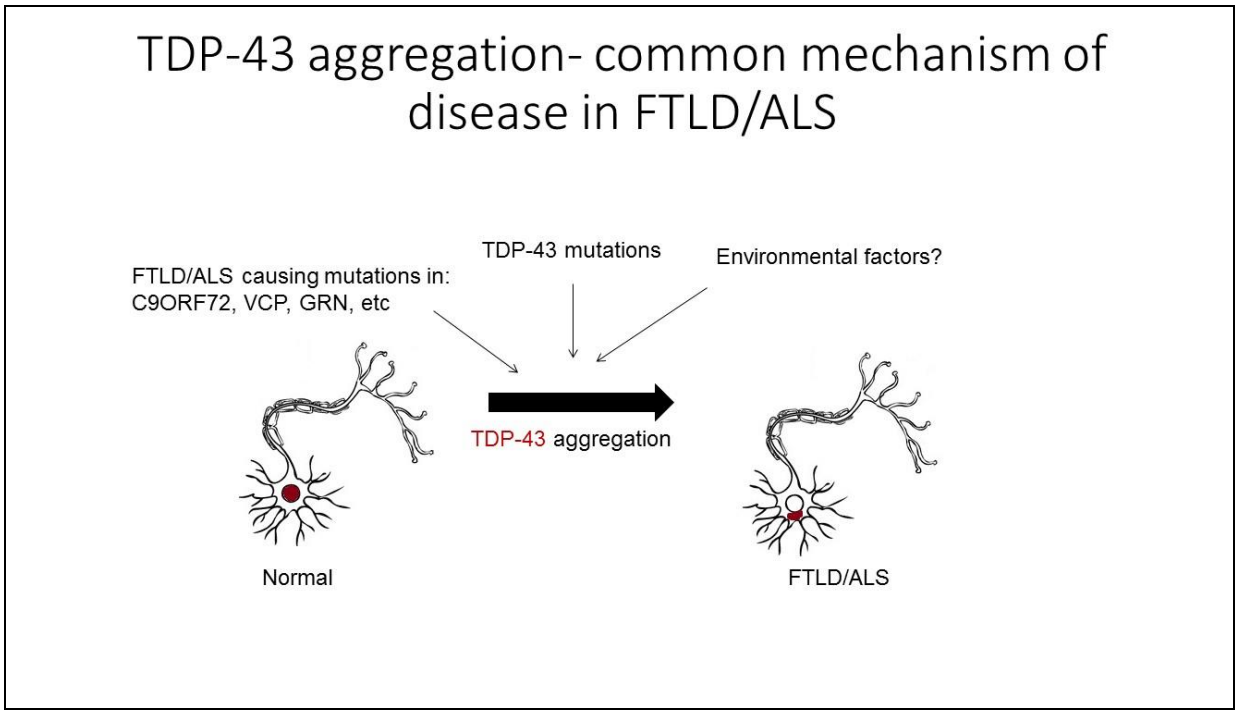

TDP-43 function:

TDP-43 is a ubiquitously expressed and highly conserved RNA-binding protein, with homologs in *C Elegans*, *D Melanogaster*, mouse, and rat [33]. Underscoring its importance, germline loss of TDP-43 is embryonic lethal for mice and causes dramatic locomotive defects in *Drosophila* [34-36]. TDP-43 overexpression is also toxic; mice overexpressing either WT human TDP-43 or WT mouse TDP-43 in the CNS have motor defects and early mortality, depending on the degree of overexpression[37-41]. In *Drosophila*, even modest amounts of overexpression cause neuronal loss [42]. Thus, cellular health requires TDP-43 expression within a very tight window. To achieve this, TDP-43 mRNA stability is autoregulated; nuclear TDP-43 protein binds the 3' UTR of TDP-43 mRNA and promotes its

degradation by enhancing the excision of the proximal poly A site [43]. This autoregulation is so robust that mice which are heterozygous for a TDP-43 null allele have same levels of TDP-43 mRNA and protein as wild-type mice [34, 36].

The tight regulation of TDP-43 suggests that it plays a critical role within the cell. However, the exact nature of this role has proved elusive. TDP-43 has long been known to influence splicing; in fact, its role in splicing was described even before its involvement in ALS. The genetic disease cystic fibrosis is caused by loss of a chloride transporter CFTR [44-46]. One of the CFTR mutations which cause cystic fibrosis is an expansion of TG repeats in exon 9, called the "T5" allele. In patients carrying the CFTR "T5" allele, TDP-43 is inappropriately recruited to CFTR mRNA, where it promotes aberrant splicing of exon 9 [47]. This aberrantly spliced mRNA encodes a nonfunctional protein [48]. The dose-dependent effect of TDP-43 on exon 9 splicing of the T5 CFTR allele is the basis for a widely-used assay to evaluate TDP-43 function. The CFTR exon 9 splicing assay uses a CFTR minigene, created by *Niksic et al*, which contains exon 9 as well as flanking sequence. This minigene generates two splicing products, and like endogenous CFTR, the ratio of the two splicing products is dependent on the dose of TDP-43 [49].

After the role of TDP-43 in ALS was uncovered, follow up studies demonstrated that TDP-43 regulation of transcriptome extended far beyond CFTR. *In vitro* studies demonstrated that RNA-binding of TDP-43 is mediated by two tandem RNA Recognition Motifs (RRMs), which preferentially bind long UG repeats. TDP-43 targets were determined *in vivo* using RIP-Seq and CLIP-seq: TDP-43 was immunoprecipitated, and the associated RNAs are sequenced. In CLIP-Seq, the interactions between TDP-43 and target RNAs were

stabilized by cross-linking, while in RIP-Seq they were not. The results of RIP-Seq of cultured rat hippocampal neurons, CLIP-Seq of mouse brain, and CLIP-Seq of human brain samples, all confirmed the *in vitro* studies: TDP-43 binds RNAs with a consensus motif of (UG)n [50-52]. Interestingly, the results of all three experimental setups also suggested that TDP-43 bound a huge number of mRNA targets (in the CLIP-Seq mouse brain study, just under a third of the mouse transcriptome), and preferentially bound introns. However, the effect of TDP-43 binding was not clear. One study attempted to address this by performing parallel RNA-Seq on mouse brain treated with either control anti-sense oligos or anti-sense oligos targeting TDP-43. There was no comprehensive fate of TDP-43 targets in the absence of TDP-43; some targets were upregulated in the absence of TDP-43, some downregulated, and some alternatively spliced [50].

However, a recent study has proposed a convincing role for TDP-43: repressing the inclusion of cryptic exons in mature mRNAs [53]. By inducing genetic deletion of TDP-43 in mouse ES cells, and taking advantage of the improvements in RNA-Seq, Ling *et al* identified multiple cryptic exons in mES cells lacking TDP-43. Notably, some of these cryptic exons were the intronic binding sites identified in earlier studies. Moreover, de-repression of cryptic exons contributed to the toxicity of TDP-43 deletion; the toxicity of TDP-43 knockout was partially rescued with expression of a TDP-43 fusion protein in which the C-terminus was replaced by a repressor. To date, of all functions which have been ascribed to TDP-43, repression of cryptic exons is the best described and understood.

TDP-43 has also been proposed to play a number of other roles within the cell. For example, TDP-43 was first identified as a protein which bound regulatory sequences in HIV

DNA, repressing HIV-1 gene expression [54]. TDP-43 has also been shown to bind DNA and repress transcription of *acrv*1, a testes-specific mouse gene [55]. TDP-43 has been shown to directly bind RNA granules in the cytosol, and enhance the transport of one of its target mRNAs, Nefl, down the axon [56]. However, whether these roles for TDP-43 generalize beyond these few described substrates is unclear. TDP-43 is also recruited into stress granules, although it is not required for stress granule formation [57].

A critical question for the field is which, if any, of these functions are directly disrupted by ALS/FTLD causing mutations. Around 30 ALS/FTLD-causing mutations in TDP-43 have been documented (http://www.molgen.ua.ac.be/FTDMutations/). With very few exceptions, these are all point mutations in the C-terminus of the protein. This region is glycine-rich and unstructured, with some homology to fungal prion proteins. The C-terminus is required for TDP-43 to be recruited into stress granules, and is required for recruitment many of TDP-43's protein partners: hnRNP A2/B1, hnRNP A1, and FUS [58-60]. Interestingly, some ALS/FTLD-causing mutations do increase association between TDP-43 and FUS [59], and some mutations have a small effect on stress granule dynamics [60]. Whether this plays a role in disease is still unknown.

The C-terminus is also required for TDP-43's effect on CFTR exon 9 skipping, and likely other splicing events [58]. None of the ALS/FTLD mutations tested disrupt exon 9 skipping [61]. However, transgenic mice expressing TDP-43 Q331K (ALS-linked mutant) do show aberrant splicing of some TDP-43 targets [62]. Arnold *et al* postulated that these aberrant splicing events were in part responsible for the toxicity seen in transgenic mice.

However, the best-supported hypothesis for the toxicity of ALS/FTLD-linked TDP-43 mutations is that they promote TDP-43 aggregation. All patients with TDP-43 mutations have TDP-43 aggregates. With few exceptions, ALS/FTLD-linked mutations are in the C-terminus, a very aggregation prone region of TDP-43 [31]. Moreover, many of the ALS/FTLD causing mutations have been demonstrated to directly increase aggregation propensity [31, 63] or increase the half-life of TDP-43 [59, 61].

TDP-43 aggregation and mislocalization are linked in ALS/FTLD

The discovery that TDP-43 is the primary component of ALS/FTLD ubiquitin-positive aggregates led to another observation: neurons containing TDP-43 aggregates also have a dramatic redistribution of TDP-43. In neurons that did not contain aggregates, as well as those in unaffected controls, TDP-43 was highly expressed and predominantly nuclear. However, neurons with TDP-43 aggregates had dramatically depleted nuclear TDP-43 [13]. Additionally, there is evidence that ALS/FTLD patients have loss of functional TDP-43 in affected brain regions; post-mortem brain tissue from ALS/FTLD patients demonstrate high rates of inclusion of cryptic exons [53]. In light of the critical role TDP-43 plays regulating the transcriptome, this raised an important question: how much of the neurotoxicity seen with TDP-43 aggregates is a direct result of the aggregate, and how much is due to the secondary loss-of-function?

However, this question has proven very difficult to answer, because TDP-43 aggregation and nuclear depletion are mechanistically linked; in cell culture, TDP-43 aggregates deplete nuclear TDP-43 within 72 hours [64]. Depletion of cytosolic TDP-43 is expected, because once a TDP-43 aggregate forms remaining soluble protein is rapidly

incorporated into it [31]. But how can an aggregate in the cytosol deplete soluble protein in the nucleus? TDP-43, although predominantly nuclear, is constantly shuttling to and from the cytosol [65]. Thus, the pool of soluble cytosolic TDP-43 is in dynamic equilibrium with the pool of soluble nuclear TDP-43. So, over time all soluble TDP-43 – both cytosolic and nuclear – is predicted to incorporate into the aggregate. Notably, the rate of nuclear depletion should be limited by the nuclear export of TDP-43. Because depletion of nuclear TDP-43 likely plays a role in the toxicity of TDP-43 aggregates, it is critical to understand the determinants of TDP-43 shuttling and localization.

TDP-43 shuttling and localization:

Like many other proteins within the hnRNP family, TDP-43 is an RNA-binding protein which is predominantly nuclear, but constantly shuttling to and from the cytosol [65]. While TDP-43 mutations which affect its RNA binding, dimerization, and protein partners have subtle effects on TDP-43 localization, the major determinants of TDP-43 localization are its nuclear import and nuclear export [65].

The nucleus is a membrane bound organelle, so all traffic between the nucleus and cytosol is restricted to the nuclear pores [66]. Nuclear pores are large multi-protein complexes which span both nuclear membranes and form a semipermeable barrier: small proteins, ions, and water can diffuse through freely, while larger molecules can only efficiently pass through with the aid of a karyopherin [67, 68]. Early studies of nuclear pores suggested a hard size cutoff of 40 kDa for diffusion through nuclear pores[69]. However, recent work suggests a soft ceiling to diffusion: even very large proteins (~130 kDa) can still diffuse through the nuclear pore, although efficiency decreases as size increases [70, 71].

Active transport through the nuclear pore is mediated by the karyopherin family of proteins. These can either selectively import proteins (from the cytosol to the nucleus), selectively export proteins (from the nucleus to the cytosol), or both. The cargoes of karyopherins are designated by small peptide sequences, called "Nuclear Localization Signals" (NLS) if they mediate import or "Nuclear Export Signals" (NES) if they mediate export; NLSs and NESs are directly recognized by a karyopherin [72]. NLSs and NESs must be solvent accessible to recruit a karyopherin, so they are usually within an unstructured domain[73]. Directionality of nuclear transport is conferred by the small G-protein Ran, which is GTP bound in the nucleus and GDP bound in the cytosol [74, 75]. Importins only bind cargo in the absence of Ran GTP, whereas exportins only bind cargo in the presence of Ran GTP[75].

Nuclear import of TDP-43 has been shown to be mediated by importin α (KPNA) binding to a nuclear localization signal (NLS) in the N-terminus of TDP-43. Knockdown of its protein partner, importin β1 (KPNB), results in cytosolic TDP-43 accumulation [76]. Culturing tBN2 cells -- a cell line with a temperature sensitive Ran gradient (temperature sensitive RCC1, Ran GEF) -- at the restrictive temperature also results in cytosolic TDP-43 accumulation [64]. Moreover, TDP-43 mutations in the NLS – lysine/arginine to alanine – also result in cytosolic accumulation [64]. Finally, TDP-43 directly binds importin α (KPNA) [76].

TDP-43 export has been less well characterized. In general, nuclear export is far less understood than nuclear import. While there are seven known exportins, an NES consensus sequence has only been described for XPO1[72, 77]. This consensus sequence is extremely

loose; consisting mainly of regularly interspersed hydrophobic residues [78]. Thus, discovering NESs based on sequence alone is fraught; the literature is filled with examples of NESs, identified based on sequence alone, which were later discovered to play no role in export [78]. One helpful rule of thumb is to take into account secondary structure as well as sequence; a true NES is more likely to be solvent exposed and relatively unstructured [79].

Figure 1.2: Domain map of TDP-43

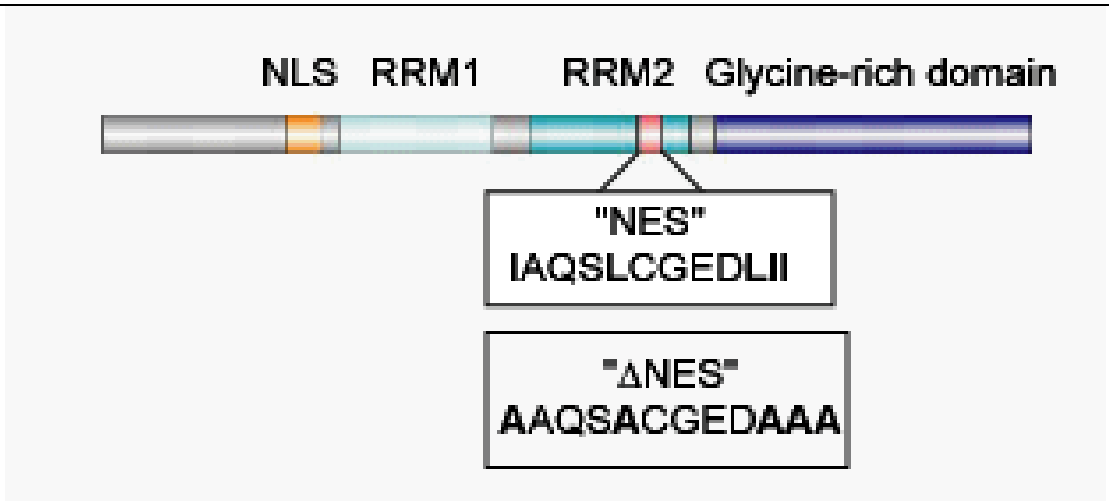

The putative NES which mediates TDP-43 export was first identified based on homology to the consensus sequence : ϕ - $X_{2,3}$ - ϕ - $X_{2,3}$ -ϕ - X - ϕ, where ϕ is a hydrophobic amino acid – Met, Val, Leu, or Ile – and X is any amino acid . However, even on the surface this NES seemed problematic. First, it is not predicted to bind XPO1 very well; one critical component of an NES is the spacing between the last two hydrophobic residues. The putative NES in TDP-43 does not maintain this spacing; it ends in LII, ϕ - ϕ - ϕ rather than ϕ - X - ϕ. Second, even if the sequence were capable of recruiting XPO1, it is not predicted to be solvent exposed. The NES is within a well-folded domain, RRM2; moreover, in an NMR

solution structure of RRM1-RRM2, the hydrophobic residues predicted to directly bind XPO1 are instead buried in RRM2 [80].

This problematic NES was also not well-supported by experimental data. The only supporting evidence that the putative NES mediated export was that TDP-43 putative NES mutants – leucine/isoleucine to alanine – aggregate in the nucleus [64]. This was interpreted as evidence that TDP-43 was accumulating in the nucleus. However, given the structural data, a more likely explanation is that these mutations disrupt the core of RRM2, making it more aggregation prone. The effect of these mutations on nuclear export itself was never assessed.

Finally, the role of XPO1 in TDP-43 nuclear export was not well-supported. Treatment of cells with a potent XPO1 inhibitor, leptomycin B, led to the formation of nuclear TDP-43 aggregates [64]. Again, this was interpreted as evidence that LMB inhibited TDP-43 nuclear export, and the effect of XPO1 inhibition on TDP-43 nuclear export was never directly assessed. Notably, XPO1 inhibitors are tolerated fairly well, and are in preclinical trials for some cancers and inflammatory diseases [81, 82]. Thus, if XPO1 inhibitors block nuclear export of TDP-43, they may have some therapeutic benefit for ALS/FTLD patients.

In summary, despite the importance of TDP-43 nucleocytoplasmic shuttling for both understanding the pathogenesis of, and potentially treating, ALS/FTLD, only nuclear import has been satisfactorily described.

Causes of TDP-43 aggregation and mislocalization in ALS/FTLD

The aggregation and mislocalization of TDP-43 is thought to play a causal role in ALS for several reasons. First, point mutations in the C-terminus of TDP-43, which enhance aggregation of the protein, are a rare cause of familial ALS/FTLD [30]. Second, TDP-43 aggregates are seen in the vast majority of ALS patients (~97%) and a plurality of FTLD patients (~45%). Third, animal models which replicate the ALS-linked redistribution of TDP-43 in motor neurons -- through overexpression of a cytosol- restricted TDP-43 mutant, an ALS-linked TDP-43 mutant, or an aggregation prone TDP-43 truncation mutant-- demonstrate the progressive muscle weakness and loss of spinal cord mass seen in patients [83-85].

There are parallels with other proteins in the hnRNP family. For example, FUS is also genetically linked to ALS/FTLD [28]. Moreover, in unstressed cells without aggregates, FUS is predominantly nuclear and continuously shutting; in a cell with a FUS aggregate, soluble FUS is depleted from the nucleus [16]. Two types of FUS mutations cause ALS/FTLD. The first are point mutations in its C-terminus which, like C-terminal TDP-43 mutations, increase propensity of FUS to aggregate [86]. The second type are point mutations within FUS NLS (Nuclear Localization Signal) which disrupt nuclear import [87]. Although no NLS mutations in TDP-43 have been found in ALS/FTLD patients, animal models which express TDP-43ΔNLS develop neuron loss and motor spasticity similar to ALS/FTLD patients [83, 84].

The cellular insults that promote TDP-43 aggregation and redistribution are incompletely understood. The C-terminal TDP-43 point mutations that cause familial

ALS/FTLD have been demonstrated to increase its aggregation propensity, both *in vitro* and *in vivo* [31, 63]. But the majority of ALS/FTLD patients with TDP-43 aggregation and redistribution do not have TDP-43 mutations. While many genetic causes of ALS/FTLD with TDP-43 aggregation have been described -- *C9ORF72* repeat expansions, loss-of function mutations in *OPTN* (optineurin), *VCP* (Valosin-containing Protein), and *GRN* (progranulin) – whether these mutations directly affect TDP-43 localization and aggregation is still unknown.

Progranulin mutations in FTLD/ALS

Progranulin is a cysteine-rich secreted protein linked to neurodegenerative disease [88]. Progranulin secretion is canonical: the extreme N-terminus encodes a signal sequence, which recruits the trafficking factor Signal Recognition Particle (SRP) during translation [89]. When SRP binds its receptor on the ER membrane, the associate ribosome-nascent chain complex docks onto the ER membrane, and progranulin is translated into the ER lumen. From the ER lumen, progranulin trafficks to the Golgi, then a secretory vesicle, and is eventually secreted outside of the cell [90]. During this process, progranulin is extensively modified: in the ER, the signal sequence is cleaved by signal peptidase, cysteines are reduced to form disulfide bonds, and the protein is N-glycosylated [89, 91]. Progranulin is further modified in the extracellular fluid. Unusually, progranulin is composed of 7.5 repeats of the ~60 amino acid granulin domain [92]. Once in the extracellular fluid, progranulin is cleaved by nonspecific proteases to release different granulins [93-97], which have distinct biological functions [98-102].

Progranulin is genetically linked to two neurodegenerative diseases: ALS/FTLD and neuronal ceroid lipofuscinosis (NCL). A loss of function (LOF) mutation in one copy of *GRN* causes ALS/FTLD with TDP-43 aggregates, while a LOF mutation in both copies of *GRN* causes NCL, a multigenic lysosomal storage disease which causes neurodegeneration in childhood [88, 103, 104]. Most LOF *GRN* mutations are either nonsense mutations or frameshifts which result in a premature termination codon and trigger nonsense-mediated decay (http://www.molgen.ua.ac.be/FTDMutations/). However, missense mutations have also been described: A9D, which is in the signal sequence, disrupts secretion, and C139R and C521Y disrupt disulfide bonds [105, 106].

As expected, patients with two LOF mutations have undetectable levels of plasma progranulin, while those carrying a single LOF mutation have markedly decreased progranulin levels, ~50% reduced compared to unaffected patients [107, 108]. Notably, FTLD/ALS patients who do not carry progranulin mutations have the same level of secreted progranulin as unaffected controls, suggesting progranulin deficiency is not a common mechanism of disease [107].

NCL patients accumulate characteristic intracellular deposits of lipofuscin, a residue of lysosomal digestion, and suffer from neurological symptoms such as seizure, ataxia, and cognitive dysfunction. Interestingly, FTLD/ALS patients with GRN mutations share some clinicopathological features of NCL, such as retinal degeneration and lipofuscin accumulation [109]. Moreover, lysosomal function is impaired in fibroblasts from GRN mutation carriers [109].

The link between progranulin haploinsufficiency and lysosomal dysfunction suggests a mechanism by which GRN mutations might predispose ALS/FTLD patients towards TDP-43 aggregates. However, there is no direct evidence that lysosomes play a role in preventing accumulation of TDP-43 aggregates.

A force opposing aggregation: Protein Quality Control

In the neurodegenerative field, the question of why affected neurons accumulate protein aggregates has attracted a great deal of time and money. However, an equally fundamental question is: Why don't all cells accumulate protein aggregates? After all, protein synthesis and folding are imperfect; and mutant and/or misfolded proteins are prone to display hydrophobic surfaces and thus aggregate. In response to the threat posed by aggregated proteins, cells have evolved quality control pathways to protect against accumulation of aberrant proteins. These pathways fall into two broad categories: pathways which find and degrade misfolded, mislocalized, or aggregated proteins, and pathways which attempt to prevent the formation of these species.

Quality control pathways which attempt to prevent formation of misfolded proteins center on the ribosome and translation. The mechanics of translation can help to identify an aberrant mRNA: for example, stem-loop structures or a truncated mRNA may lead to stalling and subsequent degradation. It is also increasingly being recognized that aberrant proteins can be recognized during translation. For example, translation of a poly-lysine tract leads to charge buildup inside ribosome, triggering quality control. More subtly, nascent chains which are not recruiting their normal trafficking factors can also be recognized as aberrant.

I will discuss the major characteristics of the quality control pathways centered on the ribosome, or ribosome QC: Nonsense-mediated decay, No-Go decay, NonStop Decay, and Regulation of Aberrant Protein Production. For each pathway, I will discuss the defect sensed, the known machinery, and the fate of the mRNA and nascent chain. Finally, I will discuss the role of these pathways in human disease.

Nonsense mediated Decay

NMD machinery and Defect sensed: Nonsense Mediated Decay (NMD) is triggered by an mRNA with a termination codon in a suboptimal context, called a premature termination codon. How a premature termination codon is distinguished from a normal termination codon is still an area of active study. However, two features predispose a termination codon to be recognized as a PTC: 1) a long 3' UTR or 2) a downstream exon-exon junction (>50 nucleotides) [110].

The RNA helicase Upf1 (Up Frameshift 1) is a master regulator of NMD; in both yeast and mammalian cells, it is absolutely required for degradation of mRNAs with PTCs [111-113]. Upf1 binding is stochastic and not specific for NMD targets; however, on mRNAs without a PTC, Upf1 binding does not initiate mRNA decay [110, 114-117]. In order to initiate NMD, Upf1 must directly contact eRF3 (eukaryotic release factor 3) on the terminating ribosome [118, 119]. This recruits the kinase SMG1 (Suppressor with morphological effect on genitalia 1), which phosphorylates Upf1 [118, 120]. Phosphorylated Upf1 acts as a tag for target mRNAs; it recruits SMG5-SMG7, a heterodimer which dephosphorylates Upf1 and directs the mRNA to p-bodies for degradation [121, 122].

Certain features of a normal mRNA antagonize the interaction between eRF3 and Upf1, which is required for NMD activation. First, there is evidence that translation termination at a normal termination codon is more efficient than at a PTC [123]. Efficient termination reduces the probability of a stochastic Upf1 binding in proximity to a terminating ribosome. Second, if poly A binding protein (PABP) is in close proximity to a termination codon, it suppresses NMD by interacting with eRF3 directly and shielding it from Upf1 [124, 125]. Surprisingly, the suppressive effect of PABP on NMD requires eukaryotic initiation factor 4G (eIF4G) [126, 127]. This has led to the model that a mature cytoplasmic mRNA is in a closed-loop conformation -- with the 5' cap and poly-A tail in close proximity -- which is resistant to NMD [128]. Conversely, in an mRNA with a very long 3'UTR (as might be seen with a PTC), the spatial orientation of the termination codon, the 5' cap, and the poly A tail may not be conducive to assuming the closed conformation.

Just as NMD can be inhibited by the closed conformation of a normal mRNA, it can be stimulated by an exon junction complex (EJC) downstream of a termination codon. The EJC is deposited approximately 24 nucleotides upstream of an exon-exon junction [129]. EJCs in the cytosol are bound by Upf2 and Upf3, but Upf2/3 are thought to be displaced during the pioneer round of translation. However, a translating ribosome will not displace Upf2/Upf3 if the EJC is far enough downstream of the termination codon. Experimental data suggests this limit is~30 nucleotides; if an exon-exon junction is >~50 nucleotides downstream of a termination codon, NMD is initiated [130, 131]

Fate of the mRNA: Upf1 phosphorylation appears to be the critical signaling event which triggers mRNA degradation. Phosphorylated Upf1 can recruit many degradation factors so

degradation can proceed along several different paths, depending on the substrate. Degradation can be initiated by endonucleolytic cleavage, by de-adenylation of the poly-A tail, or by decapping [132-138]

Fate of the protein: In yeast, the protein product of NMD is subject to proteosome dependent degradation, which is stimulated by Upf1 [139]. However, in humans, there does not appear to be a common fate for a nascent chain associated with Upf1; some of these truncated proteins can be detected in mammalian cells, while others cannot [140].

Fate of the ribosome: The fate of the ribosome translating an NMD substrate is still unclear.

No-Go Decay and Non-Stop Decay:

Machinery and Defect sensed: Both No-Go decay (NGD) and Non-Stop decay (NSD) are primarily ribosome-rescue pathways. In canonical translation, a ribosome is released from an mRNA once it reaches a termination codon; termination codons recruit the release factors eRF1/eRF3, which cleave the tRNA from the nascent chain and promote ribosome disassembly [141]. However, in the case of a truncated mRNA with no stop codon (NSD), or an mRNA with secondary structure that prevents ribosome translocation, such as a stem loop (NGD), an alternative pathway to disassemble the ribosome is required. Without ribosome rescue, ribosomes become trapped in non-productive complexes [142]. NGD and NSD rescue ribosomes from non-productive complexes: they recruit factors to disassemble the ribosome, degrade the mRNA, and ubiquitinate and degrade the nascent chain.

Both NGD and NSD rely on Dom 34 (Pelota in mammals) and Hbs1 for initial recognition of a "trapped" ribosome [143]. Cryo-EM structures of Pelota/Hbs1 on the ribosome provide a rationale for their recruitment in NSD. In both elongation and

termination, the occupant of the "A" site of the ribosome depends on the codon in the mRNA channel of the "A" site; in elongation, an aminoacyl tRNA with the correct anticodon, and in termination, the release factor eRF1, which recognizes a termination codon (reviewed in [144]). Pelota is homologous to eRF1, but contains a loop which extends deep into mRNA channel of the "A" site [145]. This explains why Hbs1/Pelota would be preferentially recruited in the case of NSD, where the mRNA channel of the "A" site does not contain a codon. This also fits with *in vitro* data suggesting Dom34/Hbs1 preferentially bind ribosomes with a short 3' end [146].

However, how Pelota/Hbs1 is recruited in NGD, when there is a codon in the mRNA channel of the "A" site, is less clear. Structures of stalled No-Go complexes isolated from a cell-free translation system, and structures of reconstituted complexes demonstrate that Pelota/Hbs1 do bind ribosomes with mRNA in the "A" site [145, 147]. Both structures showed poor density in mRNA channel, suggesting that Pelota binding may actively re-position the mRNA [145, 147]. In the case of the reconstituted complexes, a high degree of complex was formed, making it more likely that Pelota/Hbs1 binding promoted re-positioning, rather preferentially binding a subpopulation of ribosomes in which mRNA was displaced [145]. This re-positioning is likely necessary for downstream NGD events.

This presents a difficulty in understanding how Pelota/Hbs1 recognize ribosomes in need of "rescue". In the case of NSD, a vacancy in the mRNA channel of the "A" site allows for substrate recognition. If, in NGD, as the data suggests, Pelota binding is a cause, rather than a result, of the vacant mRNA channel of the "A" site, then how is an NGD substrate recognized?

One helpful piece of evidence is the various substrates which undergo NGD. The first described NGD substrate was an mRNA containing a stable stem loop, sufficient to overwhelm the helicase activity of the ribosome [148] [149]. While substrates like this have a codon in the mRNA channel of the "A" site, one might imagine that due to the tension on the mRNA, the codon might not be optimally positioned to recruit its cognate aminoacyl tRNA. An additional NGD substrate is mRNAs containing codons for which the cognate tRNAs are rare, or have been depleted or mutated [149-151]. Again, in these cases the cognate aminoacyl tRNA is inefficiently recruited. Together, these suggest a competition for the "A" site of the ribosome between eRF1, aminoacyl tRNAs, and Pelota. If the mRNA channel of the "A" site contains a termination codon, eRF1 is preferentially recruited; if the mRNA channel contains another codon, the cognate aminoacylated tRNA is preferentially recruited; if the mRNA channel is empty, Pelota is preferentially recruited. However, Pelota can be recruited even when the "A" site contains mRNA, if neither aminoacyl tRNA nor eRF1 are efficiently recruited. Fitting with this model, yeast treated with the Histidine biosynthesis inhibitor 3-AT (3-amino-1, 2, 4-triazole) show widespread ribosome pausing at His codons, and this is not exacerbated in the ΔDom34 strain[152]. These ribosomes, which we would expect contain deacylated $tRNA^{His}$ in the "A" site, are not recognized as NGD substrates. This suggests that ribosome pausing does not promote NGD, as long as the "A" site is not available for Pelota binding

If the occupancy of the "A" site is truly the signal for an NGD substrate, than the kinetics of Pelota binding an "A" site containing mRNA are probably critical to distinguishing between a physiologic translational pause and a translational stall.

Translational stalls often occur to aid in folding of the nascent chain, or recruitment of co-translational binding partners. For example, there is evidence that a translational "slow-down" is required for a secretory protein to recruit the targeting factor SRP (Signal Recognition Particle)[153]. This slow-down, which is mediated by a stretch of sub-optimal codons, does not appear to trigger NGD.

Fate of mRNA: In both NSD and NGD, mRNA degradation requires an initial recognition of the stalled ribosome by Pelota/Hbs1 [143]. In NSD, the mechanism of mRNA decay varies between yeast and mammalian cells, and has not been completely elucidated in the latter. In yeast, it requires Ski7, a component of the exosome which is not conserved in mammals [154, 155]. In mammals, the exosome also participates in mRNA decay; Ski2, Mtr4 and Dis3 are all required for efficient degradation of a non-stop reporter mRNA in mammalian cells [156].

In NGD, Pelota/Hbs1 stimulate an initial endonucleolytic cleavage and disassembly of the ribosome [143]. The re-positioning of mRNA by Pelota is likely crucial for this. The identity of the endonuclease is still unknown. Although Dom34/Pelota was proposed to have endonucleolytic activity, this activity was not required for NGD, suggesting it does not act as the endonuclease[157]. After the initial cleavage of the mRNA, 5' and 3' fragments are degraded by the exosome and Xrn1, respectively[149].

Fate of the ribosome: In both NSD and NGD, the ribosome is dissociated into its component 40S and 60S subunits. Once Pelota has been accommodated in the "A"site, Hbs1 hydrolyzes GTP, which promotes a conformational shift in Pelota. This triggers dissociation of Hbs1 from and recruitment of ABCE1, a member of the ATP Binding cassette (ABC) family of

proteins [146]. The power stroke of ABCE1 leads to dissociation of the ribosome into 60 S and 40 S subunits [158]. However, in *in vitro* studies this dissociation can only occur if the mRNA downstream of the "P" site is less than 9 nucleotides [143]. This is strong evidence for an ordered model of NGD, where the first event is Pelota/Hbs1 binding, which re-positions mRNA, followed by mRNA cleavage, followed by dissociation of the ribosomal subunits. This ordered model of NGD also suggests a convergence of NGD and NSD after mRNA cleavage.

Fate of the nascent chain: In the case of normal termination, the peptidyl-tRNA is cleaved and the peptide is released [144]. In contrast, in ribosome recycling initiated by Pelota – an eRF1 homologue which doesn't contain the GGQ motif required to cleave peptidyl-tRNA – the peptide is not released [144]. In the case of a very small peptide, dissociation of the ribosome leads to release of the intact peptidyl-tRNA into solution [143]. However, a larger peptide will remain trapped on the 60S ribosome.

A peptide is not trapped on the 60S ribosome as a consequence of normal termination, so this peptide is recognized as aberrant, and ubiquitinated and degraded [159]. The trapped peptide is recognized by an E3 ubiquitin ligase Ltn1, which preferentially binds and ubiquitinates nascent chains associated with a 60S, but not an intact 80S, ribosome. In fact, use of a GTPase deficient Hbs1, which traps the stalled 80S complex, precludes nascent chain ubiquitination [159].

Regulation of Aberrant Protein Production

Machinery and Defect sensed: Unlike NMD, NGD, and NSD, which are primarily triggered by an aberrant mRNA, Regulation of Aberrant Protein Production, or RAPP, is triggered by

an aberrant nascent chain. Specifically, RAPP recognizes a nascent chain which fails to recruit normal co-translational binding partners and triggers specific degradation of the translating mRNA. To date, RAPP has only been demonstrated in the special case of ra translating secretory protein which fails to recruit the targeting factor SRP (Signal Recognition Particle) [160]. However, this may generalize to other co-translational interactions.

RAPP is the most newly discovered ribosome QC pathway, and consequently very little mechanistic detail is known. However, RAPP is clearly distinct from the other described QC pathways. First, RAPP is triggered by the nascent chain sequence rather than the mRNA sequence; frameshift mutations in a secretory mRNA demonstrated that (-1) and (-2) mutants, which had protein sequences drastically different from WT, were subject to degradation, while the (-3) mutant was protected. Second, RAPP is clearly triggered by loss of a co-translational interaction with the nascent chain; mutant secretory proteins which abolished SRP binding were subject to degradation. Moreover, SRP knockdown led to degradation of a majority of secretory and membrane protein mRNAs (unpublished results). Finally, the machinery of RAPP, while still largely unknown, is clearly distinct from the other pathways. RAPP does not require Upf1 (required for NMD) or Pelota (required for NSD/NGD) [160].

The only protein found to play a role in RAPP is Argonaute 2 (Ago2), studied in the context of the model secretory protein preprolactin (PPL). Ago2 plays a role in RNA silencing, but has not before been linked to protein quality control [161]. When in vitro

cross-linking was performed with a range of PPL mutants with mutations of varying severity (ΔL, Δ2L, Δ3L, and Δ4L), SRP crosslinking was inversely proportional to Ago2 cross-linking. Moreover, an Ago2 immunoprecipitation pulled down preferentially Δ4L PPL mRNA and not WT PPL mRNA. Additionally, Ago2 overexpression and knockdown affected PPL mRNA levels, although this could be explained by an effect on transcription rather than mRNA turnover [160].

Fate of mRNA: The mRNAs targeted by RAPP are selectively degraded. However, the mechanism by which they are degraded is not well understood. There is some evidence that mRNA degradation is initiated by an endonucleolytic cleavage; the RAPP substrate PPL Δ4L mRNA is associated with monosomes, while WT PPL mRNA is associated with polysomes (our unpublished work). No endonuclease has been identified as cleaving RAPP substrates.

Fate of nascent chain: No full-length mutant protein is observed, suggesting that mutant nascent chains are degraded, but no details are known [160].

Quality control in genetic diseases:

A subset of genetic diseases are caused by loss of a critical protein. One common mechanism for loss-of-function (LOF) mutations is the triggering of quality control pathways which eliminate the mutant protein. For example, many nonsense mutations trigger NMD, resulting in degradation of mutant protein; ~30% of mutations which cause a genetic disease introduce PTCs [162]. Some examples include nonsense mutations in CFTR, which cause

cystic fibrosis; nonsense mutations in dystrophin, which cause muscular dystrophy; and nonsense mutations in SOX10, which cause Waardenburg syndrome type 4C [163-165].

However, mutations can also trigger other ribosome QC pathways. For example, missense mutations of a stop-codon would be predicted to trigger NSD. In fact, there are several disease causing mutations of stop codons, reviewed in Klauer et al [166]

Similarly, point mutations within the signal sequences of critical secretory proteins might trigger RAPP, leading to a LOF genetic disease. A handful of genetic diseases caused by signal sequence point mutations can be found in the literature (see table).

Table 1.2: Human diseases associated with signal sequence mutations

Disease	Gene	Signal sequence mutation	Citation
Familial isolated hypoparathyroidism	PTH	C18R	[167]
Crigler-Najjar type II	UGT1A1	L15R	[168]
Dentine dysplasia type II	DSPP	Y6D	[169]
FrontoTemporal Lobar Degeneration	GRN	A9D	[106]
Ehlers-Danlos syndrome	COL5A1	L25R L25P	[170]
Early-onset Type II diabetes	POMC	A15G	[171]

CHAPTER TWO

ACTIVE NUCLEAR IMPORT AND PASSIVE NUCLEAR EXPORT ARE THE PRIMARY DETERMINANTS OF TDP-43 LOCALIZATION

Abstract

ALS (Amyotrophic Lateral Sclerosis) is a neurodegenerative disease characterized by the redistribution of the RNA binding protein TDP-43 in affected neurons: from predominantly nuclear to aggregated in the cytosol. However, the determinants of TDP-43 localization, and the cellular insults which promote redistribution, are largely unknown. Here, we demonstrate that the putative Nuclear Export Signal (NES) is neither necessary nor sufficient for nuclear export. Moreover, the "ΔNES" mutant disrupts hydrophobic residues in the core of an RNA-binding domain, disrupting solubility and function. Furthermore, nuclear export of TDP-43 is independent of XPO1, the exportin with the broadest substrate specificity. Interestingly, TDP-43 with a large tag (tdTomato), unlike TDP-43 with a small tag (Flag), is unable to accumulate in the nucleus in the absence of active nuclear import. Moreover, nuclear export of TdtTomato-TDP-43 is significantly retarded compared to Flag-TDP-43. Together, these suggest that nuclear export of TDP-43 is predominantly driven by passive diffusion.

Introduction

Amyotrophic Lateral Sclerosis (ALS) is an adult-onset neurodegenerative disease which preferentially targets motor neurons, causing muscle weakness and eventually paralysis[172]. ALS is rapidly progressive and ultimately fatal[172]. While the mechanisms underlying the degeneration of motor neurons remain unclear, the RNA-binding protein TDP-43 has emerged as a key player in ALS pathogenesis.

TDP-43 is ubiquitously expressed and highly conserved, with homologs in *C Elegans, D Melanogaster*, mouse, and rat [33]. Underscoring its importance, germline loss of TDP-43 is embryonic lethal for mice and causes dramatic locomotive defects in *Drosophila* [34-36]. Many functions have been ascribed to TDP-43, but the best described is its role in splicing, especially in repressing inclusion of cryptic exons [48, 50-53].

Multiple lines of evidence implicate TDP-43 aggregation in the pathogenesis of ALS. First, the characteristic histopathology of ALS: affected neurons contain cytosolic protein aggregates which are composed of ubiquitinated TDP-43, with only rare exceptions [13, 14]. Notably, TDP-43 aggregation is accompanied by loss of soluble TDP-43 from the nucleus[13]. Second, point mutations in TDP-43 are a rare cause of familial ALS, and many of these mutations have been demonstrated to increase the propensity of TDP-43 to aggregate [30, 31]. Finally, animal models which replicate the ALS-linked aggregation and redistribution of TDP-43 in motor neurons -- through overexpression of a cytosol- restricted TDP-43 mutant, an ALS-linked TDP-43 mutant, or an aggregation prone TDP-43 truncation mutant-- demonstrate the progressive muscle weakness and loss of spinal cord mass seen in patients [83, 85].

Given the importance of TDP-43 localization in ALS, we sought to understand the determinants of normal TDP-43 trafficking. TDP-43 is predominantly nuclear, but constantly shuttling to and from the cytosol [65]. While TDP-43 mutations which affect its RNA binding, dimerization, and protein interactions have subtle effects on TDP-43 localization, the major determinants of TDP-43 localization are its nuclear import and nuclear export [65]. TDP-43 nuclear import is mediated by importin α, which binds to a canonical K/R nuclear localization signal (NLS) in the N-terminus of TDP-43 (Fig 1A) [64, 76]. Nuclear export of TDP-43 has been proposed to be mediated by XPO1, the exportin with the broadest substrate specificity, through direct binding to a nuclear export signal (NES) within RRM2 [64]. However, there is little experimental evidence to support this mechanism.

Here, we demonstrate that TDP-43 nuclear export is not mediated through the putative NES in RRM2. Our structural analysis demonstrates that the putative NES is not predicted to be solvent exposed, and therefore would not be available to recruit XPO1. Moreover, XPO1 binding assays demonstrate that even the exposed putative NES has low affinity for XPO1. Finally, *in vivo* assays demonstrate that the RRM2 (which contains the putative NES) is neither sufficient nor necessary for nuclear export of TDP-43. TDP-43 localization is further shown to be XPO1 independent, both in cultured HeLa cells and cultured primary hippocampal neurons. However, the fusion of a large (tdTomato) but not a small (flag) tag to TDP-43 is sufficient to significantly retard nuclear export. Together, these data support a model where TDP-43 nuclear export is largely diffusion driven.

Results

The putative NES within RRM2 is not predicted to be solvent exposed, and when accessible is incompetent to recruit XPO1

XPO1 recognizes its cargo by directly binding a short peptide sequences, termed Nuclear Export Signal (NES). XPO1 can bind a wide variety of peptide sequences in either a (+) or (-) orientation, thus the consensus sequence is very loosely defined by regularly interspersed hydrophobic residues [173]. As a result of this very loose consensus sequence, it is difficult to predict an NES based on sequence alone; predictions should take structural data into account, and must be experimentally verified.

The putative NES within TDP-43 , "IAQSLCGEDLII" only poorly fits the consensus sequence, as there are no spacers between the last three hydrophobic residues[173]. Moreover, unlike most NESs which are within unstructured domains, the putative NES in TDP-43 is within a well-folded domain, an RNA Recognition Motif (RRM) (Fig 2.1a) [64, 78].

As a rough guide to whether this proposed NES might bind XPO1, we analyzed a published NMR solution structure of the RNA binding domain (RRM1-linker-RRM2), (Fig 2.1b). The hydrophobic residues comprising the putative NES – which normally bind the NES groove of XPO1-- are mostly hidden in a surface representation of the RNA binding domain (Fig 2.1b)[80, 173]. In fact, calculating the solvent accessibility for the residues in the putative NES for TDP-43 predicts that all except I249 are predicted to be inside (Table 2.1). This suggests that these hydrophobic residues are critical for correct folding and function of RRM2, rather than recruiting XPO1.

Figure 2.1: Putative NES in TDP-43 is not solvent exposed and has a weak affinity for XPO1

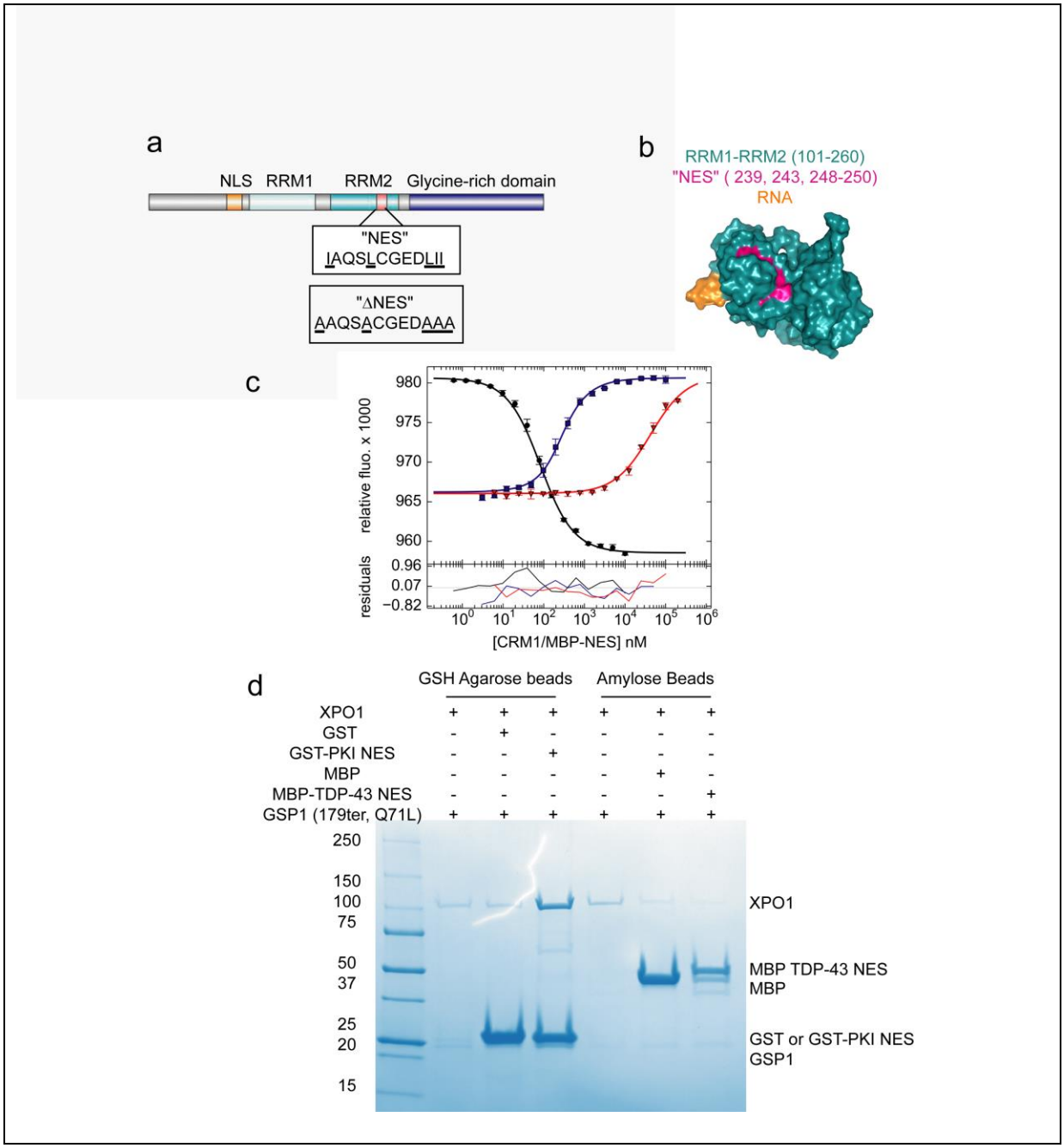

a. Domain map of TDP-43, formatted using IBS Cuckoo [174]. NLS: Nuclear Localization Signal, residues 82-98. RRM1: RNA Recognition Motif 1, residues 106-165. RRM2: RNA Recognition Motif 2, residues 191-257. "NES": putative Nuclear Export Signal, residues 239-250. "delNES": set of point mutations reported

to disrupt putative NES, I239A, L243A, L248A, I249A, I250A. Glycine-Rich domain: residues 270-414.

b. Space-filling NMR solution structure of the TDP RNA binding domain (RRM1-RRM2) [80]. Residues comprising the putative NES have been colored magenta.
c. Competition differential bleaching curves. Bleaching of a fluorescently labelled control NES, FITC-NES_{PKI}, decreases with increasing XPO1 concentration (black line). Bleaching of FITC-NES_{PKI} in the presence of fixed XPO1 and increasing concentrations of MBP-NES_{PKI} (blue line). Bleaching of FITC-NES_{PKI} in the presence of fixed XPO1 and increasing concentrations of MBP-NES_{TDP} (red line).
d. In vitro pull-down assay (Coomassie SDS PAGE) of purified human XPO1 binding to immobilized GST-NES_{PKI} (on GSH agarose beads) or MBP- NES_{TDP} (on amylose beads) in the presence of GSP1 (179ter, Q71L).

Table 2.1: Solvent Accessibility Surface of residues within TDP-43 putative NES

Amino Acid	Residue #	Total	Apolar	Backbone	Sidechain	Ratio (%)	In/Out
ILE	**239**	**27.06**	**27.06**	**2.75**	**24.31**	**16.5**	**i**
ALA	240	2.18	0	2.18	0	0	i
GLN	241	64.27	14.33	8.15	56.13	39.1	
SER	242	83.36	40	22.64	60.73	78.5	o
LEU	**243**	**9.24**	**9.24**	**0**	**9.24**	**6.3**	**i**
CYS	244	7.96	0.75	3.75	4.2	4.1	i
GLY	245	11.81	6.03	11.81	0	13.5	i
GLU	246	94.58	13.2	14.9	79.68	56.4	o
ASP	247	4.66	0.28	0.59	4.07	3.6	i
LEU	**248**	**15.67**	**15.67**	**4.2**	**11.46**	**7.8**	**i**
ILE	**249**	**39.94**	**37.53**	**2.42**	**37.53**	**25.5**	
ILE	**250**	**1.39**	**1.39**	**1.29**	**0.1**	**0.1**	**i**

However, it is conceivable that these RRMs adopt an alternate structure to expose the putative NES and facilitate export. In fact, there is NMR evidence that TDP-43 RRM2 can adopt an intermediate structure [175]. To test the ability of the exposed putative NES to recruit XPO1, the putative NES was expressed as a recombinant fusion protein in E Coli (fused to maltose binding protein to improve solubility; MBP-NES_{TDP}). In the case of TDP-43, 3 additional amino acids on either side of the putative NES were added to provide context for the NES, for a peptide sequence of DDQIAQSLCGEDLIIKGI.

First, XPO1 binding affinity was assessed using a competition differential bleaching experiment, as previously described [173]. Briefly, the binding affinity of MBP-NES_{TDP} for XPO1 was calculated by its ability to compete with a labelled probe, FITC-NES_{PKI}. The binding of FITC-NES_{PKI} to XPO1 can be determined by the kinetics of FITC bleaching, which are altered when the probe is bound to XPO1. The binding curve for the labelled probe, FITC-NES_{PKI}, yielded a Kd of 73 nM, with 68.3% confidence interval [67, 79] (Fig 2.1c, black circles). The competitive binding curve of MBP-NES_{PKI} with FITC-NES_{PKI} yielded similar result, Kd of 58 nM [47, 70], demonstrating the internal consistency of the assay (Fig 2.1c, blue circles). The competitive binding curve of MBP-NES_{TDP} yielded an affinity of 13 uM [11.3, 15.4](Fig 2.1c, red circles). While this affinity is much lower than that of a strong NES such as NES_{PKI}, it is within the range of affinities expected of a weak NES [176].

To determine whether the weak affinity of the putative NES in TDP was sufficient to recruit XPO1, *in vitro* XPO1 pull-down assays were performed. MAL-TDP_{NES} was

immobilized on amylose beads, and incubated with XPO1 in the presence or absence of yeast Ran-GTP. The TDP-43 putative NES was unable to pull down XPO1 in the presence of Ran-GTP, suggesting that even if RRM2 did adopt a conformation in which the putative NES were solvent exposed, XPO1 binding would not be sufficient to mediate export. In contrast, a control NES, GST-NES_{PKI}, immobilized on glutathione beads was able to pull down XPO1 in the presence but not the absence of Ran-GTP (Fig 2.1D).

TDP-43 RRM2 does not contain an NES: TDP-43 RRM2 is not sufficient for nuclear export

Our results have shown that the putative NES within TDP-43 is not predicted to be exposed, and even when exposed binds XPO1 only weakly. However, this does not preclude the possibility that RRM2 contains an alternate export signal. To determine whether RRM2 contained trafficking signals, we assessed whether RRM2 was sufficient and/or necessary for nuclear export of TDP-43.

To determine whether RRM2 was sufficient for nuclear export, it was fused to a reporter, 2x eYFP. As a small fusion protein, it should be able to diffuse through the nuclear pore. If it contains no trafficking signals, it will be equally distributed between the cytosol and nucleus. However, if it contains trafficking signals, steady-state localization will depend on the relative strength of those signals; a stronger NLS will concentrate the reporter within the nucleus, while a stronger NES will concentrate the reporter outside of the nucleus (Fig 2.2a). As a control for this assay, we assessed the localization of a fusion protein containing a strong NES and a weak NLS, 2x eYFP-NES_{PKI}-NLS_{SV40}. As predicted, it is concentrated outside of the nucleus (Fig 2.2b). However, when nuclear export is inhibited by treatment with the XPO1 inhibitor Leptomycin B, then the weak NLS prevails, and the fusion protein

accumulates within the nucleus. In contrast, the localization of 2x eYFP-RRM2 fusion protein is diffuse throughout the cell, suggesting an absence of any export signals (Fig 2.2b). Furthermore, introduction of the "ΔNES" point mutations causes the fusion protein to accumulate in puncta, suggesting these mutations disrupt its solubility (Fig 2.2b). Indeed, these mutations have been reported to disrupt the solubility of full-length TDP-43 as well [64]. This supports the structural evidence that the residues within the putative NES are stabilizing the core of the domain.

TDP-43 RRM2 does not contain an NES:RRM2 is not required for nuclear export of TDP-43

To test whether RRM2 is required for TDP-43 nuclear export, the heterokaryon shuttling assay was used [177]. In these assays, a "donor" cell which expresses a tagged protein of interest is fused with a "recipient" cell to make a heterokaryon containing both nuclei. Cells are treated with the translation inhibitor, cycloheximide, to prevent newly synthesized cytosolic protein from accumulating in the recipient nucleus. Thus, accumulation of the tagged protein in the recipient nucleus indicates nuclear export from the donor nucleus and re-import into the recipient nucleus (Fig 2.3a). The donor (HeLa Tet-on) and recipient (3T3) nuclei can be distinguished by the distinctive speckling in 3T3 nuclei. To quantitate shuttling, fluorescence in all nuclei of each heterokaryon were measured, and the ratio of donor: recipient nuclear fluorescence was calculated, termed "Shuttling index" or SI. To demonstrate the quantitation process, sample images of analyzed heterokaryons are shown (Figure 2.3S).

Figure 2.2: RRM2 is not sufficient for nuclear export

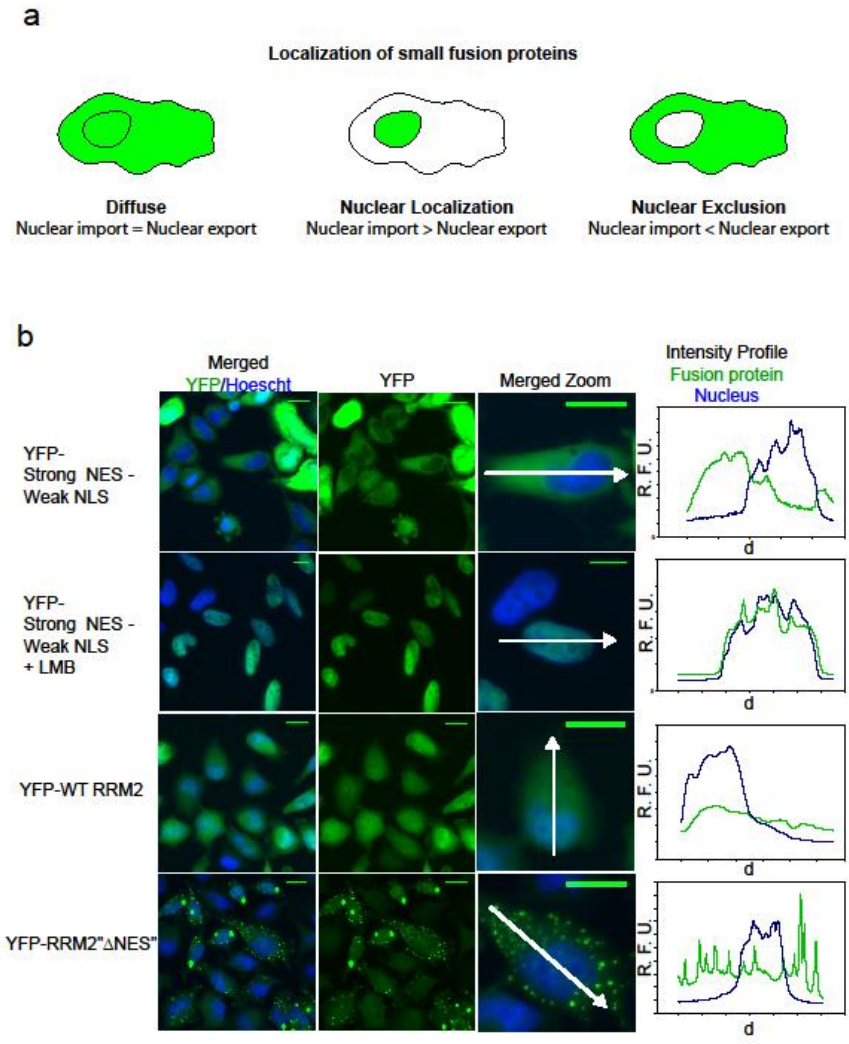

Figure 2. RRM2 is not sufficient for nuclear export

a. Schematic of predicted localization of small fusion proteins.
b. Direct fluorescence of HeLa Tet-On cells expressing the indicated fusion protein and treated with nuclear stain Hoechst. Merged image (Hoechst and YFP), YFP, and a close-up of Merged are shown. Scale bars are 10 um. Intensity plots for each image are shown; intensity was measured across the arrow in "Merged Zoom" panel. Intensity plots: y-axis is relative fluorescence, x-axis is distance. Indicated samples were treated with the XPO1 inhibitor Leptomycin B (LMB), 10 nmol for 12 hours. Results are representative of >3 independent experiments.

To confirm the integrity of the assay, YFP tagged hnRNPC was used as a negative control; hnRNPC belongs to the same protein family as TDP-43 and FUS, but does not shuttle [178]. As expected, YFP hNRNPC does not accumulate in the recipient nucleus (Fig 2.3b) and fluorescence of the recipient nucleus is only ~ 5% of donor nucleus fluorescence, an SI of 0.05 (Fig 2.3c). In contrast, WT TDP-43, which was previously shown to shuttle, accumulates efficiently in the recipient nucleus (Fig 2.3c), with an SI >1[65].

If RRM2 contains the NES responsible for TDP-43 nuclear export, then we would expect deletion of RRM2 to significantly decrease shuttling. However, TDP-43ΔRRM2 accumulates in recipient nuclei to the same degree as wild-type. Moreover, the "ΔNES" point mutations which have been assumed to abolish nuclear export do not affect TDP-43 shuttling; TDP-43"ΔNES" accumulates in the recipient nucleus to the same degree as WT (Fig 2.3b, 2.3c). Together, the evidence that RRM2 is neither sufficient for nuclear export, nor required for nuclear export of TDP-43, demonstrates that RRM2 does not contain an NES.

Figure 2.3: RRM2 is not required for nuclear export, and "ΔNES" mutations do not abolish export

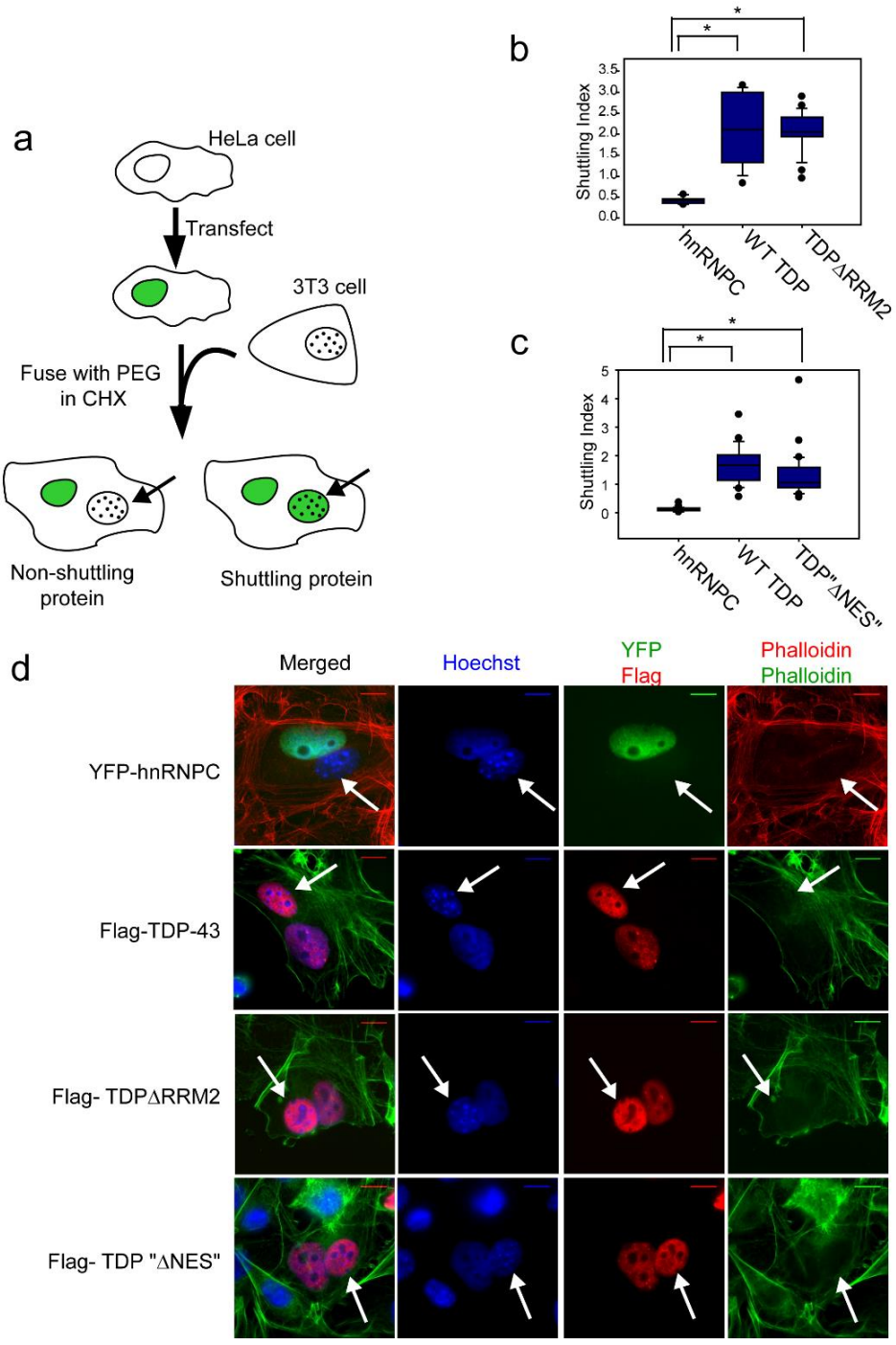

a. Schematic of heterokaryon shuttling assay.
b. Quantification of shuttling assay. For each heterokaryon counted, the ratio of fluorescence in recipient nucleus/donor nucleus was plotted (normalized to background). Results are shown in box and whiskers plot. Top: 3 independent experiments. hnRNPC- 6 heterokaryons counted; WT TDP-43 -9 heterokaryons counted; TDP-43ΔRRM2 – 19 heterokaryons counted. * indicates significant difference between groups, $p < 0.002$ using Mann-Whitney Rank Sum Test. No signicficant difference between WT and ΔRRM2.
c. Quantification of shuttling assay as in 1b. Three independent experiments. hnRNPC- 22 heterokaryons counted; WT TDP-43- 24 heterokaryons counted; TDP-43 "ΔNES" – 26 heterokaryons counted. * indicates significant difference between groups, $p < 0.001$ using Mann-Whitney Rank Sum Test. No significant difference between WT and "ΔNES".
d. Images of sample heterokaryons shown. Nuclei are stained with Hoechst. YFP-hnRNPC is detected by direct fluorescence. Flag WT TDP-43, Flag TDP-43ΔRRM2, and Flag TDP-43 "ΔNES" are detected by immunofluorescence with Flag antibody. Actin cytoskeleton visualized with phalloidin stain. Recipient nucleus (3T3) indicated by arrow. Scale bars- 10 um

Figure 2.3S: Quantitation of Heterokaryon shuttling assays

a

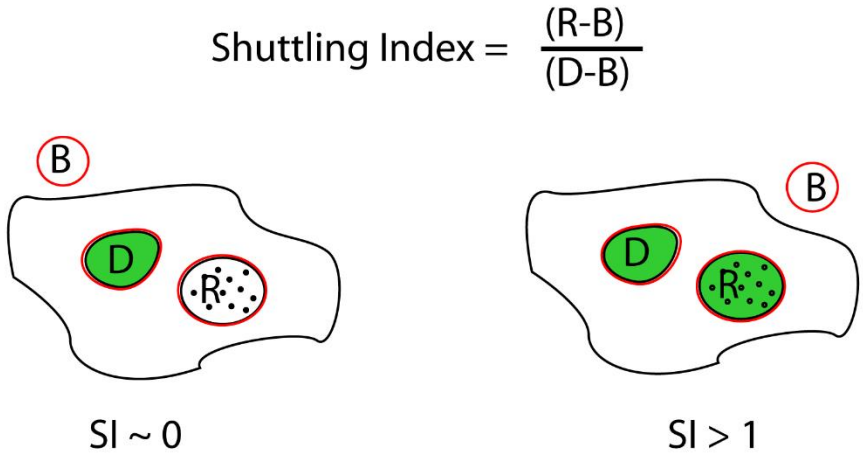

b

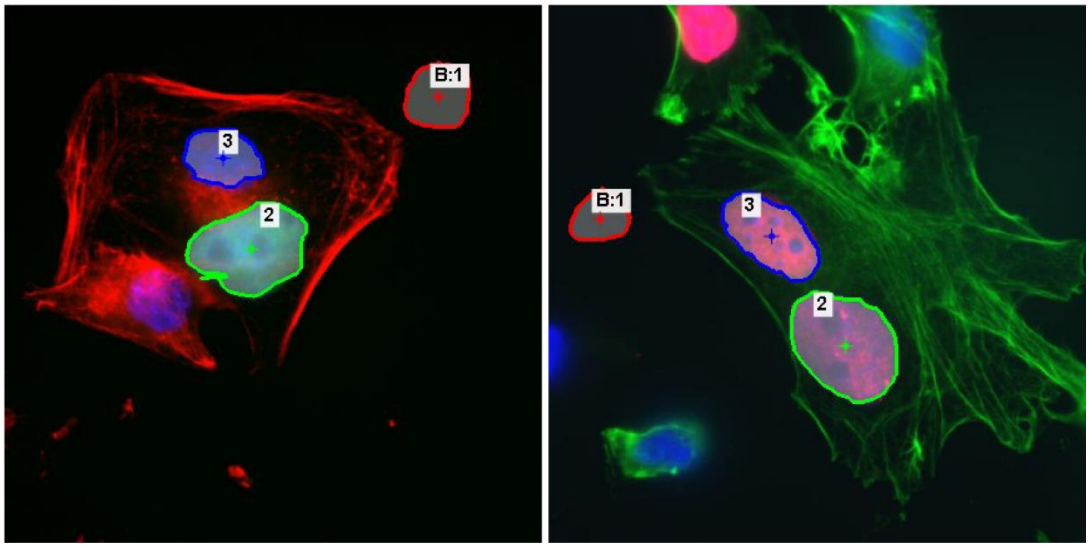

a. Schematic demonstrating quantitation of heterokaryon shuttling assays.
b. Sample images from quantitation of heterokaryon shuttling assays. "B" : background fluorescence, "D" : donor nucleus (HeLa Tet-On), "R": recipient nucleus (3T3). Shown in merged view: Left: Hoescht stain: blue, Actin skeleton: red, YFP-hnRNPC: green. Right: Hoescht stain: blue, Actin skeleton: green, Flag TDP-43: red.

"ΔNES" mutations disrupt TDP-43 function

The "ΔNES" mutations, contrary to what has been assumed in the literature, do not disrupt nuclear export of TDP-43. However, this set of point mutations does ameliorate the toxicity associated with TDP-43 overexpression, both in drosophila eye and in cell culture systems [179, 180]. Because the "NES" residues reside within the core of RRM2, and RRM2 "ΔNES" aggregates, we hypothesized that the "ΔNES" mutations disrupt TDP-43 function. This would explain the effect of these mutations on toxicity; RNA-binding is required for TDP-43 toxicity [181].

To assess the effect of the "ΔNES" mutations on TDP-43 function, we used a well-characterized assay of TDP-43 function: the CFTR exon 9 ssplicing assay. We performed in vivo splicing assays using the reporter minigene previously described [182]. This reporter was slightly modified; a silent mutation (1326A>G, K442>K) was introduced in order to disrupt a cryptic splice site, decreasing formation of an intermediate splice product (also observed in the original report [182]). This point mutation did not interfere with the TDP-43 dependent exon skipping (Figure 2.4S, Figure 2.4a).

As previously reported, WT TDP-43 mediated exon 9 skipping in a dose dependent manner (Fig 2.4a, 2.4b). However, TDP "ΔNES" had no effect on exon 9 skipping, despite adequate nuclear protein (Fig 2.4a, 2.4b). To more quantitatively assess the impact on function, we developed qPCR primers specific to the two isoforms, +9 and -9. This allowed us to more precisely quantitate each splice isoform, and also allowed us to normalize to TDP-43 expression. With this method, we compared the "ΔNES" mutations with other mutations known to disrupt function: ΔNLS, which shifts TDP-43 distribution into the cytosol[64];

F147/9L, RRM1 mutations which disrupt key RNA-stacking interactions; and F229/331L, RRM2 mutations analogous to F147/9L (Fig 2.4c) [48]. Electrophoretic mobility shift assays have demonstrated that RRM1 is required for RNA-binding, while RRM2 is not [48]. Similarly, TDP-43 mutants with either RRM2 deletion or mutations (F229/331L) still have residual function in the CFTR exon 9 splicing assay(~13% of WT), while RRM1 mutations (F147/9L) completely abrogated function. However, the "ΔNES" point mutations, which are within RRM2, also abrogate function. This suggested that these mutations disrupt more than just the local folding environment of RRM2. Lukavsky *et al* suggested that one of the residues within the putative NES, Ile 249, participates in a crucial inter-RRM interaction, which could explain the dramatic effect of the "ΔNES" mutations on TDP-43 function.

Figure 2.4: "ΔNES" Mutations profoundly disrupt TDP-43 function

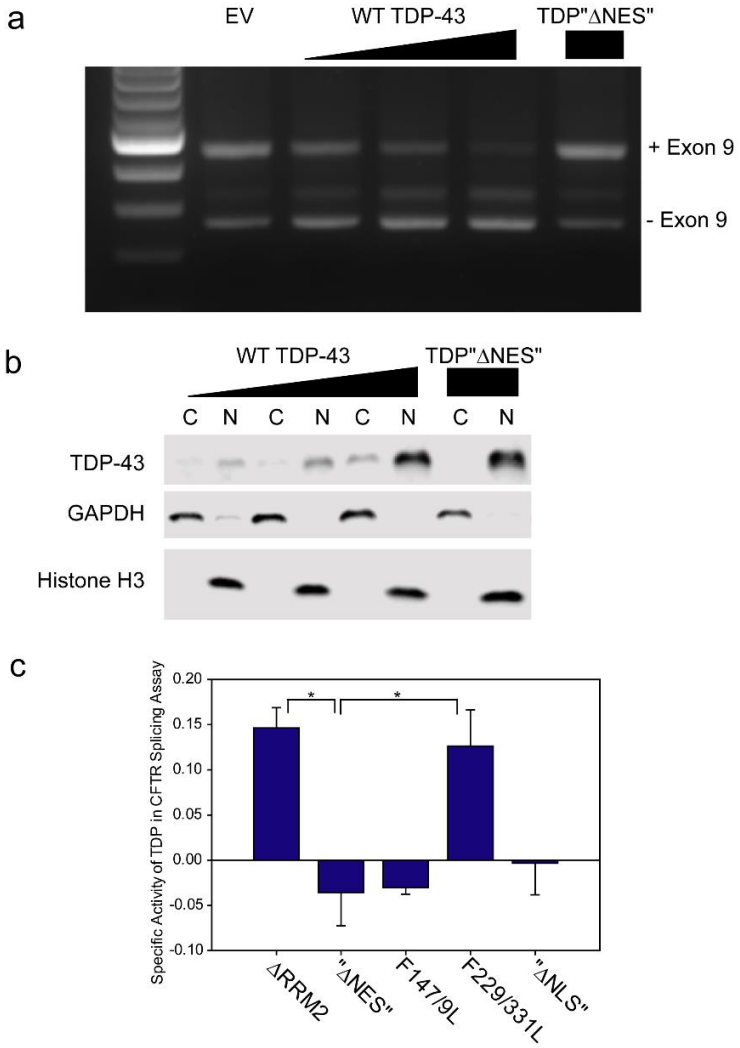

a. CFTR exon splicing Assay. cDNA from HeLa Tet-On cells co-transfected with the CFTR minigene and TDP-43 is PCR amplified and run on an agarose gel. Image is representative of three independent experiments.

b. Western blot of cytosolic "C", and nuclear, "N", fractions of lysate from cells in 3A. GAPDH (Glycaraldehyde 3 phosphate dehydrogenase) acts as a marker and loading control for the cytosolic fraction, while Histone H3 acts as a marker and loading control for the nuclear fraction. Image is representative of three independent experiments.

c. qPCR analysis of HeLa Tet-On cells co-transfected with the CFTR minigene and TDP-43. The "+9" and "-9" isoforms were detected with sequence specific primers. The specific activity: ((+9)/(-9))/(TDP-43) was calculated for each TDP-43 variant and normalized to WT. * indicates significant difference between groups, $p < 0.001$ using one-way ANOVA.

Figure 2.4S: CFTR T5 minigene with 1326A>G exhibits TDP-43 dependent CFTR exon 9 skipping.

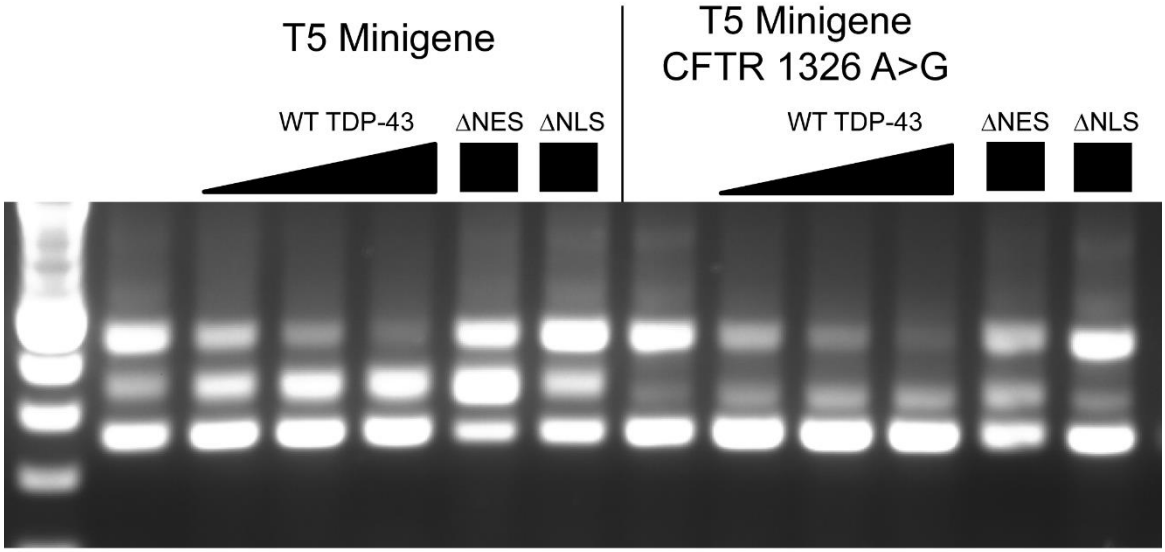

CFTR exon 9 splicing assay: HeLa Tet-on cells were cotranfected with TDP-43 and CFTR T5 minigene (original or 1326 A>G). RNA was extracted and reverse-transcribed; cDNA was PCR amplified and run on an agarose gel.

Distribution of both endogenous TDP-43 and flag WT TDP-43 in HeLa cells is almost exclusively nuclear

Our work has invalidated claims that the putative NES within RRM2 is mediating nuclear export. However, we are still left with the question of how TDP-43 nuclear export is mediated. The most likely candidate was XPO1, the exportin with the broadest substrate specificity. To determine whether TDP-43 nuclear export was dependent on XPO1, we assessed endogenous TDP-43 localization in the presence or absence of XPO1 siRNA (Figure 5Sa). However, endogenous TDP-43 is almost exclusively nuclear; cytosolic TDP-43 levels were too low to visualize. XPO1 knockdown had no apparent effect on TDP-43 localization, but the indistinguishable cytosolic TDP-43 levels in untreated cells made this result impossible to interpret. We also assessed the effect of LMB, an XPO1 inhibitor, on Flag WT TDP-43 localization(Figure 2.5Sb). Again, the extremely low cytosolic TDP-43 levels prevented a determination of whether LMB treatment diminished cytosolic TDP-43 (Figure 2.5Sb).

Figure 2.5: TDP-43 localization and nuclear export is XPO1 independent.

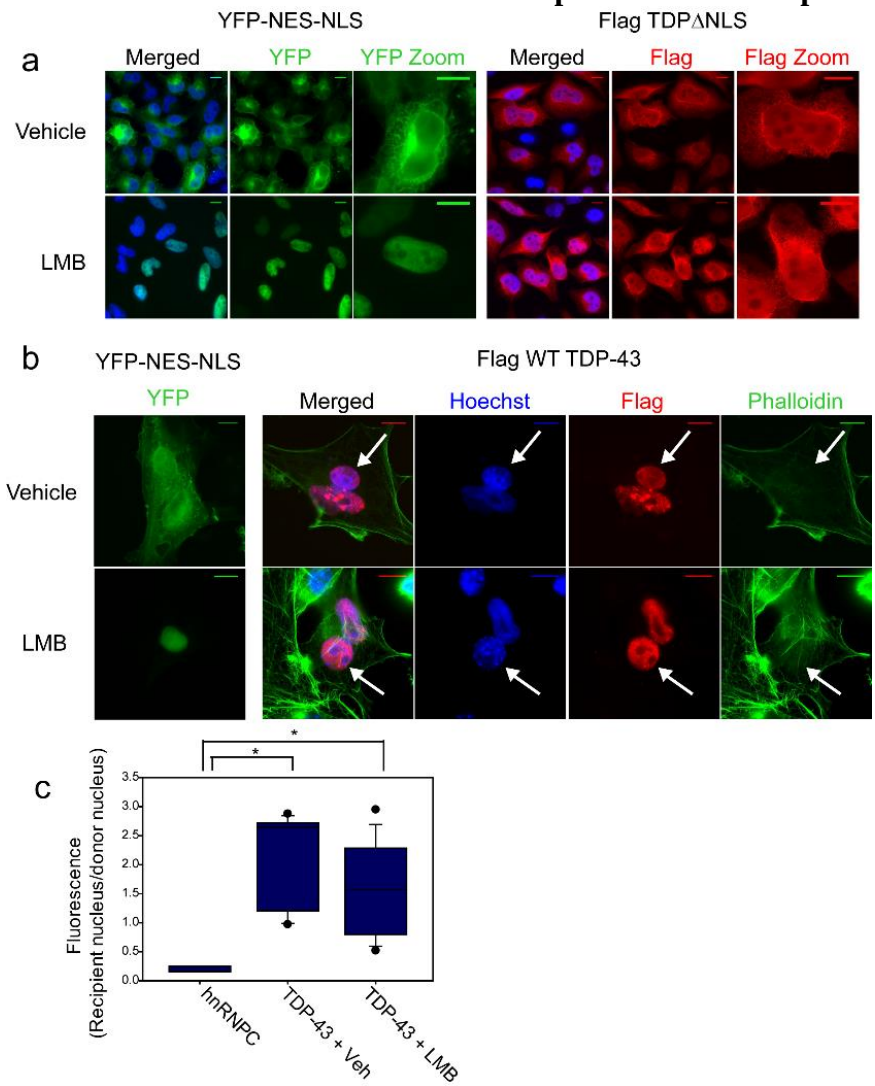

a. Direct fluorescence of HeLa Tet-On cells expressing fusion protein YFP-NES_{PKI}-NLS_{SV40} on left. Immunofluorescence using Flag antibody on HeLa Tet-On cells expressing Flag TDP-43ΔNLS on the right. Nuclei were stained using Hoechst. Cells were treated with either Vehicle (Ethanol, - 0.1% of total volume) or Leptomycin B (LMB) 10 nM for 12 hours. Scale bar- 10 um.

b. Left: direct fluorescence of HeLa cells undergoing mock shuttling assay, expressing YFP-NES_{PKI}-NLS_{SV40}. Cells were treated with either Vehicle (Ethanol, - 0.1% of total volume) or Leptomycin B (10 nM) for the duration of the assay. Right: Example heterokaryons from shuttling assay. Cells were treated with either Vehicle (Ethanol, - 0.1% of total volume) or Leptomycin B (10 nM) for the duration of the assay. Nuclei are stained with Hoechst. Flag WT TDP-43 is detected by immunofluorescence with Flag antibody. Actin cytoskeleton visualized with phalloidin stain. Recipient nucleus (3T3) indicated by arrow. Scale bars- 10 um

c. Quantification of shuttling assay as in 1b. Two independent experiments. hnRNPC-3 heterokaryons counted. Flag WT TDP-43 , vehicle treated- 8 heterokaryons counted. Leptomycin B treated- 10 heterokaryons counted. * indicates significant difference between groups, $p < 0.002$ using Mann-Whitney Rank Sum Test. No significant difference between Vehicle and LMB treated heterokaryons, but insufficient power to detect a difference.

Figure 2.5S: WT TDP-43 is predominantly nuclear and does not contain a nuclear retention signal

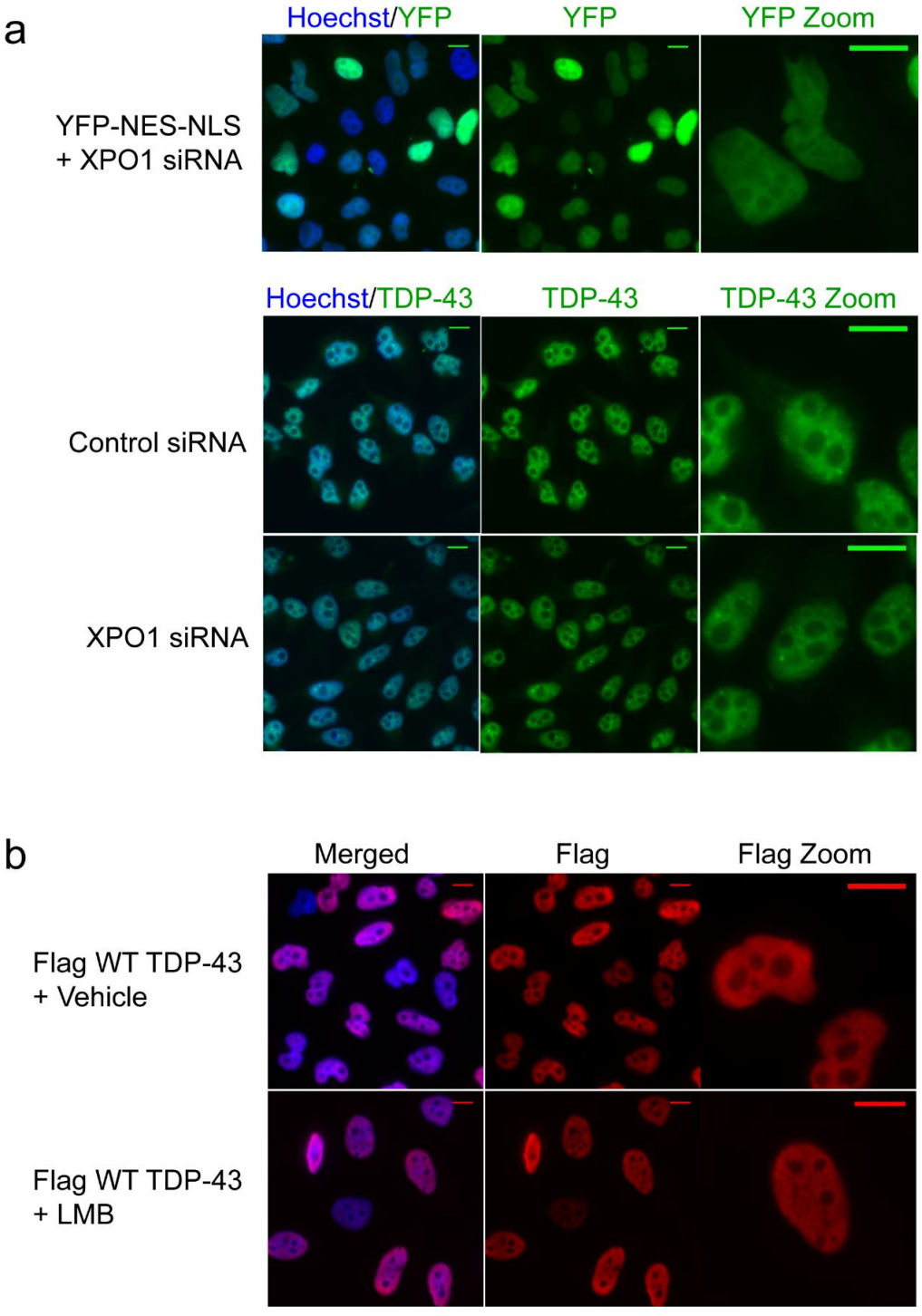

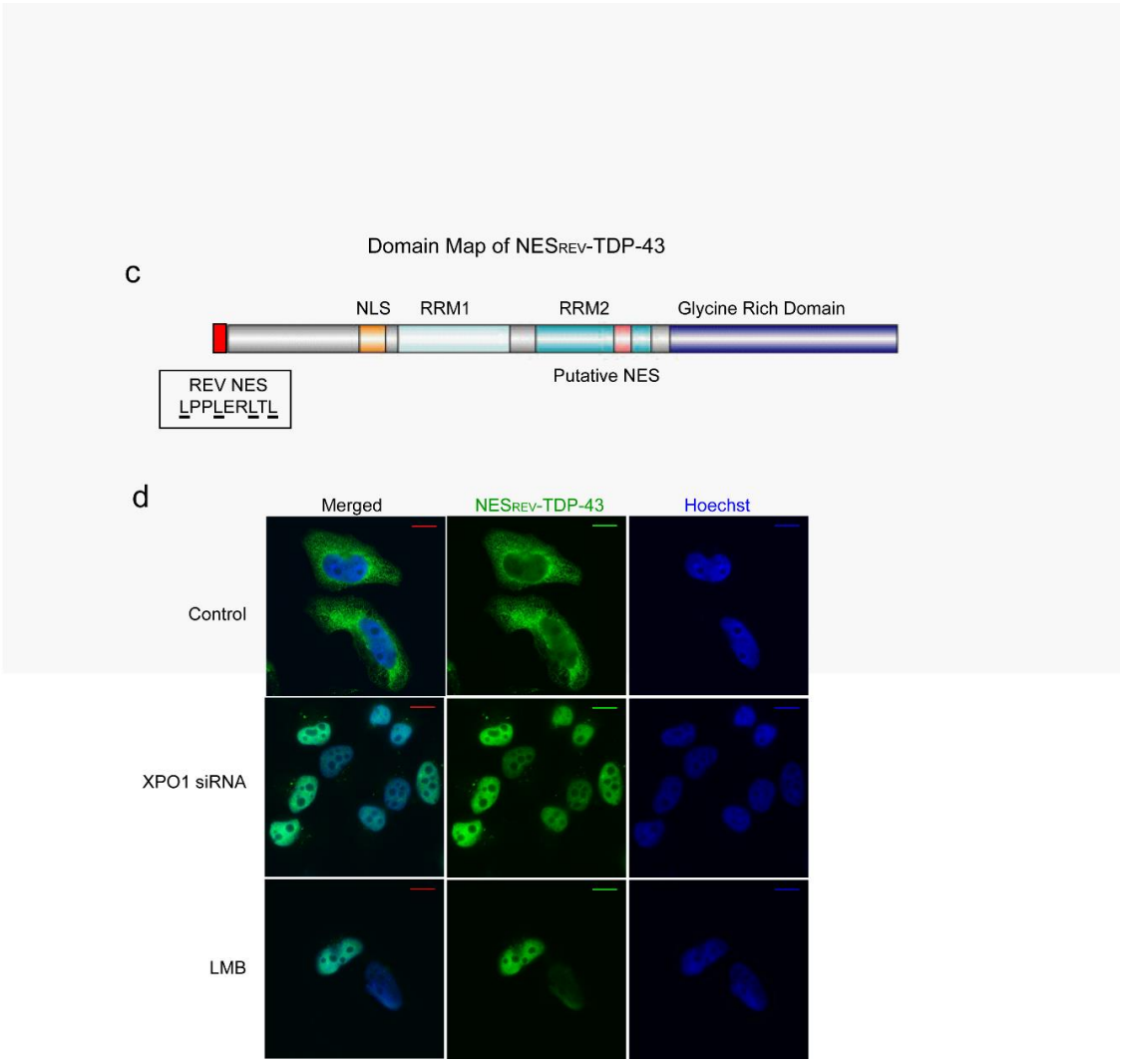

a. Top: direct fluorescence of HeLa Tet-On cells treated with XPO1 siRNA, expressing reporter YFP-NES_{PKI}-NLS_{SV40}. Bottom: Immunofluorescence of endogenous TDP-43 in HeLa Tet-On cells treated with XPO1 siRNA. Images are representative of 3 independent experiments. Nuclei are stained with Hoechst. Scale bars 10 uM.
b. Immunofluorescence of HeLa Tet-On cells expressing Flag WT TDP-43, in cells treated either by vehicle (EtOH, <0.1% volume) or Leptomycin B (10 nM). Images are representative of 3 independent experiments. Nuclei are stained with Hoechst. Scale bars 10 um.
c. Domain map of fusion protein NES_{REV}-TDP-43. Peptide sequence of REV NES is detailed. Domain map formatted using IBS Cuckoo [174].
d. Immunofluorescence of HeLat Tet-On cells expressing fusion protein NES_{REV}-TDP-43, detected using TDP-43 antibody. Indicated cells were treated with XPO1 siRNA or Leptomycin B (LMB), 10 nM for 12 hours. Nuclei were detected using Hoechst stain. Scale bars 10 um. Images are representative of 3 independent experiments.

Distribution of the TDP trafficking mutant Flag TDPΔNLS is unaffected by LMB treatment

To visualize cytosolic TDP-43, we expressed Flag-tagged TDPΔNLS, which contains mutations that disrupt the nuclear localization signal, or NLS [64]. As has been reported in the literature, this mutant is not excluded from the nucleus [65] (Figure 2.5a). Therefore, inhibition of TDP-43 nuclear export should result in an accumulation of TDP-43 ΔNLS in the nucleus, and a visible depletion of cytosolic TDPΔNLS. Treatment with LMB had no effect on cytosolic TDPΔNLS, suggesting that TDP-43 nuclear export is XPO1 independent (Figure 2.5a). XPO1 inhibition was efficient; the reporter 2 x eYFP-NES_{PKI}-NLS_{SV40} reporter construct was nuclear in LMB treated cells (Figure 2.5a).

Shuttling of TDP-43 is unaffected by Leptomycin B treatment

To more directly test the effect of XPO1 inhibition on TDP-43 nuclear export, heterokaryon shuttling assays were performed in the presence or absence of the XPO1 inhibitor Leptomycin B. TDP-43 shuttled in the presence of LMB (Fig 2.5b,c). Again, XPO1 inhibition was assessed by localization of the 2 x eYFP-NES_{PKI}-NLS_{SV40} reporter, which was cytosolic in the vehicle treated cells and nuclear in LMB treated cells (Fig 2.5b). YFP-hnRNPC was also used as a negative control for shuttling (Fig 2.5c).

TDP-43 might be non-responsive to XPO1 inhibitors because it does not contain an NES, or because an NES is antagonized by a nuclear retention sequence. To distinguish between these possibilities, we constructed a fusion protein NES_{REV}-TDP-43 (TDP-43 fused to an XPO1-dependent NES from the HIV protein Rev) (Figure 2.5Sc). This fusion protein accumulated in the nucleus after LMB treatment, suggesting that TDP-43 does not contain

any nuclear retention sequences (Figure 2.5Sd). . Thus, we conclude that TDP-43 does not contain an XPO1-dependent NES.

Distribution of TDP-43 in rat hippocampal neurons is both cytosolic and nuclear and unaffected by LMB treatment

While our results demonstrate that TDP-43 localization is XPO1 independent in HeLa cells, it is possible that the mechanism of TDP-43 nuclear export might vary based on cell type. Therefore, it was important to confirm the XPO1 independence in the most relevant cell type, neurons.

To determine the correct dose of LMB to inhibit XPO1 in cultured hippocampal neurons, we transfected neurons with the reporter YFP-NES_{PKI}-NLS_{SV40}. While transfection efficiency was low, the reporter was highly expressed in transfected cells, and was excluded from the nucleus as predicted (Fig 2.6a). LMB treatment of 10 nM for 7 hours was sufficient to redistribute the reporter from the cytosol to the nucleus (Fig 2.6a).

Next, we repeated these conditions and assessed endogenous TDP-43 localization using immunofluorescence (Figure 2.6b). Unlike in HeLa cells, and *in situ* neurons, in cultured neurons TDP-43 is evenly distributed between the cytosol and nucleus. Therefore, inhibiting TDP-43 nuclear export should lead to a profound change in localization. However, LMB treatment had no effect on TDP-43 localization, suggesting that TDP-43 localization is XPO1 independent in neurons (Figure 2.6b).

Figure 2.6 TDP-43 localization in cultured neurons is XPO1 independent.

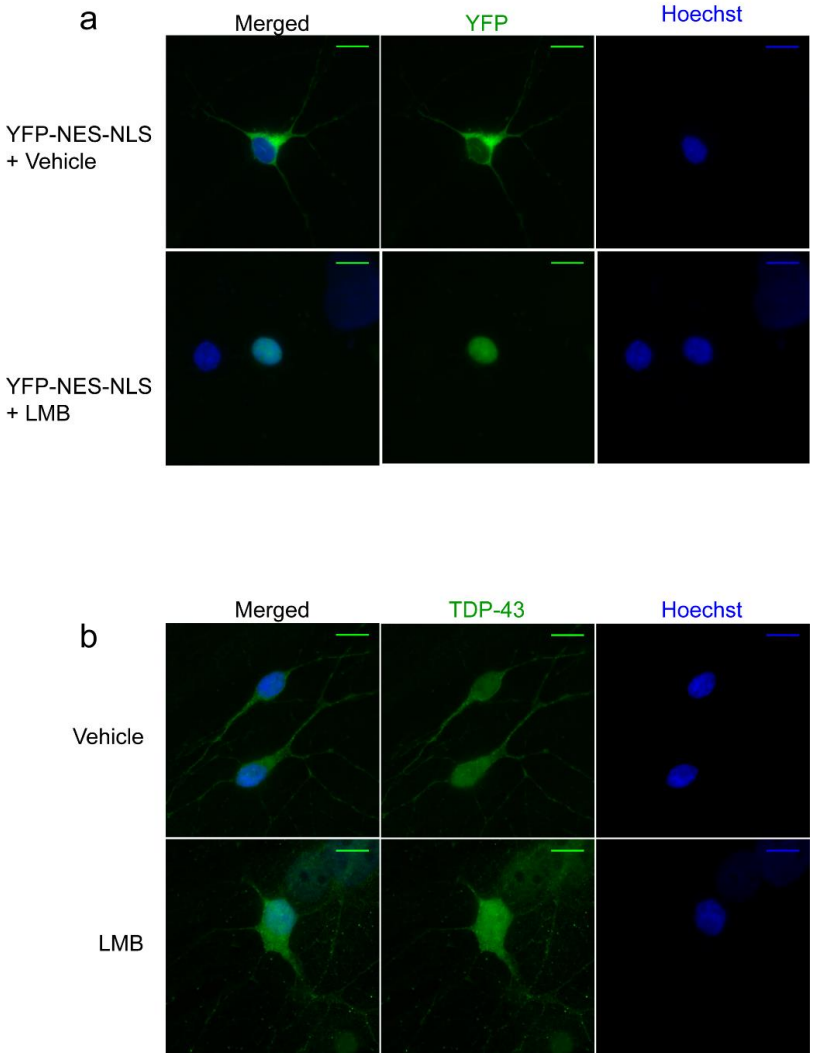

a. Hippocampal neurons were isolated and cultured. Indicated neurons were transfected with the reporter YFP-NES_{PKI}-NLS_{SV40} and treated with either vehicle (Ethanol, 0.1% of total volume) or Leptomycin B (LMB) 10 nM for 7 hours. Nuclei were stained with Hoechst and YFP-NES_{PKI}-NLS_{SV40} was detected with direct fluorescence. Images are representative of three independent experiments. Scale bar- 10 um.

b. Indicated neurons were treated with either vehicle (Ethanol, 0.1% of total volume) or Leptomycin B (LMB) 10 nM for 7 hours. Nuclei were stained with Hoechst and endogenous TDP-43 was detected with immunofluorescence using a TDP-43 antibody. Images are representative of three independent experiments. Scale bar- 10 um.

Tomato tag disrupts passive but not active nuclear import of TDP-43

We had previously noted that the FlagTDP-43ΔNLS mutant is not excluded from the nucleus. To confirm that this is a property of TDP-43ΔNLS, and not an artifact introduced by the Flag tag, we made synonymous mutations in both WT TDP-43 and TDP-43ΔNLS to confer resistance to an individual TDP-43 siRNA. Efficient knockdown of endogenous TDP-43 and addback of resistant WT TDP-43 and resistant TDP-43ΔNLS was confirmed with immunofluorescence (Fig 2.7b, Figure 2.7Sa, b). Addback experiments confirmed that, like Flag TDP-43ΔNLS, untagged TDP-43ΔNLS is partially nuclear (Figure 2.7b).

There are two possible explanations for this: first, it is possible that TDP-43 is small enough to passively diffuse through the nuclear pore. This would be consistent with some of the recent literature regarding the size cutoff for diffusion through the nuclear pores [70]. Second, it is conceivable that TDP-43 contains a redundant NLS elsewhere. To distinguish between these possibilities, we purchased a construct containing a TdTomato TDP-43 fusion protein. TdTomato is ~50 kDa, so the fusion protein is predicted to be too large to efficiently diffuse through the nuclear pore. We then mutated one site of the bipartite TDP-43 NLS (for unclear reasons, this construct proved difficult to manipulate). However, despite the incomplete mutagenesis of the NLS, tdTomato TDP-43ΔNLS was almost entirely excluded from the nucleus (Figure 2.7c).

Figure 2.7: Addition of a bulky tag on TDP-43 disrupts passive but not active nuclear import.

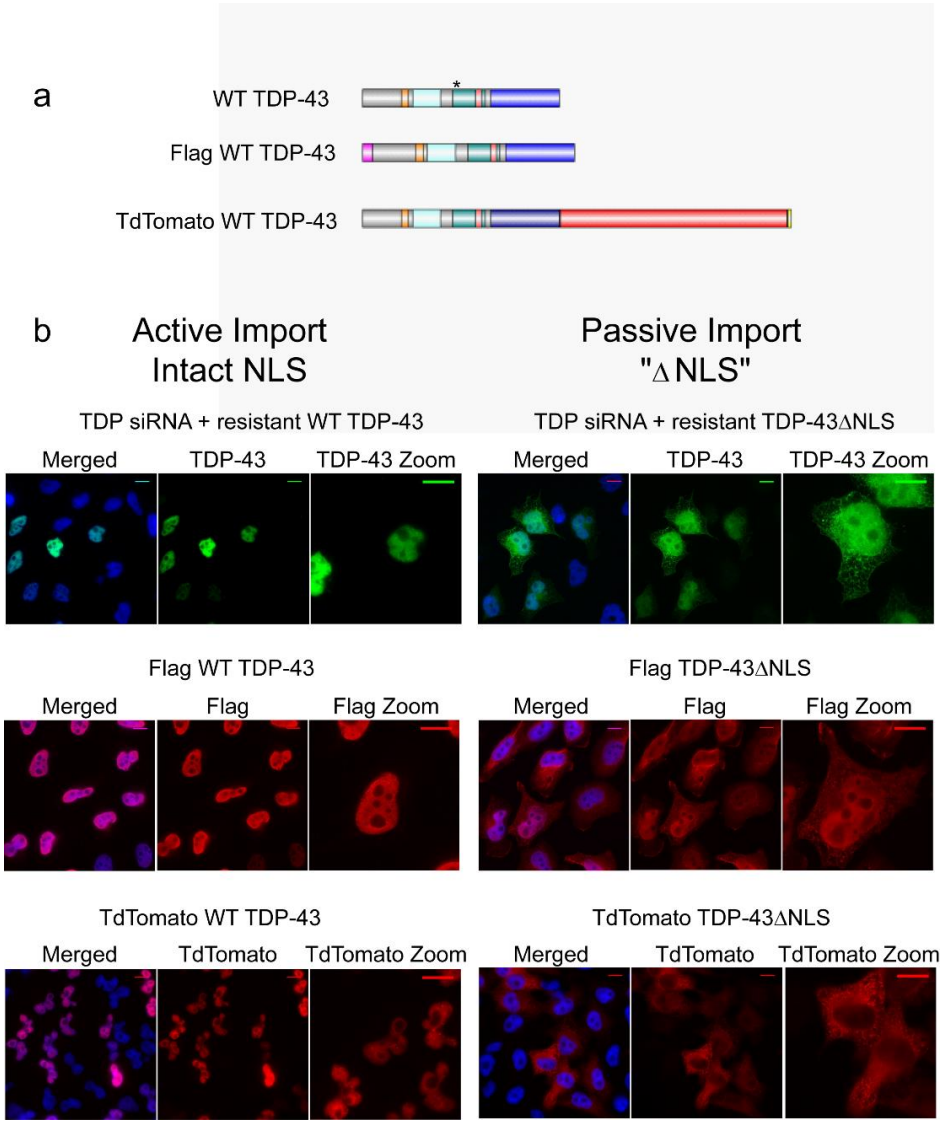

a. Domains maps (to scale) of WT TDP-43 containing synonymous mutations which confer resistance to TDP-43 siRNA (indicated by asterisk), Flag WT TDP-43, tdTomato TDP-43. Formatted using IBS cuckoo [174].

b. Immunofluorescence of HeLa Tet-On cells expressing the indicated protein. Selected samples were treated with TDP-43 siRNA to deplete endogenous TDP-43. Resistant TDP-43 was visualized via immunofluorescence with TDP-43 antibody; Flag TDP-43 was visualized via immunofluorescence with Flag antibody; tdTomato TDP-43 was visualized with direct fluorescence. Nuclei were visualized using Hoechst stain. Scale bar- 10 um. Images are representative of 3 independent experiments.

Figure 2.7S: Endogenous TDP-43 is efficiently depleted by TDP-43 siRNA, and C-terminus of TDP-43 does not contain a redundant NLS.

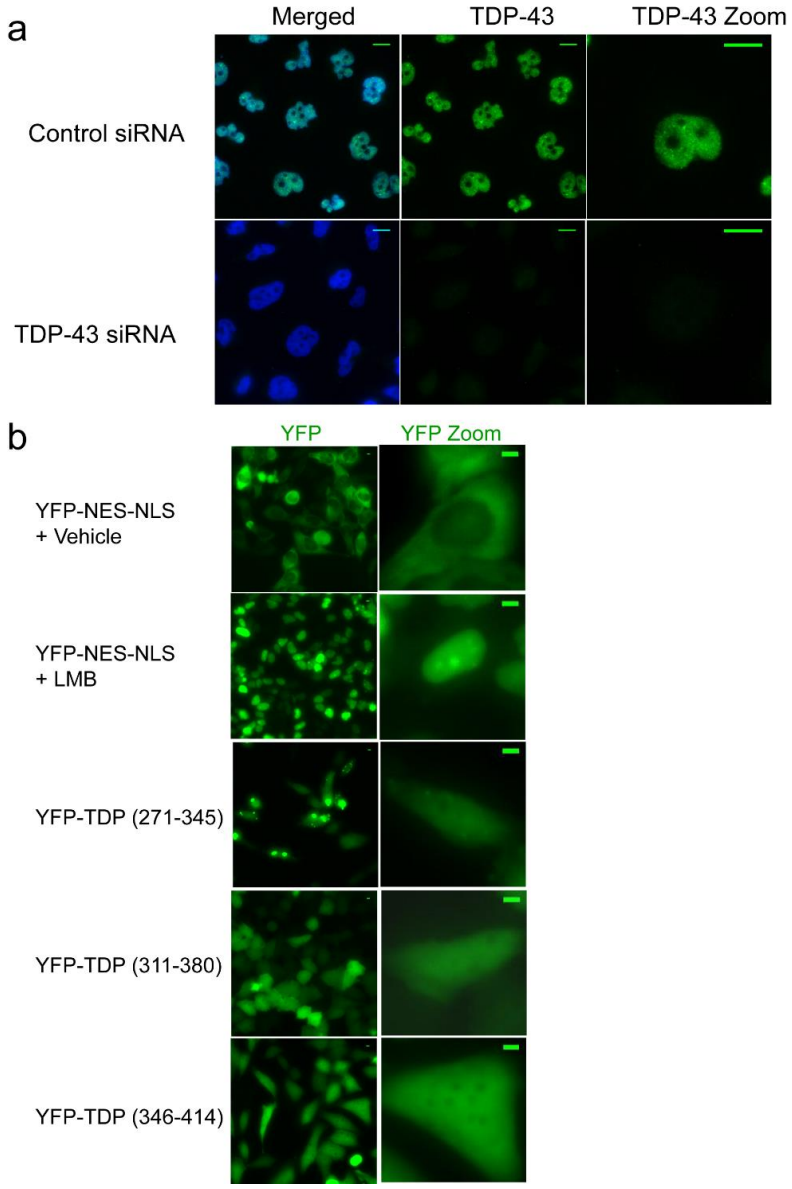

a. Immunofluorescence of endogenous TDP-43 in HeLa Tet-On cells treated with either control siRNA or TDP-43 siRNA. Scale bars 10 um. Images are representative of 3 independent experiments.
b. Direct fluorescence of HeLa Tet-On cells expressing indicated fusion proteins. Indicated cells were treated with Leptomycin B (LMB), 10 nM for 12 hours. Scale bars 10 um. Images are representative of 3 independent experiments.

We also set out to formally exclude that possibility that TDP-43 contained an alternate NLS, which was somehow occluded by the tdTomato tag (which is on the C-terminus, while the flag tag is on the N-terminus). To do this, we created several additional fusion proteins with various regions of the C-terminus fused to the reporter YFP, as in Figure 2.2. If any region of the C-terminus contained an NLS, the reporter should be nuclear. However, all fusion proteins were diffuse, suggesting the C-terminus does not contain an NLS (Figure 2.7S).

tdTomatoTDP-43 nuclear export is retarded relative to Flag TDP-43 nuclear export

Unlike active nuclear import and export, passive diffusion through the nucleus is intrinsically bidirectional. Therefore, the observation that TDP-43 passively diffuses into the nucleus implies that TDP-43 also passively diffuses out of the nucleus. We wanted to determine the contribution of passive diffusion to nuclear export of TDP-43. To do this, shuttling of Flag TDP-43 (which can passively diffuse through the nuclear pore) was directly compared to shuttling of tdTomato TDP-43 (which diffuses much less efficiently).

Heterokaryon assays were performed in which donor cells co-expressed Flag TDP-43 and tdTomato TDP-43. Shuttling index for Flag TDP-43 and tdTomatoTDP-43 was calculated as above (Fig 2.6b). As seen earlier, Flag TDP-43 efficiently accumulates in the recipient cell, with a shuttling index >1. However, tdTomato TDP accumulation in the recipient nucleus is significantly lower, with a shuttling index of ~0.3. We used the paired Wilcoxon signed rank test to compare the shuttling index of Flag TDP to tdTomato TDP for each heterokaryon. The shuttling of tdTomato WT TDP-43 was significantly impaired compared to Flag WT TDP-43 ($p < 0.001$).

Again, we wanted to formally exclude the possibility that the C-terminus contained an NES which was occluded by the large, N-terminal tdTomato tag. To do this, we assessed the contribution of the C-terminus to export. Heterokaryon shuttling assays with Flag TDPΔC-terminus demonstrated that the C-terminus is not required for shuttling (Figure 2.8S). Together, these data suggest that the primary effect of the tdTomato tag on shuttling is size dependent. As passive export, but not active export, is size dependent, this suggests that the primary driver of TDP-43 nuclear export is diffusion.

Figure 2.8: Addition of a bulky tag on TDP-43 disrupts nuclear export

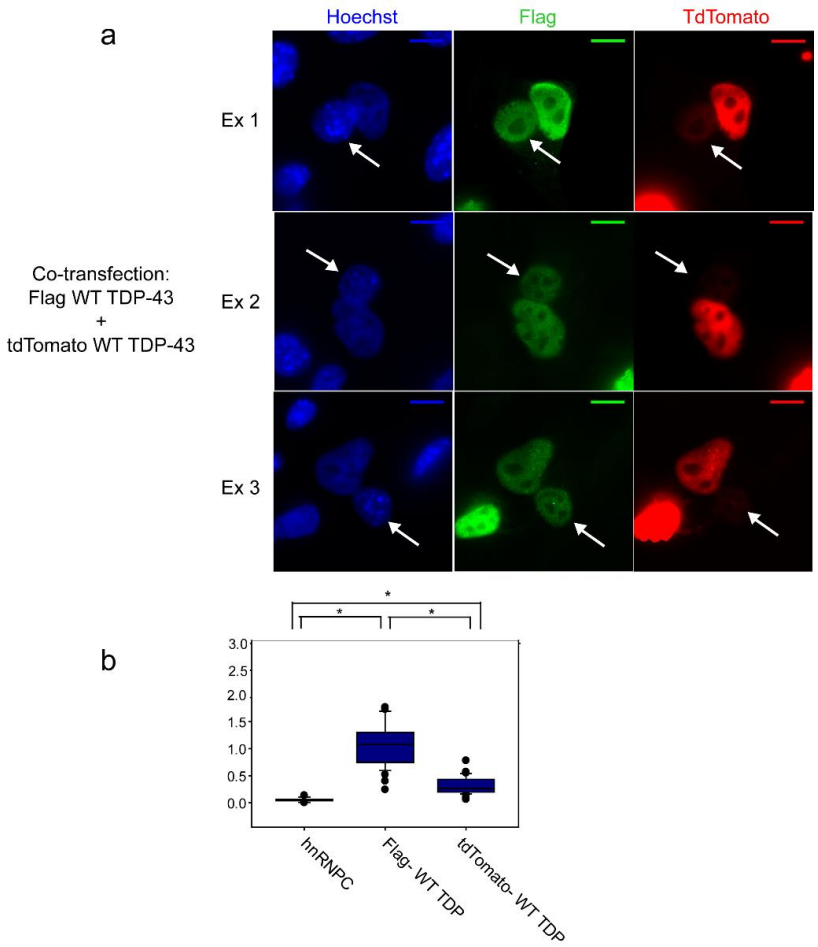

a. Example heterokaryons from a variation of the heterokaryon shuttling assay. HeLa Tet-On cells were co-transfected with Flag TDP-43 and tdTomato TDP-43 and shuttling assay was performed as in Fig 3. Heterokaryons were identified by presence of Flag TDP-43 within a recipient nucleus. Flag TDP-43 was visualized via immunofluorescence with Flag antibody, tdTomato TDP-43 was visualized via direct fluorescence. Nuclei were detected using Hoechst stain. Images are representative of 4 independent experiments. Recipient nuclei are indicated by arrow. Scale bar- 10uM.

b. Quantification of shuttling assay as in 1b. Results are pooled from 4 independent experiments. hnRNPC- 15 heterokaryons counted. Cotransfected with Flag TDP-43 and tdTomato TDP-43- 28 heterokaryons counted. * indicates significant difference between groups, $p < 0.001$. To compare hnRNPC vs Flag TDP-43, and hnRNPC vs tdTomato TDP-43, Mann Whitney rank sum test was used. To compare Flag TDP-43 vs tdTomato TDP-43, Wilcoxon signed rank test was used.

Figure 2.8S: C-terminus is not required for TDP-43 nuclear export

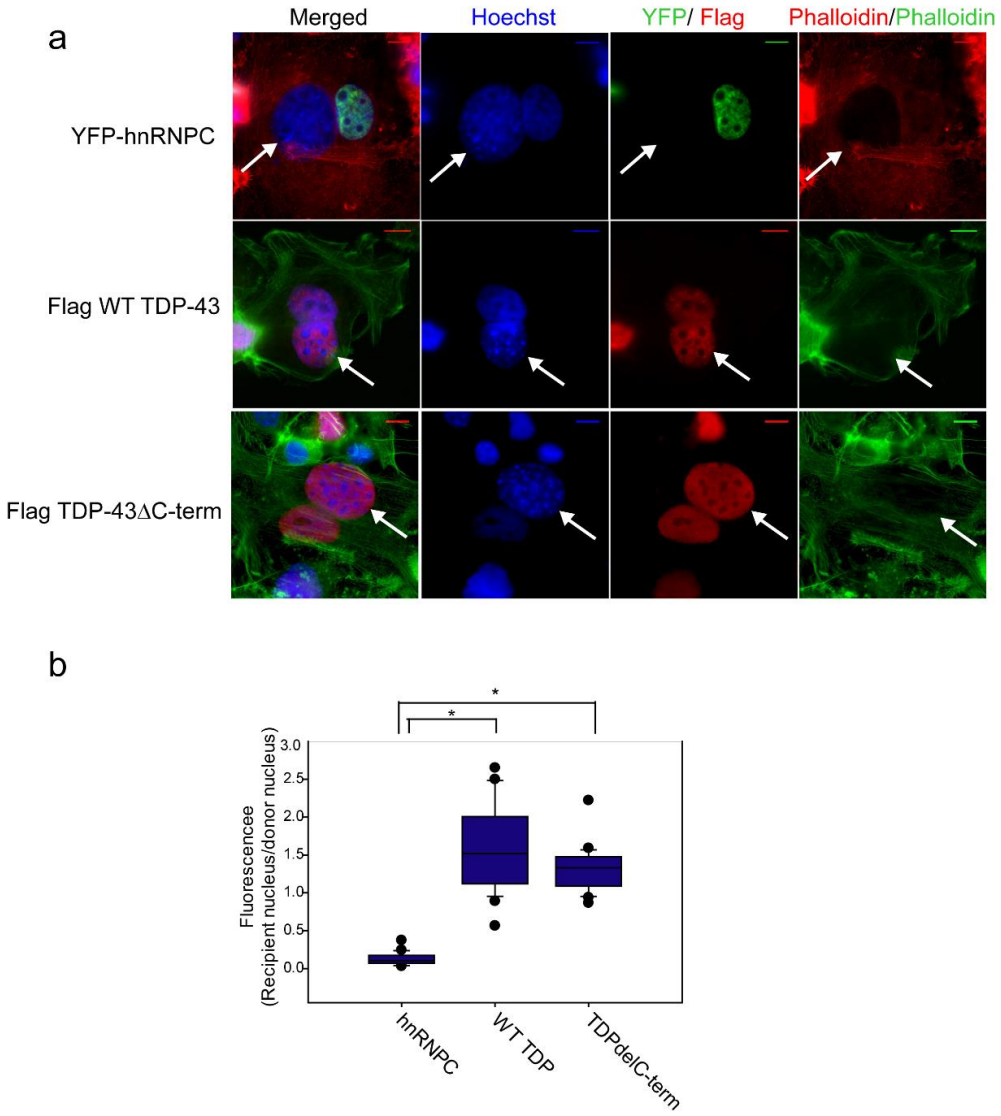

a. Example images from heterokaryon shuttling assay. YFP-hnRNPC was detected using direct fluorescence. Flag WT TDP-43 and Flag TDP-43 ΔC-terminus were detected using immunofluorescence with a Flag antibody. Nuclei were detected using Hoechst stain. Actin cytoskeleton was visualized using Phalloidin. Recipient nucleus indicated by arrow. Scale bars- 10uM.

b. Quantitation of heterokaryon shuttling assay, as in Fig 3. Heterokaryons are pooled from 2 independent experiments. hnRNPC- 15 heterokaryons counted. Flag WT TDP-43- 22 heterokaryons counted. Flag TDP-43Δ C terminus- 18 heterokaryons counted. * indicates significant difference between groups, $p < 0.001$ using Mann-Whitney Rank Sum Test. Scale bars- 10uM.

Discussion

TDP-43 mislocalization plays a causal role in the toxicity of ALS, but the cellular insults which lead to mislocalization are largely unknown. We sought to identify determinants of normal TDP-43 trafficking in order to better understand and possibly disrupt the forces that lead to TDP-43 mislocalization in ALS. Here, we have shown that TDP-43 nuclear export is not mediated by the putative XPO1 dependent NES previously reported. We have further shown that TDP-43 localization is not XPO1 dependent, and that TDP-43 nuclear export is largely diffusion driven.

This has broad implications for the therapeutic strategies which might be used to correct TDP-43 mislocalization. Because TDP-43 nuclear export is driven by diffusion rather than requiring active transport, targeting nuclear export with a small molecule inhibitor is not feasible. Moreover, it suggests that XPO1 inhibitors, which have been successful in preclinical models of several cancers and multiple sclerosis, would not correct TDP-43 mislocalization in ALS[81, 82, 183, 184]. However, XPO1 inhibitors may still ameliorate the course of ALS, by modifying the localization of downstream mediators of toxicity.

This finding also raises questions about the role of TDP-43 in the cytosol. Some roles for TDP-43 in the cytosol have been identified, such as axonal transport of one of its target mRNAs, association with translation and splicing machinery, and recruitment into stress granules [56, 185]. However, it has also been recognized that TDP-43 is prone to cytosolic aggregation, in a concentration dependent manner. Together, these would predict very tight regulation of cytosolic TDP-43 levels. This is not consistent with the unregulated, diffusion driven nuclear export of TDP-43 that we have observed. It is possible that cytosolic TDP-43

levels are in fact controlled by nuclear import alone. It is also conceivable that the roles of TDP-43 in the cytosol, which are not well-characterized, are not as general or as critical for cellular function as has been proposed.

Finally, the finding that this putative NES within TDP-43 RRM2 is not a true export signal raises questions about other putative NESs within RRMs, which have been predicted in several other members of the hnRNP family: FUS, TAF15, EWSR1, hnRNPA1, hnRNPA2B1[186]. For the most part, these predicted NESs have not been verified experimentally, and it remains to be seen whether they are truly mediating export. Possibly, nuclear export via passive diffusion is conserved throughout this family of shuttling proteins.

Figure Contributions:

Figure 2.1C was performed with Ho Yee (Joyce) Fung, Ph. D., in the lab of Yuh Min Chook Ph.D.

Figure 2.1D was the work of Tolga Cagatay, Ph. D., also in Yuh Min Chook's lab.

Figure 2.4C. Hippocampal neurons were isolated with the help of Ying Li, M.D. Ph.D. and Yemi Afuwape, M.D., Ph. D., both in the lab of Ege Kavalali Ph.D.

Materials and Methods

Constructs—cDNA encoding human TDP-43 (accession number NM 007375) in the plasmid pBUDCE was a kind gift from Jeffrey Elliot. tdTomato-TDP-43 was purchased from Addgene (Catalog # 28205). The YFP-shuttle reporter, eYFPx2-PKI NES-SV40 NLS fusion protein, was a gift from YuhMin Chook. CFTR T5 minigene was a gift from Francisco Baralle. Human hnRNPC cDNA was purchased as a Ultimate ORF clone (ThermoFisher Scientific Clone ID IOH7506). Vectors were modified as follows. Flag-TDP-43 contains an N-terminal Flag tag. The T5 minigene was modified with the synonymous mutation 1326A>G in an alternate splice acceptor site to reduce an intermediate splicing product (Supplementary Figure 3). GFP-hnRNPC contains a C-terminal GFP tag. Fusion proteins and deletions were generated using overlap extension PCR. Point mutations were generated using site-directed mutagenesis. All cloning was confirmed by sequencing.

siRNA resistant TDP-43 constructs contained the following synonymous mutations: 525C>T, 531 T>A, 534 T>A, 537T>C

With the exception of tdTomato-TDP-43, all TDP delNLS mutants contain the mutations also referred to as “delNLS1/2”: K82A, R83A, K84A; K95A, K97A, R98A.

tdTomato-TDP-43delNLS contains only a subset of these mutations:“delNLS 1”: K82A, R83A, K84A.

Rev NES TDP-43: contains an N-terminal NES from the HIV Rev protein “LPPLERLTL”.

Flag“Del C-term”: N terminal Flag Tag, TDP-43 residues 1-269

Flag TDP delRRM2: N terminal Flag tag, TDP del 191-257

YFP-RRM2: eYFPx2 fused to TDP-43 residues, 185-269

YFP- C terminal constructs: eYFPx2 fused to TDP-43 residues 271-345, 311-380, or 346-414.

Protein expression and purification

The TDP-43 putative NES with 3 surrounding residues,, was cloned into pMAL-TEV. PKI-NES and TDP-43 "NES" were expressed in BL21 E. Coli, and induced at 25 degrees celsius with 0.5 mM isopropyl β-D-1-thiogalactopyranoside for 10 hours. Cells were lysed in lysis buffer (500 mM Tris pH 7.5, 200 mM NaCl, 10% glycerol, 2mM DTT, leupeptin, benzamide, pefablock). Then PKI-NES and TDP "NES" were purified using affinity chromotography with amylose beads and then ion exchange chromotography (HiTrap Q, GE Healthcare Life Sciences) using a 0 to 15% NaCl gradient. Purified MBP-NESs were concentrated and buffer exchanged overnight for use in downstream assays.

Ran and Crm1 were expressed and purified as previously described [173].

Pull down binding assays and competition bleaching experiments

Pull down binding assays and competition bleaching experiments were performed as described in Fung et al [173]. Data for competition bleaching experiments was analyzed in PALMIST, and binding curves were generated using GUSSI.

Cell Culture

HeLa Tet-On and 3T3 cells were maintained in Dulbecco's modified Eagle's medium supplemented with 10% fetal bovine serum, 1% penicillin/streptomycin at 37 degrees in bank percentage oxygen. Hippocampal neurons were isolated from C57/BL6 rat P2 pups and cultured as previously described in Li et al [187].

Knockdown, transfection, Drugs, and antibodies

siRNAs targeting TDP-43 and XPO1 were synthesized by Dharmacon. For TDP-43, an individual siRNA was used (D-012394-04, seq:GCAAACUUCCUAAUUCUAA). For XPO1, a pool was used: M-003030-02-0005, seq: GAAAGUCUCUGUCAAAAUA, GCAAUAGGCUCCAUUAGUG, GGAACAUGAUCAACUUAUA, GGAUACAGAUUCCAUAAAU.

Cells were transfected with siRNAs using Lipofectamine RNAiMax (ThermoFisher 13778150) according to manufacturer's instructions. All transfections (including hippocampal neurons) were performed using Lipofectamine 2000 (ThermoFisher 11668019) according to manufacturer's instructions. Leptomycin B was purchased from LC Laboratories (Cat # L-6100), and stored as an ethanol solution at -20. HeLa Tet-On cells were treated with 10 nMol for 12 hours, and hippocampal neurons with 10 nMol for 7 hours.

Primary Antibodies: GAPDH (Cell Signaling 2118), TDP-43 (Proteintech 10782-2-AP), Histone H3 (Abcam ab1791), Flag (Sigma M2, F1804).

Secondary Antibodies (for western blotting): IRDye 680RD Goat anti-Rabbit (LI-COR 926-68071), IRDye 800CW Goat anti-Mouse (LI-COR 926-32210).

Secondary Antibodies (for immunofluorescence):Alexa Fluor 488 Goat anti-mouse (Life Technologies A11001), Alexa Fluor 488 anti-rabbit(?)

CFTR Splicing Assay

HeLa tet-On cells were co-transfected with T5 CFTR minigene (containing blank mutation) and either pBUD TDP-43 or empty vector. 24 hours later, RNA was harvested using the Nucleospin RNA kit (Macherey-Nagel 740955.50) . cDNA was synthesized using high-capacity cDNA reverse transcription kit (Applied Biosystems 4368814). Splicing was assessed either a) by PCR amplification of CFTR exon 9 using flanking primers (see table) followed by gel electrophoresis to separate splice variants, detected with ethidium bromide or b) quantitative real-time PCR with splice specific primers (see table).

Quantitative real-time PCR and calculation of TDP-43 specific activity

Quantitative PCR was performed on blank machine using Power SYBR Green PCR Master Mix (Applied Biosystems 4367659). HPRT was used as a loading control, and relative transcript levels were calculated using the delta delta Ct method.

To calculate TDP-43 specific activity, each experiment contained cells co-transfected with empty vector and three concentrations of WT TDP-43 (0.05 ug, 0.15 ug, and 0.5 ug). Cells expressing all other TDP-43 variants were transfected with one concentration, 0.5 ug. Transcript levels of TDP-43, CFTR +9, and CFTR -9 were calculated using quantitative

real-time PCR, using the delta delta Ct method with HPRT as a loading control. For each sample, normalized splicing index was calculated as : Normalized splicing index = (CFTR +9)/((CFTR -9)(TDP-43)). The normalized splicing index for the three WT samples was averaged. The specific activity of each TDP-43 mutant was calculated as : specific activity of mutant = (normalized splicing index of mutant)/(average normalized splicing index of WT). For each mutant, the specific activity is the average of at least three independent experiments.

Nuclear and cytosolic fractionation

Fractionation was performed as described in Gagnon et al[188]. Briefly, cells were counted and then lysed in a proportional volume of hypotonic lysis buffer (10 mM Tris, pH 7.4, 10 mM NaCl, 3 mM MgCl2, 0.3% NP-40, 10% glycerol, Protease inhibitor tablet and NaVO4) with light agitation. After a low speed spin cytosolic fraction was removed, and NaCL was added for a final concentration of 150mM Nacl. Intact nuclei were rinsed once more with hypotonic lysis buffer, then resuspended in nuclear lysis buffer (20 mM Tris, pH 7.4, 150 mM NaCl, 3 mM MgCl2, 0.3% NP-40, 10% glycerol). Cytosolic and nuclear lysates were boiled at 100 degrees celsius for 5 min in 1X Laemmli buffer, then run on a 10% Tris-Gly gel and transferred onto a PVDF membrane (Millipore). Primary and secondary antibodies used for detection listed above.

Blot was scanned using an Odessey cLx.

Live cell imaging

HeLa tet-On cells were plated in 24 well dishes and transfected as usual 24 hour later. Cells were incubated overnight, then nuclei were stained with Hoescht (Invitrogen 33342), and nuclei and fusion proteins were detected with direct fluorescence. Images are from 20X or 40X objective, gathered using Nikon Eclipse TE2000-U microscope and Photometrics CoolSNAP ES2 camera. Path analysis was performed using the Nikon elements Software.

Immunofluorescence

HeLa tet-On cells or hippocampal neurons were plated on glass coverslips and treated as indicated. Cells were processed for immunofluorescence as follows: 10 minute fixation in 4% Paraformaldehyde, 10 minute permeabilization in 0.5% Triton-X 100, 30 minute blocking in 10% Normal Goat Serum (Invitrogen 50062Z). Cells were incubated with primary antibodies overnight (listed above) and secondary antibodies for 1 hour at room temperature,followed by Hoescht staining (Invitrogen 33342) and/or phalloidin staining(Alexa Fluor 555 Phalloidin, Life Technologies A34055). Coverslips were mounted on glass slides using Prolong Gold antifade mounting reagent (Life Technologies P36934) and visualized using the 60X objective on the Nikon Eclipse TE2000-U. Images were obtained using Photometrics CoolSNAP ES2 camera. Images were analyzed using Nikon Elements software.

Heterokaryon shuttling assay and calculation of shuttling index

HeLa-tet-On cells were transfected, and 24 hours later were co-plated with 3T3 cells on glass coverslips. Cells were incubated for 3 hours, then cycloheximide was added (100 ug/ml) and cells were incubated an additional 30 minutes. Then slides were inverted on 50% poly ethylene glycol in serum-free media for 2 minutes to form heterokaryons. Slides were rinsed in PBS and returned to cycloheximide-containing media. Cells were incubated an additional 3 hours then processed for immunofluorescence as usual.

Heterokaryons were confirmed by visualizing the actin cytoskeleton. At least 5 heterokaryons were counted for each condition during each experiment, with at least three independent experiments.

Nuclear fluorescence was quantified by manually outlining the nuclei (Hoechst stained) and comparing to a manually outlined control using NIS elements software. Shuttling index, or "SI" was calculated as the normalized ratio of recipient nucleus fluorescence/donor nucleus fluorescence: (3T3 fluorescence - background)/(HeLa tet-On nuclear fluorescence-background).

Table 2.2: Primer Sequences

	Forward	Reverse
qPCR: CFTR +9	GAT ACC ATC ATC CCA GGG ATT T	AAG AGG CTG TCA TCA CCA TTA G
qPCR: CFTR -9	ATC ATC CCA GCT GTT CCT C	GGT CAC CAG GAA GTT GGT T
qPCR: TDP-43	TGC TGC TCT CCA CGG TTA C	CAG CCG GAC ACC TCT CAT A
qPCR: HPRT	CTG AGG ATT TGG AAA GGG TGT T	ATC TCC TTC ATC ACA TCT CGA G

CHAPTER THREE

PATHOGENIC SIGNAL SEQUENCE MUTATIONS IN PROGRANULIN DISRUPT SRP INTERACTIONS REQUIRED FOR MRNA STABILITY

Abstract

Proteins which accumulate in inappropriate cellular compartments can misfold or aggregate, causing toxicity. In response, cells have evolved quality control pathways to prevent mis-trafficking of proteins. One line of defense is coupling mRNA stability to the co-translational trafficking of the associated nascent chain. Thus, if a protein fails to traffic correctly, its mRNA is specifically degraded, preventing further production of the aberrant protein. This recently described quality control mechanism is termed RAPP for Regulation of Aberrant Protein Production. Data presented here demonstrate a natural RAPP substrate in man. A mutant form of a secreted neurotrophic factor, A9D progranulin, is unable to recruit the targeting factor Signal Recognition Particle (SRP). This triggers RAPP and the resulting mutant progranulin mRNA degradation. As a result, patients carrying the A9D mutation exhibit progranulin haploinsufficiency, which leads to neurodegeneration. Thus, the trafficking factor SRP plays a central role in the molecular pathology of A9D progranulin.

Introduction

Proper protein trafficking is critical for mammalian cells. An incorrectly trafficked protein can cause toxicity, either by its absence from the intended compartment, or by misfolding into a toxic new conformation in the altered folding environment of a new compartment.

The trafficking information for a typical secretory protein is embedded in its N-terminal sequence, called a signal sequence[189]. Signal sequences are recognized by the targeting factor SRP (Signal Recognition Particle) and directed to the ER membrane for translocation [190]. This interaction occurs during translation -- soon after the signal sequence emerges from the ribosomal tunnel -- and is the critical first step for secretion [190].

Recent work has indicated SRP recruitment is also critical for stability of the translating secretory mRNA. If a secretory protein fails to interact with SRP, it triggers the quality control process RAPP [160, 191]. Engaging RAPP leads to selective degradation of the translating mRNA, preventing further futile production of the aberrant protein. RAPP was discovered using engineered deletions in the secretory protein preprolactin [160].

To date, natural substrates for RAPP have not been reported, despite a preponderance of human diseases associated with a mutation in the signal sequence of a critical secretory protein (see discussion). One such example is the neurodegenerative disease FTLD (Frontotemporal Lobar Degeneration), which in some patients is a result of inheriting a single loss-of function mutation in the secretory protein progranulin. One common loss-of function mutation is A9D, which resides within the hydrophobic core of the signal sequence [88].

This mutation was previously demonstrated to disrupt secretion in a cell culture system, and is associated with a reduction of progranulin in the CSF of patients [107]. Two additional polymorphisms within the progranulin signal sequence, V5L and W7R, have been reported. Both have been found in FTLD patients, but their role in disease remained unclear [192, 193].

We hypothesized that A9D might prevent recognition of the progranulin signal sequence by SRP, triggering RAPP. Additionally, we hypothesized that the disease relevance of the two additional polymorphisms, V5L and W7R, depended on their fitness as RAPP substrates. The data presented here demonstrate the far-reaching implications of the recently discovered mRNA/protein quality pathway, RAPP, in human disease.

Results

The progranulin signal sequence mutations W7R and A9D alter interaction with the targeting factor SRP.

Signal sequences share a three domain structure: a basic "N" domain, a slightly polar "C" domain, and a central, hydrophobic "H" domain [189, 194]. All three signal sequence polymorphisms are within the "H" domain of the progranulin signal sequence. Both W7R and A9D introduce a polar amino acid, dramatically altering local hydrophobicity (Fig 3.1A). These substitutions would thus be predicted to disrupt SRP recruitment, while the more conservative V5L substitution would not.

To determine whether W7R and A9D impair SRP recruitment, we employed arrested *in vitro* translation with site-specific photocrosslinking [160, 195]. This method can identify proteins in proximity to the translating nascent chain, which are too ephemeral to detect in cells. In brief, the method is based on incorporation of a photocrosslinking probe into the nascent chain by use of a modified tRNA in an *in vitro* translation reaction of a truncated mRNA. When the translation reaction is exposed to UV light, the photocrosslinking probe forms a covalent bond to proteins in close proximity (Figure 3.1B).The nascent chain interactions detected using this method are highly dependent on a) the position of the cross-linking probe within the nascent chain, controlled by positioning the amber stop codon within the mRNA and b) the length of the nascent chain at the time of cross-linking, which the researcher controls by truncating the mRNA. In the case of progranulin, we were guided by the optimal conditions for the related protein PPL [195]. Reactions contained truncated WT or mutant GRN mRNAs with an amber-stop codon in position 13, corresponding to the

middle of the signal sequence. The mRNAs were truncated at codon 86 to produce translationally-arrested ribosome-nascent chain complexes with about 50 amino-acid residues exposed from the ribosome peptide exit tunnel. Translation reactions included S^{35}-methionine to radiolabel the nascent chains, and were separated by SDS-PAGE. Photocrosslinking adducts were detected by the shift in electrophoretic mobility of the radiolabeled nascent chain (Figure 3.1B).

In vitro translation reactions with WT PPL, WT GRN, A9D GRN, and W7R GRN 86-codon truncated mRNAs were performed in parallel. Some reactions were supplemented with purified canine SRP. Consistent with earlier findings, the WT PPL nascent chain formed an adduct with SRP54, the subunit of SRP which binds signal sequences (Figure 3.1B)[196, 197] . Because the GRN nascent chain is the same size as the PPL nascent chain, a GRN-SRP54 photoadduct would migrate similarly to a PPL-SRP54 photoadduct. As expected, WT GRN formed an adduct consistent with SRP54 (Figure 3.1B). In contrast, no detectable adducts of that size were formed with the A9D or W7R nascent chains, indicating that the disease-causing mutations inhibit this interaction (Figure 3.1B).

Figure 3.1: W7R and A9D mutations disrupt SRP recruitment, leading to inefficient expression and secretion

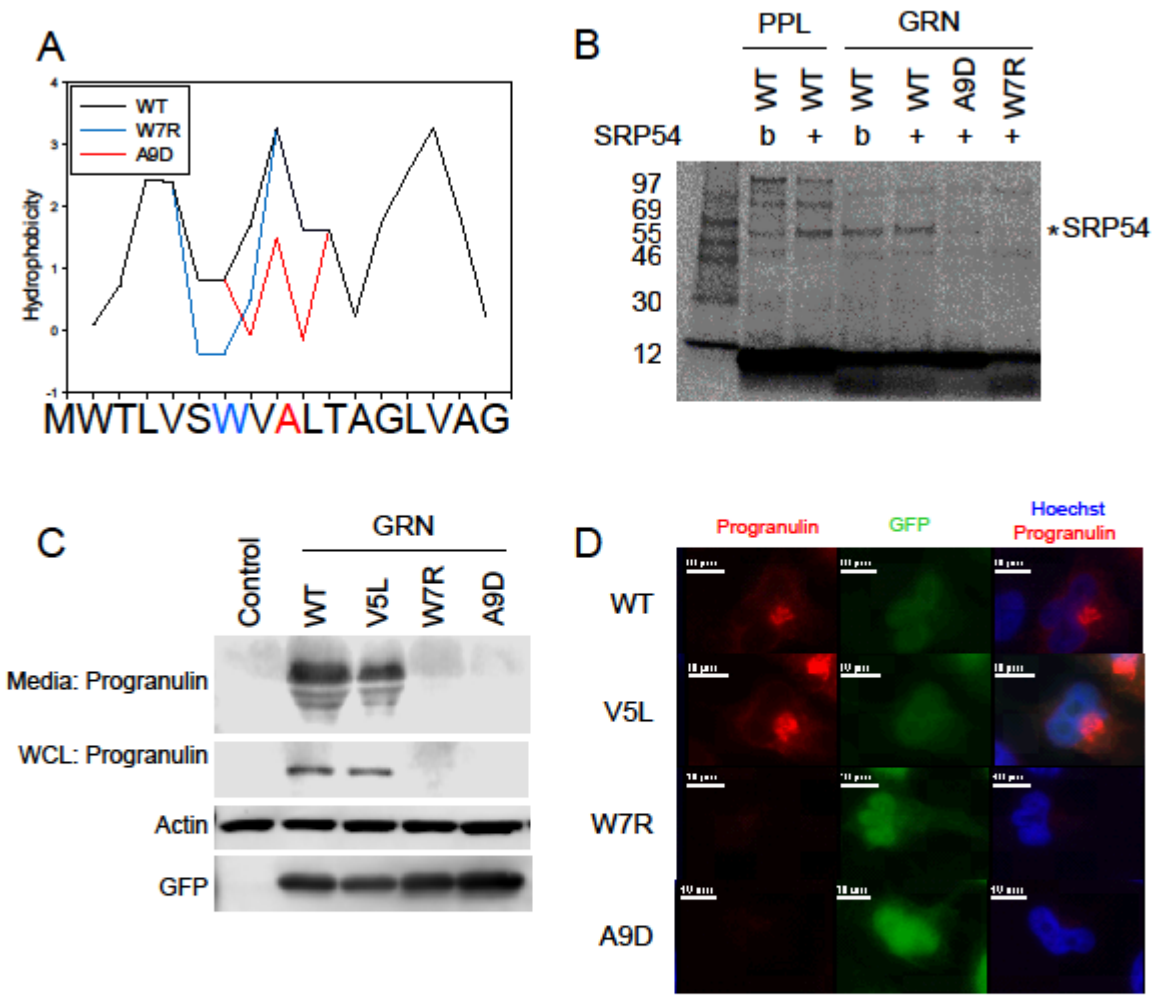

A. Kyte-Doolittle plot of hydrophobicity of either WT (black), W7R (blue), or A9D (red) GRN signal sequence.
B. Autoradiograph of electrophoresed photoadducts of 86 amino acid nascent chains- either WT PPL, WT GRN, or A9D GRN. Indicated samples were supplemented with purified SRP.
C. Western blot of media and whole-cell lysate (WCL) of HeLa Tet-On cells transfected with either WT, V5L, W7R, or A9D GRN.
D. Immunofluorescence of HeLa Tet-On cells transfected with either WT, V5L, W7R, or A9D GRN. GFP, expressed from the same plasmid, is shown as a transfection control.

Figure 3.1S: A9D is RIPA-insoluble, not glycosylated, and accumulates in puncta

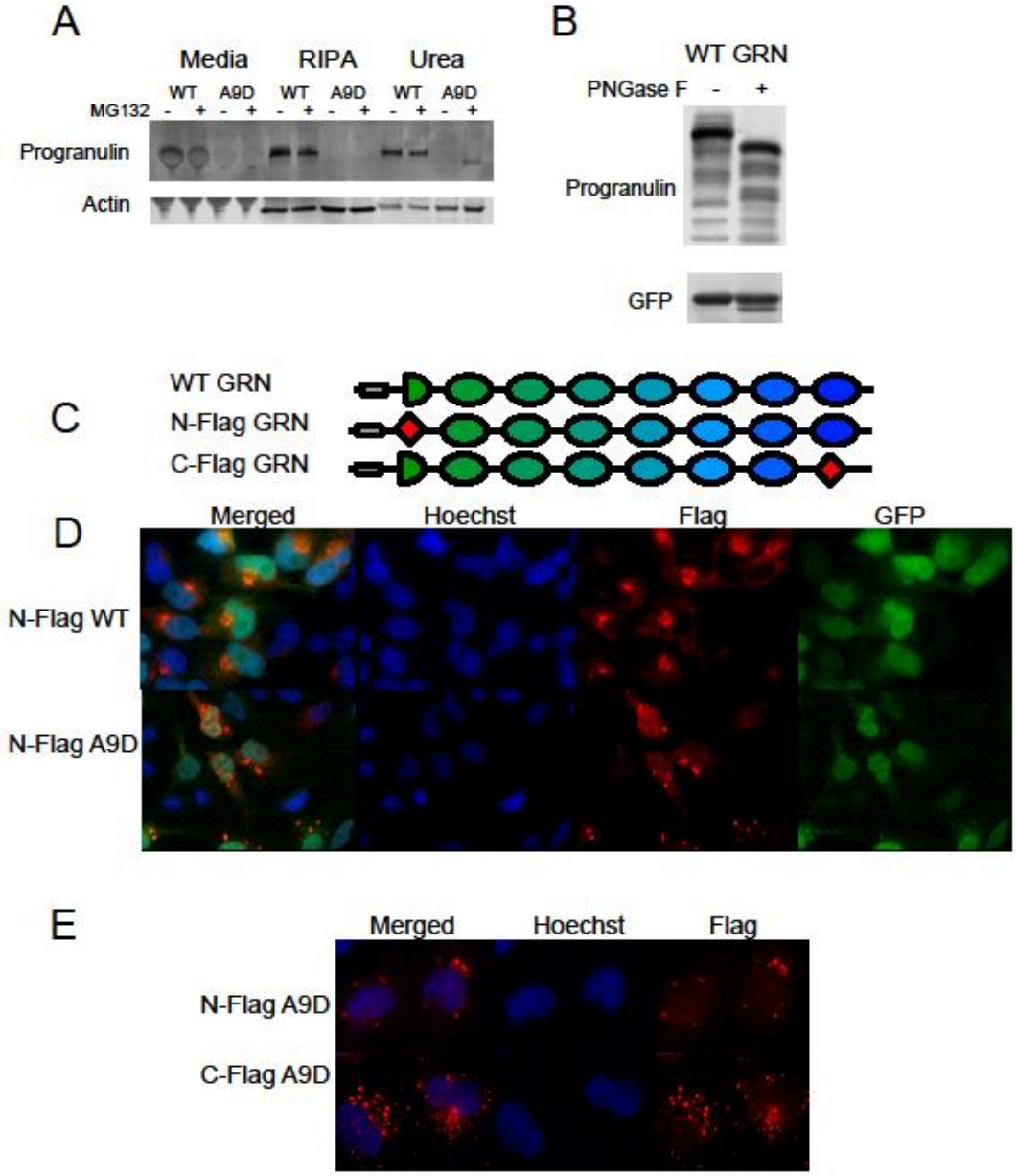

A. Western blot of HeLa Tet-On cells expressing WT or A9D progranulin, extracted sequentially with RIPA buffer and urea buffer
B. Western blot of HeLa Tet-On cells expressing WT PGRN. Indicated lysate was treated with PNGase F.
C. Domain map of Flag-tagged GRN constructs.
D. Immunofluorescence of HeLa Tet-On cells expressing indicated Flag tagged GRN
E. Immunofluorescence of HeLa Tet-On cells expressing indicated Flag tagged GRN

W7R and A9D mutations prevent secretion

To confirm that the inability of W7R and A9D to recruit targeting factor SRP impaired trafficking, we evaluated expression and secretion of the four variants. GRN variants were transiently expressed in HeLa Tet-On cells, and expression was evaluated by western blot and immunofluorescence. As predicted, V5L was expressed and secreted at similar levels to WT, while W7R and A9D were not detected in either cells or media (Figure 3.1C). Moreover, immunofluorescence confirmed the presence of WT and V5L within the secretory pathway, while W7R and A9D were not observed (Figure 3.1D).

Full-length A9D GRN accumulates in RIPA-insoluble puncta

To determine whether any A9D GRN protein was sequestered in RIPA insoluble pellet, I performed sequential extraction of whole-cell lysate. I found that a small amount of A9D GRN protein is seen in the urea soluble fraction, which is increased with MG132 treatment (Fig 3.1SA). A9D GRN migrated more quickly than WT GRN. Others have shown that WT GRN is heavily glycosylated, and this glycosylation retards migration during electrophoresis. When lysate containing WT GRN is treated with the glycosidase PNGase F, WT GRN migrates more quickly as expected (Fig 3.1SB). A9D GRN migration is unchanged with PNGase treatment (data not shown), suggesting that A9D GRN does not reach the ER.

In order to visualize A9D GRN protein in the cell, I made several tagged fusion proteins, in which a single domain of GRN was replaced by a flag-tag (Fig 3.1SC). I then performed immunofluorescence on cells overexpressing either Flag-tagged WT GRN or flag-tagged A9D GRN. The flag-tag did not affect localization of WT GRN (Fig 3.1SD). Flag

A9D GRN, unlike WT, accumulated in puncta. These puncta were unchanged by addition of MG132 (data not shown). These A9D GRN puncta also formed regardless of the location of the flag tag, suggesting the puncta represent fully translated GRN. Thus, A9D GRN is fully translated, but rather than trafficking normally, accumulates in RIPA-insoluble puncta.

W7R and A9D mRNA levels are decreased relative to WT and V5L

We hypothesized that the loss of an SRP interaction would trigger mRNA degradation. We first compared mRNA levels of WT, V5L, W7R, and A9D GRN in transfected HeLa Tet-on cells. Strikingly, the mRNA levels segregated into two groups: higher in WT and V5L, which are efficiently secreted, and ~70% lower in W7R and A9D, which cannot efficiently recruit SRP (Figure 3.2A).

Reduction in A9D mRNA is caused by a specific, transferable degradation

Reduced mutant mRNA levels could result from either decreased transcription or increased degradation. To distinguish between these two possibilities, we assessed both WT and A9D mRNA turnover. WT and A9D GRN were transiently expressed under control of a tetracycline responsive promoter in HeLa Tet-Off cells. PGRN transcription was inhibited by doxycycline, and PGRN mRNA levels were assessed, as a function of time, using qPCR. Notably, A9D PGRN mRNA was degraded significantly faster than WT, with a half-life of 1.7 hours (±S.E. 1.6, 1.9) for the mutant versus 7.9 hours for WT and (± S.E. 6, 11.4) (Figure 3.2B).

Figure 3.2: W7R and A9D mRNA are subject to specific, transferable degradation

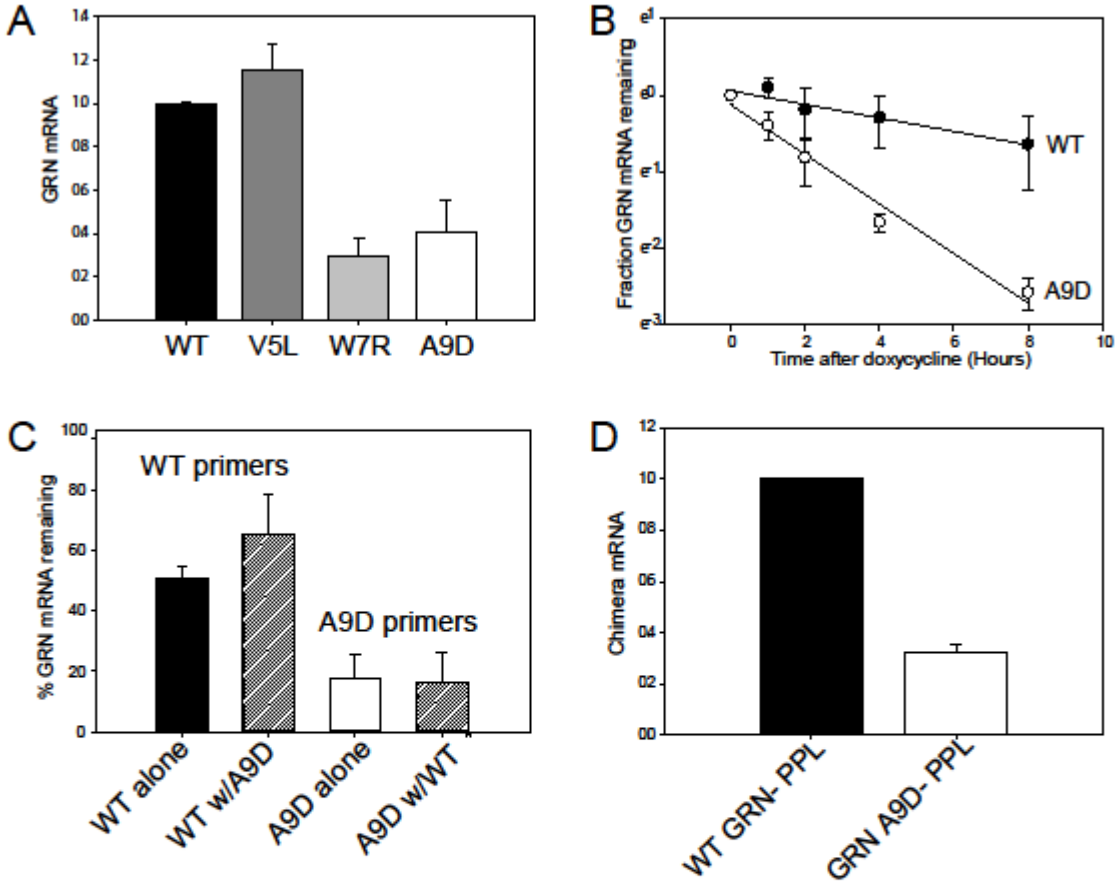

A. qPCR analysis of steady state GRN mRNA levels in cells transiently expressing WT, V5L, W7R, or A9D progranulin.
B. qPCR analysis of WT or A9D GRN mRNA levels over time after inhibition of transcription in HeLa Tet-Off cells. Data were plotted on a natural log scale.
C.qPCR analysis of WT and A9D GRN mRNA levels after 8 hours of transcriptional inhibition in HeLa Tet-Off cells expressing WT alone, A9D alone, or co-expressing WT and A9D progranulin. GRN was detected using either WT or A9D specific primers.
D. qPCR analysis of WT GRN-PPL and A9D GRN-PPL mRNA fusion of GRN signal sequence, either WT or A9D, to PPL mature protein sequence) in transiently transfected HeLa Tet-On cells. Hybrid mRNAs were detected with PPL primers.

The short half-life of A9D GRN mRNA, relative to WT, suggested that it was specifically degraded. However, stress can affect mRNA turnover, and expression of an aberrant secretory protein like A9D progranulin could provoke a nonspecific stress response. To determine whether A9D mRNA was specifically targeted, the rate of WT and A9D mRNA turnover was assessed in cells co-expressing WT and A9D GRN. As before, WT and A9D GRN were transiently expressed in HeLa Tet-On cells, and then transcription was inhibited by doxycycline. GRN mRNA levels were assessed at the time of doxycycline treatment and 8 hours later, using qPCR with sequence specific primers. The percent of WT mRNA remaining after 8 hours of transcriptional inhibition was unchanged in the presence of A9D mRNA, and *vice versa* (Figure 3.2C), consistent with mutant specific mRNA degradation.

To determine whether the mutant signal sequence alone was sufficient to confer instability to an mRNA, two fusion proteins were constructed: the signal sequence of preprolactin was replaced by either the WT or A9D progranulin signal sequence (referred to as WT PGRN-PPL or A9D PGRN-PPL). Chimeric proteins were expressed in cultured cells, and PGRN-PPL mRNA was assessed using qPCR with PPL specific primers. As predicted, the A9D PGRN-PPL mRNA was targeted for decay, while WT PGRN-PPL mRNA was not (Figure 3.2D).

SRP protects WT GRN mRNA from degradation

The mRNA levels of four GRN variants -- WT, V5L, W7R, and A9D -- segregated with the ability of the translating nascent chain to recruit SRP. To determine whether this segregation was SRP dependent, steady-state mRNA levels were assessed in control or SRP54 siRNA treated cells. As seen earlier, in control siRNA treated cells, W7R and A9D mRNA levels

were reduced compared to WT. However, in SRP54 siRNA treated cells, W7R and A9D mRNA levels were unchanged while WT and V5L mRNA levels were dramatically depleted (Figure 3.3A). As expected from the reduction in WT and V5L GRN mRNA, WT and V5L progranulin protein levels were also reduced in SRP54 siRNA treated cells (Figure 3.3C).

To confirm that the decrease in WT mRNA levels after SRP knockdown was due to a specific increase in turnover, WT and A9D GRN mRNA turnover were assessed in cells treated with either control siRNA or SRP54 siRNA. As before, the TET-Off system was used. Consistent with earlier results, the half-life for WT GRN mRNA was significantly longer than that of A9D mRNA: 5.1 hours for WT (± S.E. 4.7, 5.7), 1.7 for A9D (± S.E. 1.6, 1.8)) (Figure 3.3B). However, in SRP54 siRNA-treated cells this difference was no longer seen; WT mRNA was degraded at the same rate as A9D: half-life of 1.6 hours for WT (± S.E. 1.5, 1.7) versus 1.8 for A9D (± S.E. 1.7, 2.1)) (Fig 3.3B). Thus, co-translational recruitment of SRP54 is critical for WT mRNA stability.

Mutant mRNA degradation is translation dependent

To test whether translation was necessary for W7R and A9D mRNA degradation, we used the elongation inhibitor cycloheximide (CHX). In CHX treated cells, where no nascent chain was produced and exposed, W7R and A9D mRNA levels were restored to WT (and V5L) levels (Figure 3.3D). As expected, translation inhibition by CHX was robust, dramatically reducing progranulin protein (Figure 3.3E). This result demonstrates that the mRNA degradation requires translation and may be initiated on translating ribosomes.

Figure 3.3: Differential stability of WT GRN mRNA is SRP dependent and translation dependent

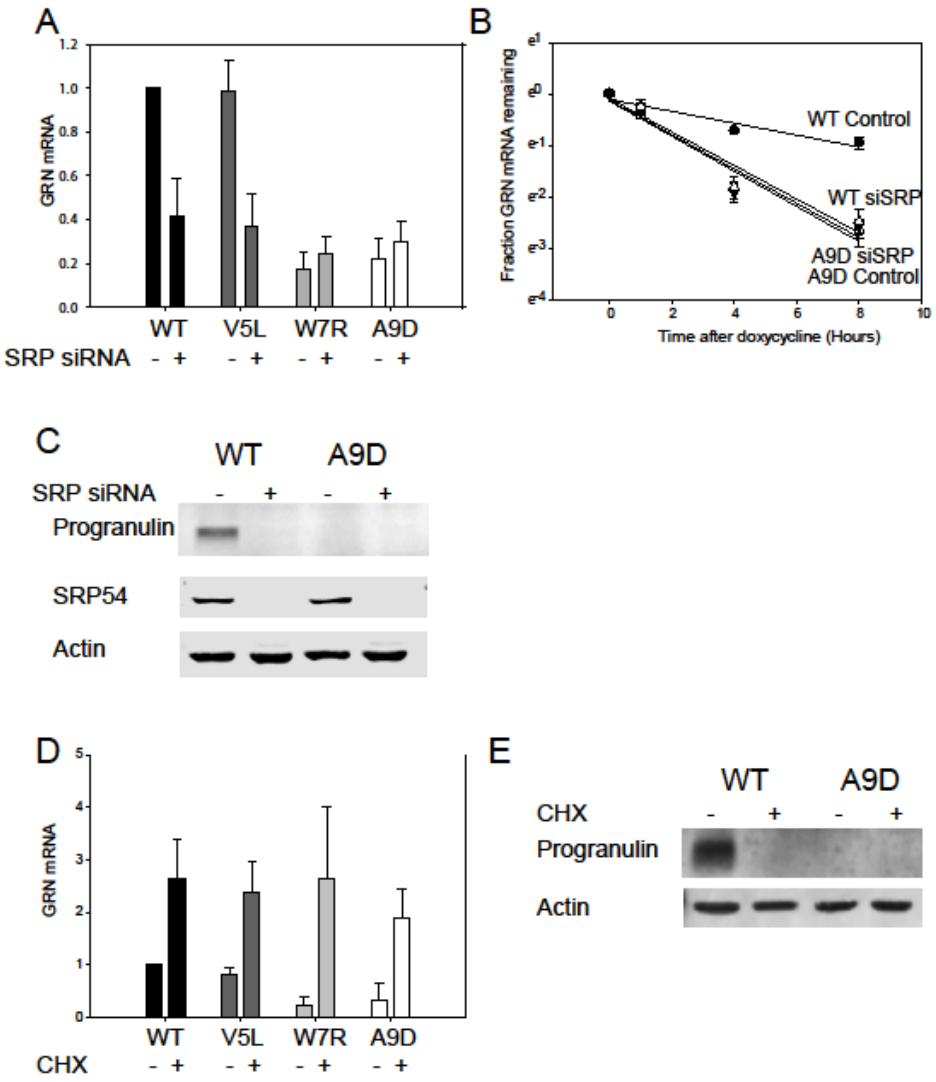

A. qPCR analysis of GRN mRNA levels in cells transiently expressing WT, V5L, W7R, or A9D progranulin, in the presence or absence of SRP54 siRNA.
B. qPCR analysis of WT or A9D GRN mRNA levels over time after inhibition of transcription, in HeLa Tet-Off cells treated with control siRNA or SRP54 siRNA.
C. Western blot of HeLa tet-On cells treated with control or SRP54 siRNA, transiently expressing WT or A9D progranulin.
D. qPCR analysis of GRN mRNA levels in cells transiently expressing WT, V5L, W7R, or A9D progranulin, in the presence or absence of CHX.
E. Western blot of HeLa tet-On cells treated with control or CHX, transiently expressing WT or A9D progranulin.

Based on these results, we conclude that W7R and A9D progranulin are RAPP substrates, while V5L is not. While we have not tested the function of V5L progranulin, the signal sequence is generally cleaved in the ER [198], so we would expect secreted V5L to be identical to secreted WT progranulin and therefore functional. Thus, we predict that V5L is a benign polymorphism, while W7R, like A9D, disrupts progranulin secretion and causes FTLD.

A9D progranulin triggers RAPP in patient-derived fibroblasts

To determine whether endogenous A9D GRN is a RAPP substrate in the context of human disease, we obtained fibroblasts from an FTLD patient carrying the A9D mutation. Sequencing confirmed that the fibroblasts are heterozygous for the A9D mutation (Figure 3.4A).

We inferred A9D GRN mRNA degradation in patient cells by assessing steady-state WT and A9D mRNA levels. First, we used a previously employed [88] qualitative approach-sequencing cDNA from patient cells and comparing WT and A9D peak heights, which correspond to cDNA (and thus mRNA) abundance (Figure 3.4A). The WT and A9D peaks were of similar height in the genomic DNA tracing, but the A9D peak was far smaller than the WT peak in the cDNA sequencing tracing, consistent with the previous report [88]. In addition, we used a more quantitative method: qPCR with WT and A9D specific primers. By this method, only ~8% of the GRN mRNA in the patient fibroblasts is A9D (Figure 3.4B). Together, these results demonstrate that A9D mRNA is significantly underrepresented in patient fibroblasts.

Figure 3.4: A9D mRNA is specifically degraded in patient derived cells, and mRNA degradation is translation dependent.

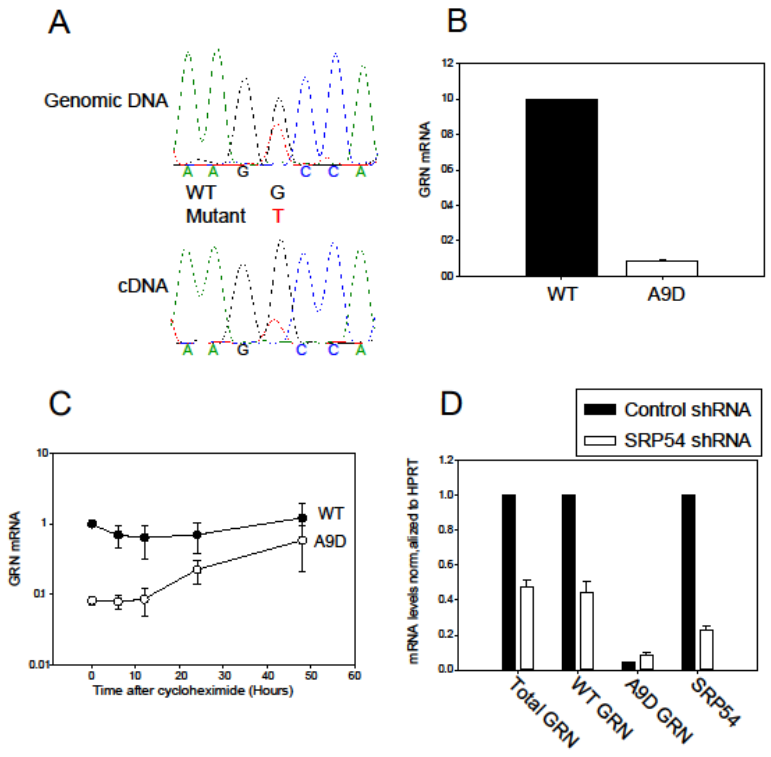

A. Sequence traces of PGRN from primary human fibroblasts. Patient had FTLD and was carrying the A9D PGRN mutation. Top: genomic DNA, bottom: cDNA (mRNA).
B. qPCR analysis of GRN mRNA in patient fibroblasts, using genotype specific primers.
C. qPCR analysis of GRN mRNA levels in patient fibroblasts over time after inhibiting translation with CHX. Genotype specific primers were used for WT (closed circle) and A9D (open circle) GRN variants. GRN mRNA levels were plotted on a log 10 scale.
D. qPCR analysis of WT, A9D, and total GRN mRNA levels in patient fibroblasts treated with either control virus or shRNA SRP54 virus. SRP54 knockdown was confirmed via qPCR.

To test whether A9D mRNA reduction was translation-dependent, fibroblasts were treated with CHX and WT and A9D mRNA levels were assessed over time, using qPCR. While WT mRNA levels showed little response to CHX treatment, A9D mRNA levels increased ~8 fold over 48 hours (Figure 3.4C). At the last time point, the percent of total GRN mRNA which was A9D had more than quadrupled, to about 35% of WT from the initial value of ~8%.

Finally, to confirm that the reduction in A9D mRNA is SRP dependent, I used a virus carrying a shRNA targeting SRP54 to knockdown SRP54 in patient fibroblasts (Fig 3.4D). As predicted, both total GRN mRNA and WT GRN mRNA levels decreased. However, A9D GRN mRNA levels were unchanged (Fig 3.4D.

Figure 3.5: Model of RAPP (Regulation of Aberrant Protein Production)

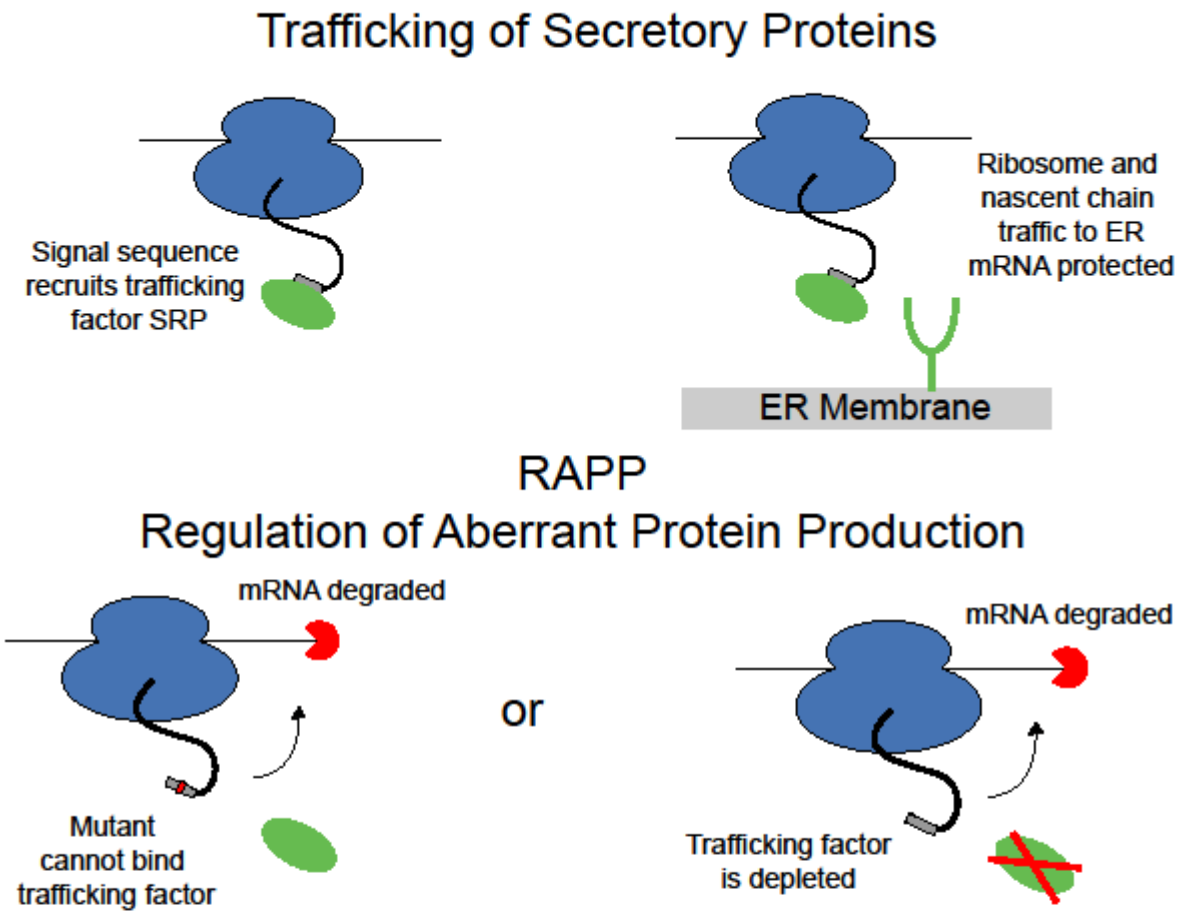

Discussion

Here, we present evidence that two mutant forms of progranulin, W7R and A9D, are targeted by the RNA/protein quality control pathway RAPP. In patients carrying these mutations, the consequence of RAPP activation is progranulin haploinsufficiency and the neurodegenerative disease FTLD. Additionally, our study suggests that another signal sequence mutation, V5L, is a benign variant. We have shown that both W7R and A9D progranulin fail to recruit the targeting factor SRP, triggering the specific translation-dependent degradation of their mRNAs. Moreover, translation-dependent, mutant specific mRNA degradation is also seen in FTLD patient-derived fibroblasts. This is the first evidence that RAPP plays a role in the pathophysiology of human diseases caused by signal sequence mutations.

Mutant progranulin is clearly subject to RAPP. However, there are some differences between mutant progranulin and PPLΔ4L, the first described RAPP substrate. For example, in the original report, PPL mRNA stability depended on the balance between two interactions of the nascent chain: SRP and Ago2. This was based on evidence of proximity: Ago2 crosslinked preferentially to the mutant nascent chain, and an Ago2 IP pulled down specifically mutant PPL mRNA. Additionally, there was functional evidence that Ago2 played a role in mRNA degradation--overexpression decreased PPL mRNA, while knockdown protected mutant PPL mRNA. By contrast, for progranulin, while SRP plays a very similar role, we did not observe evidence of Ago2 participation. Neither Ago2 knockdown nor overexpression had measurable effect on either mutant or WT GRN mRNA

turnover under the conditions employed (data not shown), suggesting the role of Ago2 may be substrate specific.

The existence of natural RAPP substrates confirms the physiological relevance of this quality control pathway. However, we anticipate that this expanded role for RAPP will be central for many disparate genetic diseases. In fact, a survey of the literature demonstrates a handful of disease-causing signal sequence mutations which would be predicted to disrupt SRP recruitment. For example, the L15R mutation in *UGT1A1*, which causes Crigler-Najjar Type II [168] and the L25R mutation in *COL5A1*, which causes Ehlers-Danlos [170], both substitute a polar amino acid for a hydrophobic residue. Additional potential RAPP substrates include C18R in *PTH*, which causes Familial isolated hypoparathyroidism [167] and the Y6D mutation in *DSPP*, which causes dentine dysplasia type II [169]. There are also signal sequence mutations would not be predicted to disrupt SRP recruitment, but are nevertheless associated with loss of secretion, such as the A15G mutation in *POMC*, associated with obesity [171]. This study of A9D progranulin reveals a new mechanism of molecular pathology that likely underlies multiple genetic diseases.

Figure Contributions:

Figure 1B was the work of Andrey Karamyshev, Ph. D.

Materials and Methods:

Cell Lines and Drug Concentrations

HeLa Tet-On (Clontech) and HeLa Tet-Off cells (Clontech) were maintained in Dulbeco's Modified Eagle Medium (DMEM, Sigma) supplemented with 10% Fetal Bovine Serum (Gemini); 50,000 U Penicillin; and 50 mg Streptomycin (Gibco). Cultures were maintained in 37 incubator with 5% CO2. Cells were treated with cycloheximide (CHX) at 50 ug/ml for 24 hours. Cells were treated with Doxycycline (Sigma) at 1 ug/ml for indicated times.

The patient fibroblasts were obtained from the NINDS Human Genetics Resource Center DNA and Cell Line Repository (https://catalog.coriell.org/1/ninds) . NINDS Repository sample numbers corresponding to the samples used are: ND40082. Untransformed fibroblasts were cultured in Media X (4 parts DMEM to 1 part medium 199; Hyclone, cat. no. SH3A1845.02) supplemented with FBS and antibiotics in coated flasks, and grown under low oxygen (2% oxygen, 5% CO_2 and 93% nitrogen) at 37 degrees [199] . Fibroblasts were subcultured with Trypsin/EDTA (Cascade Biologics, cat. no. R-001-100). All experiments were performed on fibroblasts between p.9-12.

Fibroblasts were treated with cycloheximide at 10 ug/ml, for the indicated time period.

Plasmids, DNA Techniques, and tRNA

GRN cDNA was obtained from DNASU(HsCD00022162)and cloned into pBI-eGFP (Clontech) vector using restriction sites for SalI and EcoRV.

V5L, W7R, A9D, and amber stop codons were introduced using site-directed mutagenesis (see Supp Table 1 for primers). To generate the tet-dependent PGRN constructs, WT and

A9D PGRN were pcr amplified (see Supp Table 1 for primers) and subcloned into pTRE2-hyg (Clontech) vector using BamHI and EcoRV restriction sites.

All constructs were sequenced to confirm.

DNA fragments for in vitro transcription were generated by standard PCR techniques. For in vitro translation and photocrosslinking experiments mRNAs were transcribed in vitro using SP6 RNA polymerase and PCR-produced DNA fragments of the desired length as before [200] and purified using the RNeasy Mini kit (QIAGEN). N^{ε}-(5-azido-2-nitrobenzoyl)-Lys-$tRNA^{amb}$ (εANB-Lys-$tRNA^{amb}$) was prepared as described earlier [200] and [201]. This tRNA contains an anticodon that recognizes an amber stop codon in mRNA. Briefly, $tRNA^{amb}$ was synthesized in vitro by T7 RNA polymerase, purified by chromatography on MonoQ column, aminoacylated with [^{14}C]Lys in vitro, purified again on the same column, and chemically modified with ANB. This εANB-Lys-$tRNA^{amb}$ was used for photocrosslinking experiments.

cDNA Synthesis and qRT-PCR

RNA was extracted using the Macherey-Nagel Nucleospin kit according to manufacturer's instructions (740955). Samples were reverse transcribed using high-capacity cDNA reverse transcription kit (Thermoscientific 4368813). qPCR was performed using a 7900HT Fast Real-time PCR system (Applied Biosystems) and Power SYBR green master mix (Applied Biosystems 4367659). Primer sequences can be found in Table 1. GFP was used as a normalization control. Relative expression levels were determined using the ΔΔCT method. All experiments use a minimum of three technical replicates per sample and at least three biological replicates per analysis.

For the mRNA turnover experiments, mRNA quantity at each timepoint was normalized to "time 0" using the ΔΔCt method, where GFP was used as a loading control. For both WT and A9D, data points were fit onto a two-parameter exponential decay curve using SigmaPlot 12.0, y = a* exp (-b*x). Half-life was calculated as ln (2/b). The standard error in half-life was calculated using e, the standard error of b: ln (2/b-e) and ln (2/b+e).

SRP54 knockdown in patient fibroblasts

Fibroblasts were plated at ~50% density and treated with polybrene (5ug/ml) and either control shRNA (SHC200V) or shRNA targeting SRP54 (TRCN0000278368), both purchased from Sigma-Aldrich. Two days later, infected fibroblasts were selected with puromycin (1.5 mg/ml). Nine days after treatment with virus, total RNA was isolated as described earlier.

RNAi and PGRN mRNA Stability Experiments

The following siRNAs were synthesized by Dharmacon: SRP54 siRNA (sense:GAAAUGAACAGGAGUCAAUdTdT) [202]; Ago2 specific siRNAs, purchased as a pool (Dharmacon siGENOME smartpool, Cat # M=004639-00), as published[203]. The control siRNA used was purchased from Ambion, Silencer Negative Control #1 siRNA.

For the siRNA experiments, HeLa Tet-On cells were transfected using Lipofectamine RNAiMax, according to manufacturer's instructions. The next day, cells were transfected with WT or mutant GRN plasmids using Lipofectamine 2000, according to manufacturer's instructions.

For the mRNA turnover experiments, HeLa Tet-Off cells were co-transfected with the pTRE2hyg WT or A9D GRN and pBI-CMV2 AcGFP plasmid (for normalization). Thus, WT and A9D GRN were under a promoter with a Tet-responsive element, while GFP was

not. 20 hours after transfection, cells were treated with doxycycline (1 ug/ml) to inhibit transcription of GRN. Cells were harvested, and total RNA collected, at 1,2,4, and 8 hours after doxycycline treatment. Untreated cells were harvested at time 0 as controls. Total RNA was purified using the NucleoSpin RNA II kit (Clontech). WT or mutant PGRN mRNA levels were determined by qPCR.

The SRP knockdown experiments were performed identically, with the exception of siRNA transfection 48 hours prior to transfection of WT or A9D GRN.

Western Blots and Antibodies

Samples for western blotting were prepared as follows: Media was heated at 95 degrees celsius for 10 min in 5X Laemmli buffer (0.3 M Tris-HCl pH 6.8, 50% glycerol (v/v), .05% Bromophenol blue, 0.1 M DTT, 10% SDS(w/v)). Whole cell lysate was prepared either by lysing cells directly in 2X Laemmli or in modified RIPA (1% (w/v)deoxycholic acid (Na salt), 1% (v/v)Triton X-100, 0.1% (w/v)SDS, 50 mM Tris, 150 mM NaCl, pH 7.4 , 1X protease inhibitor (Roche 11836170001). Samples were separated by SDS-PAGE and transferred onto PVDF membranes (Millipore Immobilon-FL IPFL00010). Blots were probed with primary antibodies:PGRN (Proteintech 18410-1-AP), Actin (Millipore JLA20), GFP (Clontech JL-8), SRP54 (BD Bioscience 610940). Secondary antibodies: LI-COR Goat anti-Mouse (926-68070) and LI-COR Goat anti-Rabbit (926-32211). Blots were visualized using the LI-COR Odyssey CLx or film.

Solubility and Glycosylation Analysis

Sequential extractions were performed to compare the solubility profile of WT vs A9D progranulin. Cells were washed with phosphate-buffered saline and lysed in ice cold RIPA (containing protease and phosphatase inhibitors). Lysates were bath sonicated (4 rounds, 30 sec on 30 sec off) then spun at 100,000Xg for 30 min at 4 degrees. Supernatant was taken as "RIPA" fraction. Pellets were resuspended in freshly-made urea buffer (7M Urea, 2M thiourea, 4% CHAPS, 30 mM Tris, pH 8.5) and bath sonicated using the same protocol. Lysates were spun again at 100,000 x g for 30 min at 4 degrees, and supernatant was taken as the "Urea" fraction.

To determine migration of unglycosylated WT GRN, lysate from HeLa tet-On cells transiently expressing WT progranulin was harvested as usual. 20 ul lysate was incubated with 125U of PNGase F for 1 hour at 37 degrees.

For both sequentially extracted and PNGase treated lysates, 5X laemmli buffer was added and samples were boiled at 95 degrees for 10 min. Western blotting analysis was performed as described earlier.

Immunofluorescence Microscopy

HeLa Tet-On cells were cultured on coverslips using standard culture conditions. Then cells were fixed with 4% paraformaldehyde, permeabilized with 0.5% Triton-X 100, and blocked with 10% Normal Goat serum ((Invitrogen 50062Z). Antibodies against PGRN (Proteintech 18410-1-AP) were applied at 1:50, in 10% normal goat serum. PGRN was visualized using the secondary antibody Alexa 594-anti mouse (Thermo Fisher Scientific A11005). Nuclei were stained with Hoescht (Invitrogen 33342). Coverlips were mounted

with Prolong Gold antifade (life technologies P36934), and imaged on a Nikon Eclipse TE2000-U with NIS Elements software, under 60X magnification.

Sequencing of genomic DNA and cDNA

Genomic DNA was isolated from fibroblasts using Wizard Genomic DNA Purification kit from Promega (A1120). Fibroblast cDNA was prepared as above. GRN gDNA was amplified using specific primers used by [88], (see table). GRN cDNA was amplified using a different primer set (see table). Cycling conditions were an initial denaturation of 95°x 2 min, followed by 30 cycles of 95° x 30 sec, 54.2° x 20 sec, 72° x 1 min; this was followed by a final elongation step, 72° x 3min. Reactions were run on agarose gel, and the band was gel-extracted (Using Promega Wizard SV Gel and PCR Clean Up System, A9281). The PCR product was then sequenced in both directions by the McDermott Sanger Sequencing core, using Life Technologies® (LT) Dye Terminator 3.1 chemistry and 3730XL Genetic Analyzers. Tracings from the reverse sequence are shown.

Table 3.1: Primer Sequences

Mutagenesis		Forward	Reverse

	V5L	catgtggaccctgttgagctgggtggc	gccacccagctcaacagggtccacatg
	W7R	gaccctggtgagcagggtggccttaac	gttaaggccaccctgctcaccagggtc
	A9D	ggtgagctgggtggacttaacagcaggc	gccctgctgttaagtccacccagctcacc
subcloning into pTRE2		ggactcggatccgccaccatgtggaccctggt	gactcgatatcctacagcagctgtctcaagg
qPCR	pBI GRN	gaaccgtcagatccgctagg	acagggcagaactgaccatc
	total GRN	atacctgctgccgagacaac	aaacacttggtacccctggc
	WT specific	ctggtgagctgggtggc	gccatttgtccagaagggga
	A9D specific	cctggtgagctgggtgga	gccatttgtccagaagggga
	AcGFP	gaagtagatcatgtgatcgcg	ctgctgcccgataaccact
PGRN cDNA amplification		atgtggaccctggtgagct	gccatttgtccagaagggga
PGRN gDNA amplification [88]		gggctagggtactgagtgac	agtgttgtgggccatttg
qPCR	Actin	caccttctacaatgagctgcg	tagcacagcctggatagcaac
qPCR[160]	PPL 3’	aagtttgccagggaatggatc	acaactgctaagcccacattcat
qPCR[160]	PPL exon 2-3	caaattcgttgaacatttccg	ctgccaggtatcccttcgagac

CHAPTER FIVE

Conclusions and Recommendations

The rapid progression of FTLD/ALS, combined with a lack of disease-modifying therapies, make this a truly devastating diagnosis. The development of an even moderately efficacious therapy would have a significant impact on these patients. However, a therapeutic strategy must be informed by the underlying pathological changes, which as of now are not well-understood. This can be improved by focusing on two areas: First, the causes and consequences of a common pathological change in FTLD, the aggregation and mislocalization of TDP-43. Second, the quality control mechanisms which combat aggregation, such as RAPP (Regulation of Aberrant Protein Production).

Mislocalization and aggregation of the RNA-binding protein TDP-43 is commonly seen in FTLD/ALS patients. In an unstressed cell, TDP-43 is predominantly nuclear, but constantly shuttling to and from the cytosol. In ALS/FTLD, TDP-43 is aggregated in the cytosol and depleted from the nucleus. Converging lines of evidence suggest that cytosolic aggregation and nuclear depletion of TDP-43 are a cause of toxicity in FTLD/ALS, although the contribution of each of these to toxicity is still a matter of debate. Thus, facilitating nuclear import and/or inhibiting nuclear export of TDP-43 are attractive potential therapeutic strategies.

Despite this, there is relatively little known about normal trafficking of TDP-43. In this work, I have made contributions to our understanding of the steady-state trafficking of TDP-43. TDP-43 trafficking is comprised of nuclear import and nuclear export. In the course of my initial experiments on TDP-43 nuclear trafficking, I found that the published

mechanism of nuclear export was incorrect: TDP-43 nuclear export did not require the putative NES (Nuclear Export Signal), or did it appear to be XPO1 dependent. After determining that no region of TDP-43 was required for its export, and performing a few fortituous experiments with differently sized tags, I came to a surprising conclusion- TDP-43 nuclear export appeared to be driven by passive diffusion through the nuclear pore.

The phenomenon of diffusion through the nuclear pore has been largely ignored. Initial studies in the 70s with differently sized beads indicated that most proteins are unable to diffuse through; this led to the oft-repeated statement through the literature that any protein larger than 40 kDa cannot diffuse through the NPC. Additionally, the observation that many proteins much smaller than contain trafficking signals – for example, the 13kDa Rev protein– suggested that even small proteins could only traffic efficiently with the aid of a karyopherin [204].

However, more recently this finding has been re-examined, with several studies suggesting that in fact much larger proteins have the capability to diffuse through the NPC. My study provides, to my knowledge, the first practical example that a protein can shuttle efficiently without active nuclear export. My study suggests that other members of the hnRNP family of proteins, which also contain dubious NESs, may also exit the nucleus via passive diffusion. Moreover, my study offers an experimental paradigm to test this hypothesis: assess nuclear export of protein of interest fused to tags of various sizes.

While the passive nuclear export of TDP-43 is interesting from a scientific standpoint, from a therapeutic standpoint it is rather disappointing. Blocking nuclear export with small molecules is not only feasible, but is well-tolerated by patients. By contrast,

inhibiting passive nuclear export is likely both technically challenging and toxic. However, I hope the insight I provide into the steady-state trafficking of TDP-43 can help answer the critical next questions: what are the fundamental events that incite pathological mislocalization and aggregation of TDP-43? And are there any cellular events which directly affect TDP-43 import, export, or aggregation, that might play a part in either inciting or propagating these pathological states?

There is also a great deal of work to be done in understanding quality control pathways, which have evolved to curb accumulation of potentially toxic misfolded and mislocalized proteins. Our lab recently described the quality control pathway RAPP (Regulation of Aberrant Protein Production). This quality control pathway acts to prevent formation of mis-localized proteins by specifically degrading mRNA of proteins which fail to recruit the correct trafficking factors during translation. This was originally demonstrated in the case of a mutant secretory protein, PPLΔ4L (preprolactin) which could not recruit the trafficking factor SRP (Signal Recognition Particle).

I extended our understanding of RAPP by demonstrating an endogenous, disease-related substrate: GRN A9D (progranulin). Patients which carry a single loss-of-function mutation in progranulin develop the neurodegenerative disease FTLD. Most of the FTLD-causing GRN mutations are nonsense, but one of the most common mutations is A9D, a missense mutation within the signal sequence. I showed that A9D GRN is a RAPP substrate when transiently expressed in cultured cells. Moreover, A9D GRN is a RAPP substrate in culture fibroblasts isolated from an FTLD patient. This demonstrates that RAPP plays a role in suppressing the expression of mutated secretory proteins in disease. A preliminary

literature search suggests that this may be a general mechanism of genetic diseases caused by loss of a critical secretory protein.

However, many questions about RAPP remain unanswered. First, there are mechanistic details: how are RAPP substrates recognized? What is the eventual fate of the nascent chain and translating ribosome? And what are the nucleases and other protein players in this process? Second, there are physiological questions about RAPP: is suppression of mutant secretory proteins, such as A9D GRN, helpful or harmful? And what are the consequences, for the cell and the organism, of loss of RAPP?

The most pressing question is which proteins/RNAs are involved in sensing and mediating RAPP. I and previous lab members have already done a candidate-based search, looking at proteins involved in other QC pathways: NSD, NGD, and NMD. The logical next step is to do an unbiased screen for RAPP mediators. This could be a siRNA screen, a small molecule screen, or a CRISPR screen. Because this RAPP is an RNA decay pathway, proteins involved in RNAi mediated silencing may play a role in RAPP, so a CRISPR screen may be preferable. A small molecule inhibitor of RAPP would be very useful for answering key questions about RAPP, so conducting a small molecule screen in parallel is worth consideration.

BIBLIOGRAPHY

1. Kochanek, K.D., et al., *Deaths: Final Data for 2014.* Natl Vital Stat Rep, 2016. **65**(4): p. 1-122.
2. Worms, P.M., *The epidemiology of motor neuron diseases: a review of recent studies.* J Neurol Sci, 2001. **191**(1-2): p. 3-9.
3. Lindsay, J., et al., *Risk factors for Alzheimer's disease: a prospective analysis from the Canadian Study of Health and Aging.* Am J Epidemiol, 2002. **156**(5): p. 445-53.
4. Van Den Eeden, S.K., et al., *Incidence of Parkinson's disease: variation by age, gender, and race/ethnicity.* Am J Epidemiol, 2003. **157**(11): p. 1015-22.
5. Dickson, D.W., *Parkinson's disease and parkinsonism: neuropathology.* Cold Spring Harb Perspect Med, 2012. **2**(8).
6. Bertram, L. and R.E. Tanzi, *The genetic epidemiology of neurodegenerative disease.* J Clin Invest, 2005. **115**(6): p. 1449-57.
7. Brooks, B.R., et al., *El Escorial revisited: revised criteria for the diagnosis of amyotrophic lateral sclerosis.* Amyotroph Lateral Scler Other Motor Neuron Disord, 2000. **1**(5): p. 293-9.
8. Neary, D., et al., *Frontotemporal lobar degeneration: a consensus on clinical diagnostic criteria.* Neurology, 1998. **51**(6): p. 1546-54.
9. Strong, M.J., et al., *Consensus criteria for the diagnosis of frontotemporal cognitive and behavioural syndromes in amyotrophic lateral sclerosis.* Amyotroph Lateral Scler, 2009. **10**(3): p. 131-46.
10. Ringholz, G.M., et al., *Prevalence and patterns of cognitive impairment in sporadic ALS.* Neurology, 2005. **65**(4): p. 586-90.
11. Seltman, R.E. and B.R. Matthews, *Frontotemporal lobar degeneration: epidemiology, pathology, diagnosis and management.* CNS Drugs, 2012. **26**(10): p. 841-70.
12. Rosen, D.R., *Mutations in Cu/Zn superoxide dismutase gene are associated with familial amyotrophic lateral sclerosis.* Nature, 1993. **364**(6435): p. 362.
13. Neumann, M., et al., *Ubiquitinated TDP-43 in frontotemporal lobar degeneration and amyotrophic lateral sclerosis.* Science, 2006. **314**(5796): p. 130-3.
14. Mackenzie, I.R., et al., *Pathological TDP-43 distinguishes sporadic amyotrophic lateral sclerosis from amyotrophic lateral sclerosis with SOD1 mutations.* Ann Neurol, 2007. **61**(5): p. 427-34.
15. Davidson, Y., et al., *Ubiquitinated pathological lesions in frontotemporal lobar degeneration contain the TAR DNA-binding protein, TDP-43.* Acta Neuropathol, 2007. **113**(5): p. 521-33.
16. Neumann, M., et al., *A new subtype of frontotemporal lobar degeneration with FUS pathology.* Brain, 2009. **132**(Pt 11): p. 2922-31.
17. Sieben, A., et al., *The genetics and neuropathology of frontotemporal lobar degeneration.* Acta Neuropathol, 2012. **124**(3): p. 353-72.
18. Gibson, S.B., et al., *Familial clustering of ALS in a population-based resource.* Neurology, 2014. **82**(1): p. 17-22.

19. Majounie, E., et al., *Frequency of the C9orf72 hexanucleotide repeat expansion in patients with amyotrophic lateral sclerosis and frontotemporal dementia: a cross-sectional study.* Lancet Neurol, 2012. **11**(4): p. 323-30.
20. Deng, H.X., et al., *Mutations in UBQLN2 cause dominant X-linked juvenile and adult-onset ALS and ALS/dementia.* Nature, 2011. **477**(7363): p. 211-5.
21. Johnson, J.O., et al., *Exome sequencing reveals VCP mutations as a cause of familial ALS.* Neuron, 2010. **68**(5): p. 857-64.
22. Watts, G.D., et al., *Inclusion body myopathy associated with Paget disease of bone and frontotemporal dementia is caused by mutant valosin-containing protein.* Nat Genet, 2004. **36**(4): p. 377-81.
23. Skibinski, G., et al., *Mutations in the endosomal ESCRTIII-complex subunit CHMP2B in frontotemporal dementia.* Nat Genet, 2005. **37**(8): p. 806-8.
24. Hutton, M., et al., *Association of missense and 5'-splice-site mutations in tau with the inherited dementia FTDP-17.* Nature, 1998. **393**(6686): p. 702-5.
25. Miller, R.G., et al., *Riluzole for amyotrophic lateral sclerosis (ALS)/motor neuron disease (MND).* Cochrane Database Syst Rev, 2002(2): p. CD001447.
26. Azbill, R.D., X. Mu, and J.E. Springer, *Riluzole increases high-affinity glutamate uptake in rat spinal cord synaptosomes.* Brain Res, 2000. **871**(2): p. 175-80.
27. Shibata, N., et al., *Intense superoxide dismutase-1 immunoreactivity in intracytoplasmic hyaline inclusions of familial amyotrophic lateral sclerosis with posterior column involvement.* J Neuropathol Exp Neurol, 1996. **55**(4): p. 481-90.
28. Vance, C., et al., *Mutations in FUS, an RNA processing protein, cause familial amyotrophic lateral sclerosis type 6.* Science, 2009. **323**(5918): p. 1208-11.
29. Kwiatkowski, T.J., Jr., et al., *Mutations in the FUS/TLS gene on chromosome 16 cause familial amyotrophic lateral sclerosis.* Science, 2009. **323**(5918): p. 1205-8.
30. Sreedharan, J., et al., *TDP-43 mutations in familial and sporadic amyotrophic lateral sclerosis.* Science, 2008. **319**(5870): p. 1668-72.
31. Johnson, B.S., et al., *TDP-43 is intrinsically aggregation-prone, and amyotrophic lateral sclerosis-linked mutations accelerate aggregation and increase toxicity.* J Biol Chem, 2009. **284**(30): p. 20329-39.
32. Snowden, J.S., et al., *The most common type of FTLD-FUS (aFTLD-U) is associated with a distinct clinical form of frontotemporal dementia but is not related to mutations in the FUS gene.* Acta Neuropathol, 2011. **122**(1): p. 99-110.
33. Wang, H.Y., et al., *Structural diversity and functional implications of the eukaryotic TDP gene family.* Genomics, 2004. **83**(1): p. 130-9.
34. Wu, L.S., et al., *TDP-43, a neuro-pathosignature factor, is essential for early mouse embryogenesis.* Genesis, 2010. **48**(1): p. 56-62.
35. Feiguin, F., et al., *Depletion of TDP-43 affects Drosophila motoneurons terminal synapsis and locomotive behavior.* FEBS Lett, 2009. **583**(10): p. 1586-92.
36. Sephton, C.F., et al., *TDP-43 is a developmentally regulated protein essential for early embryonic development.* J Biol Chem, 2010. **285**(9): p. 6826-34.
37. Stallings, N.R., et al., *Progressive motor weakness in transgenic mice expressing human TDP-43.* Neurobiol Dis, 2010. **40**(2): p. 404-14.

38. Xu, Y.F., et al., *Wild-type human TDP-43 expression causes TDP-43 phosphorylation, mitochondrial aggregation, motor deficits, and early mortality in transgenic mice.* J Neurosci, 2010. **30**(32): p. 10851-9.
39. Wils, H., et al., *TDP-43 transgenic mice develop spastic paralysis and neuronal inclusions characteristic of ALS and frontotemporal lobar degeneration.* Proc Natl Acad Sci U S A, 2010. **107**(8): p. 3858-63.
40. Shan, X., et al., *Altered distributions of Gemini of coiled bodies and mitochondria in motor neurons of TDP-43 transgenic mice.* Proc Natl Acad Sci U S A, 2010. **107**(37): p. 16325-30.
41. Tsai, K.J., et al., *Elevated expression of TDP-43 in the forebrain of mice is sufficient to cause neurological and pathological phenotypes mimicking FTLD-U.* J Exp Med, 2010. **207**(8): p. 1661-73.
42. Vanden Broeck, L., et al., *TDP-43 loss-of-function causes neuronal loss due to defective steroid receptor-mediated gene program switching in Drosophila.* Cell Rep, 2013. **3**(1): p. 160-72.
43. Avendano-Vazquez, S.E., et al., *Autoregulation of TDP-43 mRNA levels involves interplay between transcription, splicing, and alternative polyA site selection.* Genes Dev, 2012. **26**(15): p. 1679-84.
44. Rommens, J.M., et al., *Identification of the cystic fibrosis gene: chromosome walking and jumping.* Science, 1989. **245**(4922): p. 1059-65.
45. Riordan, J.R., et al., *Identification of the cystic fibrosis gene: cloning and characterization of complementary DNA.* Science, 1989. **245**(4922): p. 1066-73.
46. Kerem, B., et al., *Identification of the cystic fibrosis gene: genetic analysis.* Science, 1989. **245**(4922): p. 1073-80.
47. Chu, C.S., et al., *Variable deletion of exon 9 coding sequences in cystic fibrosis transmembrane conductance regulator gene mRNA transcripts in normal bronchial epithelium.* EMBO J, 1991. **10**(6): p. 1355-63.
48. Buratti, E. and F.E. Baralle, *Characterization and functional implications of the RNA binding properties of nuclear factor TDP-43, a novel splicing regulator of CFTR exon 9.* J Biol Chem, 2001. **276**(39): p. 36337-43.
49. Niksic, M., et al., *Functional analysis of cis-acting elements regulating the alternative splicing of human CFTR exon 9.* Hum Mol Genet, 1999. **8**(13): p. 2339-49.
50. Polymenidou, M., et al., *Long pre-mRNA depletion and RNA missplicing contribute to neuronal vulnerability from loss of TDP-43.* Nat Neurosci, 2011. **14**(4): p. 459-68.
51. Sephton, C.F., et al., *Identification of neuronal RNA targets of TDP-43-containing ribonucleoprotein complexes.* J Biol Chem, 2011. **286**(2): p. 1204-15.
52. Tollervey, J.R., et al., *Characterizing the RNA targets and position-dependent splicing regulation by TDP-43.* Nat Neurosci, 2011. **14**(4): p. 452-8.
53. Ling, J.P., et al., *TDP-43 repression of nonconserved cryptic exons is compromised in ALS-FTD.* Science, 2015. **349**(6248): p. 650-5.
54. Ou, S.H., et al., *Cloning and characterization of a novel cellular protein, TDP-43, that binds to human immunodeficiency virus type 1 TAR DNA sequence motifs.* J Virol, 1995. **69**(6): p. 3584-96.
55. Lalmansingh, A.S., C.J. Urekar, and P.P. Reddi, *TDP-43 is a transcriptional repressor: the testis-specific mouse acrv1 gene is a TDP-43 target in vivo.* J Biol Chem, 2011. **286**(13): p. 10970-82.

56. Alami, N.H., et al., *Axonal transport of TDP-43 mRNA granules is impaired by ALS-causing mutations.* Neuron, 2014. **81**(3): p. 536-43.
57. Colombrita, C., et al., *TDP-43 is recruited to stress granules in conditions of oxidative insult.* J Neurochem, 2009. **111**(4): p. 1051-61.
58. Buratti, E., et al., *TDP-43 binds heterogeneous nuclear ribonucleoprotein A/B through its C-terminal tail: an important region for the inhibition of cystic fibrosis transmembrane conductance regulator exon 9 splicing.* J Biol Chem, 2005. **280**(45): p. 37572-84.
59. Ling, S.C., et al., *ALS-associated mutations in TDP-43 increase its stability and promote TDP-43 complexes with FUS/TLS.* Proc Natl Acad Sci U S A, 2010. **107**(30): p. 13318-23.
60. Dewey, C.M., et al., *TDP-43 is directed to stress granules by sorbitol, a novel physiological osmotic and oxidative stressor.* Mol Cell Biol, 2011. **31**(5): p. 1098-108.
61. Watanabe, S., K. Kaneko, and K. Yamanaka, *Accelerated disease onset with stabilized familial amyotrophic lateral sclerosis (ALS)-linked mutant TDP-43 proteins.* J Biol Chem, 2013. **288**(5): p. 3641-54.
62. Arnold, E.S., et al., *ALS-linked TDP-43 mutations produce aberrant RNA splicing and adult-onset motor neuron disease without aggregation or loss of nuclear TDP-43.* Proc Natl Acad Sci U S A, 2013. **110**(8): p. E736-45.
63. Guo, W., et al., *An ALS-associated mutation affecting TDP-43 enhances protein aggregation, fibril formation and neurotoxicity.* Nat Struct Mol Biol, 2011. **18**(7): p. 822-30.
64. Winton, M.J., et al., *Disturbance of nuclear and cytoplasmic TAR DNA-binding protein (TDP-43) induces disease-like redistribution, sequestration, and aggregate formation.* J Biol Chem, 2008. **283**(19): p. 13302-9.
65. Ayala, Y.M., et al., *Structural determinants of the cellular localization and shuttling of TDP-43.* J Cell Sci, 2008. **121**(Pt 22): p. 3778-85.
66. Stevens, B.J. and H. Swift, *RNA transport from nucleus to cytoplasm in Chironomus salivary glands.* J Cell Biol, 1966. **31**(1): p. 55-77.
67. Ribbeck, K. and D. Gorlich, *Kinetic analysis of translocation through nuclear pore complexes.* EMBO J, 2001. **20**(6): p. 1320-30.
68. Gorlich, D. and U. Kutay, *Transport between the cell nucleus and the cytoplasm.* Annu Rev Cell Dev Biol, 1999. **15**: p. 607-60.
69. Paine, P.L. and C.M. Feldherr, *Nucleocytoplasmic exchange of macromolecules.* Exp Cell Res, 1972. **74**(1): p. 81-98.
70. Timney, B.L., et al., *Simple rules for passive diffusion through the nuclear pore complex.* J Cell Biol, 2016. **215**(1): p. 57-76.
71. Wang, R. and M.G. Brattain, *The maximal size of protein to diffuse through the nuclear pore is larger than 60kDa.* FEBS Lett, 2007. **581**(17): p. 3164-70.
72. Pemberton, L.F. and B.M. Paschal, *Mechanisms of receptor-mediated nuclear import and nuclear export.* Traffic, 2005. **6**(3): p. 187-98.
73. Xu, D., A. Farmer, and Y.M. Chook, *Recognition of nuclear targeting signals by Karyopherin-beta proteins.* Curr Opin Struct Biol, 2010. **20**(6): p. 782-90.
74. Moore, M.S. and G. Blobel, *The GTP-binding protein Ran/TC4 is required for protein import into the nucleus.* Nature, 1993. **365**(6447): p. 661-3.
75. Melchior, F., *Ran GTPase cycle: oOne mechanism -- two functions.* Curr Biol, 2001. **11**(7): p. R257-60.

76. Nishimura, A.L., et al., *Nuclear import impairment causes cytoplasmic trans-activation response DNA-binding protein accumulation and is associated with frontotemporal lobar degeneration.* Brain, 2010. **133**(Pt 6): p. 1763-71.
77. Fornerod, M., et al., *CRM1 is an export receptor for leucine-rich nuclear export signals.* Cell, 1997. **90**(6): p. 1051-60.
78. Xu, D., et al., *Sequence and structural analyses of nuclear export signals in the NESdb database.* Mol Biol Cell, 2012. **23**(18): p. 3677-93.
79. Xu, D., et al., *LocNES: a computational tool for locating classical NESs in CRM1 cargo proteins.* Bioinformatics, 2015. **31**(9): p. 1357-65.
80. Lukavsky, P.J., et al., *Molecular basis of UG-rich RNA recognition by the human splicing factor TDP-43.* Nat Struct Mol Biol, 2013. **20**(12): p. 1443-9.
81. Lapalombella, R., et al., *Selective inhibitors of nuclear export show that CRM1/XPO1 is a target in chronic lymphocytic leukemia.* Blood, 2012. **120**(23): p. 4621-34.
82. Haines, J.D., et al., *Nuclear export inhibitors avert progression in preclinical models of inflammatory demyelination.* Nat Neurosci, 2015. **18**(4): p. 511-20.
83. Zhou, H., et al., *Transgenic rat model of neurodegeneration caused by mutation in the TDP gene.* PLoS Genet, 2010. **6**(3): p. e1000887.
84. Igaz, L.M., et al., *Dysregulation of the ALS-associated gene TDP-43 leads to neuronal death and degeneration in mice.* J Clin Invest, 2011. **121**(2): p. 726-38.
85. Dayton, R.D., et al., *Selective Forelimb Impairment in Rats Expressing a Pathological TDP-43 25 kDa C-terminal Fragment to Mimic Amyotrophic Lateral Sclerosis.* Mol Ther, 2013. **21**(7): p. 1324-1334.
86. Corrado, L., et al., *Mutations of FUS gene in sporadic amyotrophic lateral sclerosis.* J Med Genet, 2010. **47**(3): p. 190-4.
87. Zhang, Z.C. and Y.M. Chook, *Structural and energetic basis of ALS-causing mutations in the atypical proline-tyrosine nuclear localization signal of the Fused in Sarcoma protein (FUS).* Proc Natl Acad Sci U S A, 2012. **109**(30): p. 12017-21.
88. Gass, J., et al., *Mutations in progranulin are a major cause of ubiquitin-positive frontotemporal lobar degeneration.* Hum Mol Genet, 2006. **15**(20): p. 2988-3001.
89. Songsrirote, K., et al., *Development and application of mass spectrometric methods for the analysis of progranulin N-glycosylation.* J Proteomics, 2010. **73**(8): p. 1479-90.
90. Hu, F., et al., *Sortilin-mediated endocytosis determines levels of the frontotemporal dementia protein, progranulin.* Neuron, 2010. **68**(4): p. 654-67.
91. Tolkatchev, D., et al., *Structure dissection of human progranulin identifies well-folded granulin/epithelin modules with unique functional activities.* Protein Sci, 2008. **17**(4): p. 711-24.
92. Bateman, A. and H.P. Bennett, *Granulins: the structure and function of an emerging family of growth factors.* J Endocrinol, 1998. **158**(2): p. 145-51.
93. Butler, G.S., et al., *Pharmacoproteomics of a metalloproteinase hydroxamate inhibitor in breast cancer cells: dynamics of membrane type 1 matrix metalloproteinase-mediated membrane protein shedding.* Mol Cell Biol, 2008. **28**(15): p. 4896-914.
94. Bai, X.H., et al., *ADAMTS-7, a direct target of PTHrP, adversely regulates endochondral bone growth by associating with and inactivating GEP growth factor.* Mol Cell Biol, 2009. **29**(15): p. 4201-19.

95. Kessenbrock, K., et al., *Proteinase 3 and neutrophil elastase enhance inflammation in mice by inactivating antiinflammatory progranulin.* J Clin Invest, 2008. **118**(7): p. 2438-47.
96. Zhu, J., et al., *Conversion of proepithelin to epithelins: roles of SLPI and elastase in host defense and wound repair.* Cell, 2002. **111**(6): p. 867-78.
97. Suh, H.S., et al., *Regulation of progranulin expression in human microglia and proteolysis of progranulin by matrix metalloproteinase-12 (MMP-12).* PLoS One, 2012. **7**(4): p. e35115.
98. Culouscou, J.M., G.W. Carlton, and M. Shoyab, *Biochemical analysis of the epithelin receptor.* J Biol Chem, 1993. **268**(14): p. 10458-62.
99. Plowman, G.D., et al., *The epithelin precursor encodes two proteins with opposing activities on epithelial cell growth.* J Biol Chem, 1992. **267**(18): p. 13073-8.
100. Shoyab, M., et al., *Epithelins 1 and 2: isolation and characterization of two cysteine-rich growth-modulating proteins.* Proc Natl Acad Sci U S A, 1990. **87**(20): p. 7912-6.
101. Liau, L.M., et al., *Identification of a human glioma-associated growth factor gene, granulin, using differential immuno-absorption.* Cancer Res, 2000. **60**(5): p. 1353-60.
102. Van Damme, P., et al., *Progranulin functions as a neurotrophic factor to regulate neurite outgrowth and enhance neuronal survival.* J Cell Biol, 2008. **181**(1): p. 37-41.
103. Canafoglia, L., et al., *Recurrent generalized seizures, visual loss, and palinopsia as phenotypic features of neuronal ceroid lipofuscinosis due to progranulin gene mutation.* Epilepsia, 2014. **55**(6): p. e56-9.
104. Almeida, M.R., et al., *Portuguese family with the co-occurrence of frontotemporal lobar degeneration and neuronal ceroid lipofuscinosis phenotypes due to progranulin gene mutation.* Neurobiol Aging, 2016. **41**: p. 200 e1-5.
105. Wang, J., et al., *Pathogenic cysteine mutations affect progranulin function and production of mature granulins.* J Neurochem, 2010. **112**(5): p. 1305-15.
106. Shankaran, S.S., et al., *Missense mutations in the progranulin gene linked to frontotemporal lobar degeneration with ubiquitin-immunoreactive inclusions reduce progranulin production and secretion.* J Biol Chem, 2008. **283**(3): p. 1744-53.
107. Finch, N., et al., *Plasma progranulin levels predict progranulin mutation status in frontotemporal dementia patients and asymptomatic family members.* Brain, 2009. **132**(Pt 3): p. 583-91.
108. Smith, K.R., et al., *Strikingly different clinicopathological phenotypes determined by progranulin-mutation dosage.* Am J Hum Genet, 2012. **90**(6): p. 1102-7.
109. Ward, M.E., et al., *Individuals with progranulin haploinsufficiency exhibit features of neuronal ceroid lipofuscinosis.* Sci Transl Med, 2017. **9**(385).
110. Kurosaki, T. and L.E. Maquat, *Rules that govern UPF1 binding to mRNA 3' UTRs.* Proc Natl Acad Sci U S A, 2013. **110**(9): p. 3357-62.
111. Mendell, J.T., C.M. ap Rhys, and H.C. Dietz, *Separable roles for rent1/hUpf1 in altered splicing and decay of nonsense transcripts.* Science, 2002. **298**(5592): p. 419-22.
112. Bhattacharya, A., et al., *Characterization of the biochemical properties of the human Upf1 gene product that is involved in nonsense-mediated mRNA decay.* RNA, 2000. **6**(9): p. 1226-35.
113. Sun, X., et al., *A mutated human homologue to yeast Upf1 protein has a dominant-negative effect on the decay of nonsense-containing mRNAs in mammalian cells.* Proc Natl Acad Sci U S A, 1998. **95**(17): p. 10009-14.

114. Hogg, J.R. and S.P. Goff, *Upf1 senses 3'UTR length to potentiate mRNA decay.* Cell, 2010. **143**(3): p. 379-89.
115. Kurosaki, T., et al., *A post-translational regulatory switch on UPF1 controls targeted mRNA degradation.* Genes Dev, 2014. **28**(17): p. 1900-16.
116. Hurt, J.A., A.D. Robertson, and C.B. Burge, *Global analyses of UPF1 binding and function reveal expanded scope of nonsense-mediated mRNA decay.* Genome Res, 2013. **23**(10): p. 1636-50.
117. Zund, D., et al., *Translation-dependent displacement of UPF1 from coding sequences causes its enrichment in 3' UTRs.* Nat Struct Mol Biol, 2013. **20**(8): p. 936-43.
118. Kashima, I., et al., *Binding of a novel SMG-1-Upf1-eRF1-eRF3 complex (SURF) to the exon junction complex triggers Upf1 phosphorylation and nonsense-mediated mRNA decay.* Genes Dev, 2006. **20**(3): p. 355-67.
119. Czaplinski, K., et al., *The surveillance complex interacts with the translation release factors to enhance termination and degrade aberrant mRNAs.* Genes Dev, 1998. **12**(11): p. 1665-77.
120. Yamashita, A., et al., *Human SMG-1, a novel phosphatidylinositol 3-kinase-related protein kinase, associates with components of the mRNA surveillance complex and is involved in the regulation of nonsense-mediated mRNA decay.* Genes Dev, 2001. **15**(17): p. 2215-28.
121. Ohnishi, T., et al., *Phosphorylation of hUPF1 induces formation of mRNA surveillance complexes containing hSMG-5 and hSMG-7.* Mol Cell, 2003. **12**(5): p. 1187-200.
122. Chakrabarti, S., et al., *Phospho-dependent and phospho-independent interactions of the helicase UPF1 with the NMD factors SMG5-SMG7 and SMG6.* Nucleic Acids Res, 2014. **42**(14): p. 9447-60.
123. Peixeiro, I., et al., *Interaction of PABPC1 with the translation initiation complex is critical to the NMD resistance of AUG-proximal nonsense mutations.* Nucleic Acids Res, 2012. **40**(3): p. 1160-73.
124. Silva, A.L., et al., *Proximity of the poly(A)-binding protein to a premature termination codon inhibits mammalian nonsense-mediated mRNA decay.* RNA, 2008. **14**(3): p. 563-76.
125. Kozlov, G. and K. Gehring, *Molecular basis of eRF3 recognition by the MLLE domain of poly(A)-binding protein.* PLoS One, 2010. **5**(4): p. e10169.
126. Joncourt, R., et al., *Eukaryotic initiation factor 4G suppresses nonsense-mediated mRNA decay by two genetically separable mechanisms.* PLoS One, 2014. **9**(8): p. e104391.
127. Fatscher, T., et al., *The interaction of cytoplasmic poly(A)-binding protein with eukaryotic initiation factor 4G suppresses nonsense-mediated mRNA decay.* RNA, 2014. **20**(10): p. 1579-92.
128. Amrani, N., et al., *Translation factors promote the formation of two states of the closed-loop mRNP.* Nature, 2008. **453**(7199): p. 1276-80.
129. Le Hir, H., et al., *The spliceosome deposits multiple proteins 20-24 nucleotides upstream of mRNA exon-exon junctions.* EMBO J, 2000. **19**(24): p. 6860-9.
130. Zhang, J., et al., *At least one intron is required for the nonsense-mediated decay of triosephosphate isomerase mRNA: a possible link between nuclear splicing and cytoplasmic translation.* Mol Cell Biol, 1998. **18**(9): p. 5272-83.
131. Sun, X., P.M. Moriarty, and L.E. Maquat, *Nonsense-mediated decay of glutathione peroxidase 1 mRNA in the cytoplasm depends on intron position.* EMBO J, 2000. **19**(17): p. 4734-44.

132. Gatfield, D. and E. Izaurralde, *Nonsense-mediated messenger RNA decay is initiated by endonucleolytic cleavage in Drosophila.* Nature, 2004. **429**(6991): p. 575-8.
133. Glavan, F., et al., *Structures of the PIN domains of SMG6 and SMG5 reveal a nuclease within the mRNA surveillance complex.* EMBO J, 2006. **25**(21): p. 5117-25.
134. Eberle, A.B., et al., *SMG6 promotes endonucleolytic cleavage of nonsense mRNA in human cells.* Nat Struct Mol Biol, 2009. **16**(1): p. 49-55.
135. Unterholzner, L. and E. Izaurralde, *SMG7 acts as a molecular link between mRNA surveillance and mRNA decay.* Mol Cell, 2004. **16**(4): p. 587-96.
136. Yamashita, A., et al., *Concerted action of poly(A) nucleases and decapping enzyme in mammalian mRNA turnover.* Nat Struct Mol Biol, 2005. **12**(12): p. 1054-63.
137. Loh, B., S. Jonas, and E. Izaurralde, *The SMG5-SMG7 heterodimer directly recruits the CCR4-NOT deadenylase complex to mRNAs containing nonsense codons via interaction with POP2.* Genes Dev, 2013. **27**(19): p. 2125-38.
138. Cho, H., K.M. Kim, and Y.K. Kim, *Human proline-rich nuclear receptor coregulatory protein 2 mediates an interaction between mRNA surveillance machinery and decapping complex.* Mol Cell, 2009. **33**(1): p. 75-86.
139. Kuroha, K., T. Tatematsu, and T. Inada, *Upf1 stimulates degradation of the product derived from aberrant messenger RNA containing a specific nonsense mutation by the proteasome.* EMBO Rep, 2009. **10**(11): p. 1265-71.
140. Anczukow, O., et al., *Does the nonsense-mediated mRNA decay mechanism prevent the synthesis of truncated BRCA1, CHK2, and p53 proteins?* Hum Mutat, 2008. **29**(1): p. 65-73.
141. Frolova, L.Y., T.I. Merkulova, and L.L. Kisselev, *Translation termination in eukaryotes: polypeptide release factor eRF1 is composed of functionally and structurally distinct domains.* RNA, 2000. **6**(3): p. 381-90.
142. Davis, L. and J. Engebrecht, *Yeast dom34 mutants are defective in multiple developmental pathways and exhibit decreased levels of polyribosomes.* Genetics, 1998. **149**(1): p. 45-56.
143. Pisareva, V.P., et al., *Dissociation by Pelota, Hbs1 and ABCE1 of mammalian vacant 80S ribosomes and stalled elongation complexes.* EMBO J, 2011. **30**(9): p. 1804-17.
144. Dever, T.E. and R. Green, *The elongation, termination, and recycling phases of translation in eukaryotes.* Cold Spring Harb Perspect Biol, 2012. **4**(7): p. a013706.
145. Shao, S., et al., *Decoding Mammalian Ribosome-mRNA States by Translational GTPase Complexes.* Cell, 2016. **167**(5): p. 1229-1240 e15.
146. Shoemaker, C.J. and R. Green, *Kinetic analysis reveals the ordered coupling of translation termination and ribosome recycling in yeast.* Proc Natl Acad Sci U S A, 2011. **108**(51): p. E1392-8.
147. Becker, T., et al., *Structure of the no-go mRNA decay complex Dom34-Hbs1 bound to a stalled 80S ribosome.* Nat Struct Mol Biol, 2011. **18**(6): p. 715-20.
148. Qu, X., et al., *The ribosome uses two active mechanisms to unwind messenger RNA during translation.* Nature, 2011. **475**(7354): p. 118-21.
149. Doma, M.K. and R. Parker, *Endonucleolytic cleavage of eukaryotic mRNAs with stalls in translation elongation.* Nature, 2006. **440**(7083): p. 561-4.
150. Letzring, D.P., K.M. Dean, and E.J. Grayhack, *Control of translation efficiency in yeast by codon-anticodon interactions.* RNA, 2010. **16**(12): p. 2516-28.
151. Ishimura, R., et al., *RNA function. Ribosome stalling induced by mutation of a CNS-specific tRNA causes neurodegeneration.* Science, 2014. **345**(6195): p. 455-9.

152. Guydosh, N.R. and R. Green, *Dom34 rescues ribosomes in 3' untranslated regions.* Cell, 2014. **156**(5): p. 950-62.
153. Pechmann, S., J.W. Chartron, and J. Frydman, *Local slowdown of translation by nonoptimal codons promotes nascent-chain recognition by SRP in vivo.* Nat Struct Mol Biol, 2014. **21**(12): p. 1100-5.
154. van Hoof, A., et al., *Exosome-mediated recognition and degradation of mRNAs lacking a termination codon.* Science, 2002. **295**(5563): p. 2262-4.
155. Frischmeyer, P.A., et al., *An mRNA surveillance mechanism that eliminates transcripts lacking termination codons.* Science, 2002. **295**(5563): p. 2258-61.
156. Saito, S., N. Hosoda, and S. Hoshino, *The Hbs1-Dom34 protein complex functions in non-stop mRNA decay in mammalian cells.* J Biol Chem, 2013. **288**(24): p. 17832-43.
157. Passos, D.O., et al., *Analysis of Dom34 and its function in no-go decay.* Mol Biol Cell, 2009. **20**(13): p. 3025-32.
158. Becker, T., et al., *Structural basis of highly conserved ribosome recycling in eukaryotes and archaea.* Nature, 2012. **482**(7386): p. 501-6.
159. Shao, S., K. von der Malsburg, and R.S. Hegde, *Listerin-dependent nascent protein ubiquitination relies on ribosome subunit dissociation.* Mol Cell, 2013. **50**(5): p. 637-48.
160. Karamyshev, A.L., et al., *Inefficient SRP interaction with a nascent chain triggers a mRNA quality control pathway.* Cell, 2014. **156**(1-2): p. 146-57.
161. Hammond, S.M., et al., *Argonaute2, a link between genetic and biochemical analyses of RNAi.* Science, 2001. **293**(5532): p. 1146-50.
162. Miller, J.N. and D.A. Pearce, *Nonsense-mediated decay in genetic disease: friend or foe?* Mutat Res Rev Mutat Res, 2014. **762**: p. 52-64.
163. Kerr, T.P., et al., *Long mutant dystrophins and variable phenotypes: evasion of nonsense-mediated decay?* Hum Genet, 2001. **109**(4): p. 402-7.
164. Inoue, K., et al., *Molecular mechanism for distinct neurological phenotypes conveyed by allelic truncating mutations.* Nat Genet, 2004. **36**(4): p. 361-9.
165. Howard, M., R.A. Frizzell, and D.M. Bedwell, *Aminoglycoside antibiotics restore CFTR function by overcoming premature stop mutations.* Nat Med, 1996. **2**(4): p. 467-9.
166. Klauer, A.A. and A. van Hoof, *Degradation of mRNAs that lack a stop codon: a decade of nonstop progress.* Wiley Interdiscip Rev RNA, 2012. **3**(5): p. 649-60.
167. Arnold, A., et al., *Mutation of the signal peptide-encoding region of the preproparathyroid hormone gene in familial isolated hypoparathyroidism.* J Clin Invest, 1990. **86**(4): p. 1084-7.
168. Seppen, J., et al., *A mutation which disrupts the hydrophobic core of the signal peptide of bilirubin UDP-glucuronosyltransferase, an endoplasmic reticulum membrane protein, causes Crigler-Najjar type II.* FEBS Lett, 1996. **390**(3): p. 294-8.
169. Rajpar, M.H., et al., *Mutation of the signal peptide region of the bicistronic gene DSPP affects translocation to the endoplasmic reticulum and results in defective dentine biomineralization.* Hum Mol Genet, 2002. **11**(21): p. 2559-65.
170. Symoens, S., et al., *COL5A1 signal peptide mutations interfere with protein secretion and cause classic Ehlers-Danlos syndrome.* Hum Mutat, 2009. **30**(2): p. E395-403.
171. Mencarelli, M., et al., *A novel missense mutation in the signal peptide of the human POMC gene: a possible additional link between early-onset type 2 diabetes and obesity.* Eur J Hum Genet, 2012. **20**(12): p. 1290-4.

172. Zarei, S., et al., *A comprehensive review of amyotrophic lateral sclerosis.* Surg Neurol Int, 2015. **6**: p. 171.
173. Fung, H.Y., et al., *Structural determinants of nuclear export signal orientation in binding to exportin CRM1.* Elife, 2015. **4**.
174. Liu, W., et al., *IBS: an illustrator for the presentation and visualization of biological sequences.* Bioinformatics, 2015. **31**(20): p. 3359-61.
175. Mackness, B.C., et al., *Folding of the RNA recognition motif (RRM) domains of the amyotrophic lateral sclerosis (ALS)-linked protein TDP-43 reveals an intermediate state.* J Biol Chem, 2014. **289**(12): p. 8264-76.
176. Kutay, U. and S. Guttinger, *Leucine-rich nuclear-export signals: born to be weak.* Trends Cell Biol, 2005. **15**(3): p. 121-4.
177. Pinol-Roma, S. and G. Dreyfuss, *Shuttling of pre-mRNA binding proteins between nucleus and cytoplasm.* Nature, 1992. **355**(6362): p. 730-2.
178. Nakielny, S. and G. Dreyfuss, *The hnRNP C proteins contain a nuclear retention sequence that can override nuclear export signals.* J Cell Biol, 1996. **134**(6): p. 1365-73.
179. Barmada, S.J., et al., *Cytoplasmic mislocalization of TDP-43 is toxic to neurons and enhanced by a mutation associated with familial amyotrophic lateral sclerosis.* J Neurosci, 2010. **30**(2): p. 639-49.
180. Miguel, L., et al., *Both cytoplasmic and nuclear accumulations of the protein are neurotoxic in Drosophila models of TDP-43 proteinopathies.* Neurobiol Dis, 2011. **41**(2): p. 398-406.
181. Voigt, A., et al., *TDP-43-mediated neuron loss in vivo requires RNA-binding activity.* PLoS One, 2010. **5**(8): p. e12247.
182. Buratti, E., et al., *Nuclear factor TDP-43 and SR proteins promote in vitro and in vivo CFTR exon 9 skipping.* EMBO J, 2001. **20**(7): p. 1774-84.
183. Etchin, J., et al., *Antileukemic activity of nuclear export inhibitors that spare normal hematopoietic cells.* Leukemia, 2013. **27**(1): p. 66-74.
184. Kim, J., et al., *XPO1-dependent nuclear export is a druggable vulnerability in KRAS-mutant lung cancer.* Nature, 2016. **538**(7623): p. 114-117.
185. Freibaum, B.D., et al., *Global analysis of TDP-43 interacting proteins reveals strong association with RNA splicing and translation machinery.* J Proteome Res, 2010. **9**(2): p. 1104-20.
186. Lorenzo-Betancor, O., et al., *Analysis of nuclear export sequence regions of FUS-Related RNA-binding proteins in essential tremor.* PLoS One, 2014. **9**(11): p. e111989.
187. Li, Y.C., et al., *Synaptotagmin-1- and Synaptotagmin-7-Dependent Fusion Mechanisms Target Synaptic Vesicles to Kinetically Distinct Endocytic Pathways.* Neuron, 2017. **93**(3): p. 616-631 e3.
188. Gagnon, K.T., et al., *RNAi factors are present and active in human cell nuclei.* Cell Rep, 2014. **6**(1): p. 211-21.
189. von Heijne, G., *Signal sequences. The limits of variation.* J Mol Biol, 1985. **184**(1): p. 99-105.
190. Walter, P., I. Ibrahimi, and G. Blobel, *Translocation of proteins across the endoplasmic reticulum. I. Signal recognition protein (SRP) binds to in-vitro-assembled polysomes synthesizing secretory protein.* J Cell Biol, 1981. **91**(2 Pt 1): p. 545-50.
191. Popp, M.W. and L.E. Maquat, *Defective secretory-protein mRNAs take the RAPP.* Trends Biochem Sci, 2014. **39**(4): p. 154-6.

192. Lopez de Munain, A., et al., *Mutations in progranulin gene: clinical, pathological, and ribonucleic acid expression findings.* Biol Psychiatry, 2008. **63**(10): p. 946-52.
193. Le Ber, I., et al., *Phenotype variability in progranulin mutation carriers: a clinical, neuropsychological, imaging and genetic study.* Brain, 2008. **131**(Pt 3): p. 732-46.
194. von Heijne, G., *On the hydrophobic nature of signal sequences.* Eur J Biochem, 1981. **116**(2): p. 419-22.
195. Nilsson, I., et al., *The code for directing proteins for translocation across ER membrane: SRP cotranslationally recognizes specific features of a signal sequence.* J Mol Biol, 2015. **427**(6 Pt A): p. 1191-201.
196. Walter, P. and G. Blobel, *Signal recognition particle: a ribonucleoprotein required for cotranslational translocation of proteins, isolation and properties.* Methods Enzymol, 1983. **96**: p. 682-91.
197. Krieg, U.C., P. Walter, and A.E. Johnson, *Photocrosslinking of the signal sequence of nascent preprolactin to the 54-kilodalton polypeptide of the signal recognition particle.* Proc Natl Acad Sci U S A, 1986. **83**(22): p. 8604-8.
198. von Heijne, G., *Patterns of amino acids near signal-sequence cleavage sites.* Eur J Biochem, 1983. **133**(1): p. 17-21.
199. Wright, W.E. and J.W. Shay, *Inexpensive low-oxygen incubators.* Nat Protoc, 2006. **1**(4): p. 2088-90.
200. Flanagan, J.J., et al., *Signal recognition particle binds to ribosome-bound signal sequences with fluorescence-detected subnanomolar affinity that does not diminish as the nascent chain lengthens.* J Biol Chem, 2003. **278**(20): p. 18628-37.
201. McCormick, P.J., et al., *Cotranslational protein integration into the ER membrane is mediated by the binding of nascent chains to translocon proteins.* Mol Cell, 2003. **12**(2): p. 329-41.
202. Ren, Y.G., et al., *Differential regulation of the TRAIL death receptors DR4 and DR5 by the signal recognition particle.* Mol Biol Cell, 2004. **15**(11): p. 5064-74.
203. Chu, Y., et al., *Involvement of argonaute proteins in gene silencing and activation by RNAs complementary to a non-coding transcript at the progesterone receptor promoter.* Nucleic Acids Res, 2010. **38**(21): p. 7736-48.
204. Meyer, B.E. and M.H. Malim, *The HIV-1 Rev trans-activator shuttles between the nucleus and the cytoplasm.* Genes Dev, 1994. **8**(13): p. 1538-47.